HHS Public Access

Author manuscript

Q Rev Biophys. Author manuscript; available in PMC 2019 January 04.

Published in final edited form as:

Q Rev Biophys. 2011 February ; 44(1): 1–93. doi:10.1017/S0033583510000181.

Nucleases: Diversity of Structure, Function and Mechanism

Wei Yang

Laboratory of Molecular Biology, National Institute of Diabetes and Digestive and Kidney Diseases, National Institutes of Health, 9000 Rockville Pike, Bldg. 5, Rm B1-03, Bethesda, MD 20892, USA

Abstract

Nucleases cleave the phosphodiester bonds of nucleic acids and may be endo or exo, DNases or RNases, topoisomerases, recombinases, ribozymes, or RNA splicing enzymes. In this review I survey nuclease activities with known structures and catalytic machinery and classify them by reaction mechanism and metal ion dependence and by their biological function ranging from DNA replication, recombination, repair, RNA maturation, processing, interference, to defense, nutrient regeneration or cell death. Several general principles emerge from this analysis. There is little correlation between catalytic mechanism and biological function. A single catalytic mechanism can be adapted in a variety of reactions and biological pathways. Conversely a single biological process can often be accomplished by multiple tertiary and quaternary folds and by more than one catalytic mechanism. Two-metal-ion dependent nucleases comprise the largest number of different tertiary folds and mediate the most diverse set of biological functions. Metal-ion dependent cleavage is exclusively associated with exonucleases producing monomucleotides and endonucleases that cleave double- or single-stranded substrates in helical and base-stacked conformations. All metal-ion independent RNases generate 2′,3′-cyclic phosphate products, and all metal-ion independent DNases form phospho-protein intermediates. I also find several previously unnoted relationships between different nucleases and shared catalytic configurations.

Keywords

RNase; DNase; topoisomerase; ribozyme; repair; replication; recombination; splicing; maturation; decay; interference; restriction; CRISPR; toxin; immunity; metal ion

1. Introduction

Nucleases catalyzing DNA and RNA cleavage are indispensible for life (Table 1). Nuclease activities are integral parts of DNA replication; the 5′ to 3′ exo- and endonucleases are needed to remove RNA primers (Kao & Bambara, 2003; Shen et al., 2005), and the 3′ to 5′ exonuclease for proofreading (Reha-Krantz, 20010). Two other major DNA metabolic processes, recombination and repair, are initiated by nucleases (Marti & Fleck, 2004; Mimitou & Symington, 2009). Nuclease activity is also required for structural alterations of nucleic acids, for example, topoisomerization (Champoux, 2001; Schoeffler & Berger, 2008; Wang, 2002), site-specific recombination (Grindley et al., 2006), and RNA splicing (Patel & Steitz, 2003), during which a phosphodiester bond is temporarily broken and reformed after strand passing or transfer to a new target. In addition nuclease activities are essential in RNA

processing, maturation, and RNA interference (Abelson et al., 1998; Chu & Rana, 2007; Moore & Proudfoot, 2009; Nowotny & Yang, 2009). RNA and DNA degradation is an essential component of microbial defense mechanisms (James et al., 1996; Sorek et al., 2008; Tock & Dryden, 2005). Nucleases are even essential for programmed cell death (Parrish & Xue, 2006). Defective DNase and RNase activities have been associated with various autoimmune diseases due to incomplete removal of endogenously produced nucleic acids (Crow & Rehwinkel, 2009; Stephenson, 2008).

RNA and DNA present only two types of phosphodiester bonds for cleavage, 5′ or 3′ of a scissile phosphate (Fig. 1a)), and the fundamental chemistry is bimolecular nucleophilic substitution or S_N2 in short. Nonetheless, structures and catalytic mechanisms of RNA and DNA nucleases are greatly varied and complex. Nucleases can be protein or RNA and use water, (deoxy)ribose, inorganic phosphate, or the sidechains of Ser, Tyr or His as a nucleophile. Catalysis may or may not require metal ions. In addition, nuclease activities are strictly regulated by stringent substrate specificity (Pingoud et al., 2005; Stoddard, 2005), confined localization, or by potent inhibitors (Chowdhury et al., 2006; Kolade et al., 2002; Widlak & Garrard, 2005) to avoid unwanted or uncontrolled degradation of cellular DNA and RNA.

Individual nuclease families or superfamilies, for example topoisomerases (Schoeffler & Berger, 2008), sequence-specific recombinases (Grindley et al., 2006), metal ion-independent ribozymes (Cochrane & Strobel, 2008), Holliday junction resolvases (Declais & Lilley, 2008), and DNA nucleases (Horton, 2008) have been recently reviewed. This particular review is intended to summarize all DNases and RNases with known atomic structures and focus on catalytic mechanisms. The aim is to compare and contrast structural and mechanistic diversity in the context of shared functionality.

2. Nucleolytic reactions

2.1 Basic chemistry

A nuclease is a phosphodiesterase that cleaves one of the two bridging P-O bonds, 3′ or 5′, in a nucleic acid polymer (Fig. 1a). Cleavage of phosphodiester bonds is thought to be by a general acid-base catalysis, where the general base activates the nucleophile by deprotonation and the general acid facilitates product formation by protonating the leaving group. Perhaps because of the stability of nucleic acid phosphodiester bonds, the cleavage reaction is usually of the associative S_N2 type (Gerlt et al., 1983). The reaction can be divided into three stages: nucleophilic attack, formation of a highly negatively charged penta-covalent intermediate, and breakage of the scissile bond. Cleavage of the P-O_3′ bond, which generates 5′-phosphate and 3′-OH products, requires a nucleophile to be on the 5′ side poised for the in-line attack (Fig. 1a). In the penta-covalent bipyramid intermediate, the O_5′ moves to the center plane, which consists of the phosphorus and two non-bridging oxygens, and the attacking nucleophile and O_3′ leaving group are opposite each other at the apices of the bipyramid. In the cleaved product the stereo configuration of the phosphorus is inverted in this one-step reaction. Although phosphate in nucleic acid is achiral due to two chemically indistinguishable non-bridging oxygen atoms, the stereo inversion is evident when one of the non-bridging oxygen is replaced by a heavy isotope or sulfur (Eckstein,

1985; Gerlt et al., 1983). Hence the two non-bridging oxygens are referred to as pro-Sp and pro-Rp. A double inversion, which returns the phosphorus to its original configuration, requires a two-step reaction and occurs if an enzyme-nucleic acid covalent intermediate forms (Fig. 1b). To generate 3′-PO_4 and 5′-OH products, the reaction configuration has to be reversed, and the nucleophile has to attack on the 3′ side of the scissile phosphate (Fig. 1a).

2.2 Nucleophiles

Nucleases utilize a variety of nucleophiles to cleave a scissile phosphate bond (Fig. 2a). The most common nucleophiles are water molecules deprotonated by a general base for direct hydrolysis. A hydroxyl group of the 3′ end of DNA or RNA can also be the nucleophile as during RNA splicing, DNA strand transfer or hairpin formation (Doudna & Cech, 2002; van Gent et al., 1996) (Fig. 2b-c). For DNA cleavage, the side chains of Ser, Tyr and His have been observed to serve as nucleophiles to form a covalent DNA phosphoryl-protein intermediate, which is subsequently resolved either by phosphoryl transfer reaction back to DNA as during recombination and topoisomerization (Fig. 2d) or by hydrolysis in two-step cleavage reactions (Grindley et al., 2006; Stuckey & Dixon, 1999).

The 2′ hydroxyls of RNA or free ribonucleotides are additional nucleophiles utilized by RNases. The 2′-OH adjacent to a scissile phosphate often serves as the nucleophile and leads to the formation of a labile 2′,3′-cyclic phosphate (Fig. 2e, Fig. 3b-c), which is then hydrolyzed to produce a 3′ phosphate as exemplified by RNase A (Raines, 1998) or occasionally a 2′ phosphate as catalyzed by the yeast RNA ligase during tRNA splicing (Abelson et al., 1998). Finally, RNase PH and polynucleotide phosphorylases (PNPases) use inorganic phosphate as a nucleophile to degrade ssRNA by phosphorolysis and produce nucleoside 5′-diphosphates (Deutscher et al., 1988)(Fig. 2f). The pKa of these nucleophiles are 6.0 (His), 10.0 (Tyr), 12–14 (2′-OH of ribose), 13 (Ser), and 16 (H_2O) (Saenger, 1984; Voet & Voet, 2004). If water is the nucleophile, a general base is necessary to deprotonate it for efficient cleavage. Similarly, the 2′-OH of ribose also needs deprotonation to be an efficient nucleophile.

2.3 Double versus single stranded substrate

If the scissile phosphate is in a double helix, the options for placement of an external nucleophile (that is not within the nucleic acid itself) are limited. Looking down the helical axis, a nucleophile can approach the nucleic acid backbone only from outside the double helix because the inside is occupied by sugars and bases (Fig. 3a). If a nucleic acid is single stranded and bases are unstacked, approach of a nucleophile is not as resctricted. For example, RNA cleavage using the 2′-OH adjacent to a scissile phosphate can only occur with ssRNA because the reaction coordinate is incompatible with the double helix conformation and requires a distorted backbone phosphate with bases surrounding the scissile phosphate unstacked and splayed (Buckle & Fersht, 1994; Cochrane & Strobel, 2008; Correll et al., 2004) (Fig. 3b-c).

Potential reaction coordinates for nicking double-stranded nucleic acids are far less varied than possibilities for cleaving single stranded nucleic acids. Most often DNA is in a double

helix. Even RNA substrates in pre-mRNA splicing or RNAi-mediated cleavage are often based paired in a double-helical conformation (Nowotny & Yang, 2009; Patel & Steitz, 2003; Stahley & Strobel, 2006). To date, the nucleases that cleave double-stranded substrates all approach RNA and DNA from the minor groove side, where scissile phosphates are easier to reach than from the major groove side (Fig. 3a). Sequence-specific interactions, which usually take place in the major groove, are often accomplished by additional domains attached to catalytic centers (Lee et al., 2005).

2.4 Products of 5′ or 3′ phosphate

Nucleolytic cleavage products are most often 5′-phosphates and 3′-OH groups. This type of cleavage is preferred (over 3′-phosphate and 5′-OH) likely because firstly the 3′-OH can be passed onto other nucleic acid enzymes and used directly as the nucleophile, e.g. RNA and DNA polymerases, DNA ligases, transposases, spliceosomes, CCA-adding enzymes, and aa-tRNA synthetases. Secondly, the 5′-phosphate is a ready substrate for DNA ligation at the end of replication, repair and recombination. The two main exceptions are RNA cleavage via the 2′,3′-cyclic phosphodiester intermediate and DNA cleavage by Tyr-dependent site-specific recombinases and Type IB topoisomerases. For the DNA enzymes, a 3′-phosphotyrosyl bond is a transient intermediate and is reversed back to a phosphodiester bond in the product (Champoux, 2001; Grindley et al., 2006). In the RNA cases, either the 3′-phosphate is an end product or these RNA molecules require further hydrolysis and dephosphorylation. For example, the 2′,3′-cyclic phosphodiester formed in the tRNA splicing is hydrolyzed to form 3′-OH and 2′-phosphate (Abelson et al., 1998), which require several enzymatic activities to alter the phosphorylation states in a process referred to as healing (Nandakumar et al., 2008) before RNA fragements can be ligated.

3. Diversity and classification of nucleases

Nucleases are a very diverse group and include both proteins and catalytic RNAs (ribozyes). There is no simple way to classify and divide them. Based on substrate preference, nucleases may be divided to DNases and RNases, yet quite a number of nucleases are sugar nonspecific and can cleave both RNA and DNA (Hsia et al., 2005; Laskowski, 1985; Rangarajan & Shankar, 2001). Depending on whether a 5′ or 3′ end is required for substrate recognition and whether cleavage products are single or oligo nucleotides, they may be divided to exo- and endo-nucleases. For instance, all self-cleaving ribozymes found to date only cleave RNAs endonucleolytically (Cochrane & Strobel, 2008; Lilley, 2005). Exonucleases, which remove one nucleotide at a time from the end of a strand, can be further divided to two groups by the 5′ to 3′ versus 3′ to 5′ polarity. However, the fundamental chemistry of endo- and exo- cleavage is the same, and it is not unusual that a single active site may contain both exo and endonuclease activities. For example, members of the Flap endonuclease 1 (FEN1) family have the 5′ to 3′ exonuclease activity in addition to the endonuclease activity (Harrington & Lieber, 1994; Lyamichev et al., 1993), and Mre11, which is involved in DNA double-strand break (DSB) repair, has both endo and 3′ to 5′ exo-nuclease activities (Paull & Gellert, 1998; Usui et al., 1998).

According to catalytic mechanism, all nucleases may be divided into three major classes based on whether none, one or two metal ions are involved. However, each of these classes includes many different families and superfamilies. For instance, two-metal-ion dependent nucleases include both protein enzymes and ribozymes and can be vastly different in tertiary structure, metal ion-coordination motif, and cellular function. The following are just a few examples of diversity among nucleases.

3.1 The lack of correlation in structure, mechanism and biological function

Similar biological outcomes are often achieved by molecules with unrelated tertiary structures and drastically different mechanisms. For example, sequence specific restriction endonucleases encompass at least five structural families and employ at a minimum four different catalytic mechanisms (Orlowski & Bujnicki, 2008) (Table 1). For an up-to-date complete list of restriction endonucleases, please consult the REBASE database (rebase.neb.com)(Roberts et al.). In parallel, Holliday-junction resolvases are composed of five different structural and mechanistic families (Declais & Lilley, 2008; Ip et al., 2008) (Table 1). Conversely, similar tertiary structures may adopt different catalytic properties. For example, the Cas6 and Cas2 nucleases share the ferredoxin fold, but their active sites are unrelated (Beloglazova et al., 2008; Carte et al., 2008). Cas2 is metal-ion dependent and Cas6 metal independent. Furthermore, structural and mechanistic conservation are not necessarily correlated with identical functions. For example, molecules with the RNase H-like fold that utilizes two-metal ion catalysis are invovled in RNA processing, DNA cleavage, transposition and Holliday junction resolution (Nowotny et al., 2005; Yang & Steitz, 1995b).

3.2 Different catalytic mechanisms of ribozymes

RNA is thought to be the primordial nucleic acid and can function as both genetic material and a catalytic entity (Chen et al., 2007b; Yarus, 2002). It is not surprising that RNases and ribozymes display great mechanistic diversity. Naturally occurring ribozymes can be metal-dependent or independent (Lilley, 2005). The self-cleaving hammerhead, hairpin, glmS, HDV and VS ribozymes cleave extended single-stranded RNA by a metal-ion independent mechanism (Cochrane & Strobel, 2008), whereas group I and II introns cleave exon-intron junctions embedded in dsRNA by a two-metal-ion mechanism (Stahley & Strobel, 2005; Toor et al., 2009). Different catalytic mechanisms lead to the different types of cleavage products. The two-metal-ion dependent ribozymes generate 5′-phosphate and 3′-OH products, whereas the metal-independent ribozymes use 2′-OH as the nucleophile and generate 2′,3′-cyclic phosphate and 5′-OH products.

3.3 Different catalytic mechanisms of topoisomerases

All topoisomerases cleave DNA using a Tyr sidechain as the nucleophile to produce a covalent phosphotyrosyl DNA-enzyme intermediate for strand passing (see reviews by (Schoeffler & Berger, 2008; Wang, 2002)). Following cleavage and topological change, DNA is religated using the DNA hydroxyl group generated in the cleavage step as the nucleophile to cleave the phosphotyrosyl bond and religate the DNA, which regenerates a free topoisomerase (Fig. 2d). In this coupled cleavage-religation scheme, the phosphodiester bond energy is preserved and an external energy source is not necessary. The active site of

all topoisomerases consists of an essential Tyr nucleophile. Type IA and type II topoisomerases share a conserved catalytic core and require Mg^{2+} for efficient cleavage and religation, whereas type IB topoisomerases are different and don't need a divalent cation. Correlated with the metal ion dependence, type II and IA topoisomerases form 5′-phosphotyrosine and 3′-OH cleavage products, whereas type IB form 3′-phosphotyrosine and 5′-OH products (Schoeffler & Berger, 2008). Type IA and type II topoisomerases further differ in ATP and DNA substrate requirements. Type IA requires no ATP and cleaves ssDNA, whereas type II requires ATP and cleaves dsDNA (Schoeffler & Berger, 2008).

3.4 A two-way approach of categorization in this review

Because of the great diversity of nucleases, their classification cannot be accomplished explicitly by any single criterion. For convenience I separate nucleases into three major classes based on their metal-ion dependence and catalytic mechanism. In each class, nucleases are further divided to families or superfamilies according to sequence and structure conservation and functional diversity. Because the catalytic mechanisms of some nucleases are yet to be determined, uncertainty in their classification is indicated. To complement the classification by catalytic mechanism, nucleases are also divided by their biological function and summarized in Table 1. Diverse catalytic mechanisms involved in each biological pathway are then cross referenced to the relevant chapters and sections.

Before going into details of each class and superfamily of nucleases according to this metal-centric classification, the properties of Mg^{2+} and divalent cations and the main characteristics of metal-dependent and independent catalyses are first summarized.

4. Basic properties of Mg^{2+} and divalent cations

Mg^{2+} and Ca^{2+} are the most abundant divalent cations in living organisms (Cowan, 2002; Lyons & Eide, 2006), and Mg^{2+} is the most abundant divalent cation inside cells (Maguire & Cowan, 2002; Romani & Scarpa, 1992). Other ions like Fe^{2+}, Zn^{2+} and Cu^{2+} are widespread, and Mn^{2+} and Ni^{2+} are essential but found at low concentrations (Lyons & Eide, 2006). The principal quality of these divalent cations is the high density of positive charge, which makes them efficient for charge neutralization of phospholipids and nucleic acids. The second common property is hydration and the specific ligand requirement. By the atomic or covalent radius Ca^{2+} is the largest (1.9Å), Mg^{2+} the second (1.6Å), and the rest are similarly smaller (1.3Å). However, when hydrated, Mg^{2+} is larger than Ca^{2+} because Mg^{2+} is associated with multiple shells of ligated water molecules (Maguire & Cowan, 2002). In biological systems these metal ions never exist without water or ligand. Therefore ionic (Shannon) radii (Pauling, 1961) are inapplicable. The most common ligand coordination geometry is octahedral or tetrahedral (Harding, 1999) (Fig. 4). Mg^{2+} prefers to have six inner-sphere ligands arranged in an octahedral configuration, and so does Fe^{2+} (Harding, 1999). Ca^{2+} and Zn^{2+} can have octahedral coordination, but Zn^{2+} is frequently coordinated by four ligands in a tetrahedron (Christianson, 1991), and Ca^{2+} by seven, eight or even nine ligands (Pidcock & Moore, 2001). The number and length of ligand bonds of metal ions are empirically determined and vary within a very narrow range (Harding, 1999). Metal ion

coordination is far more sensitive to the ligand type and geometry than hydrogen bonds or salt bridges observed in macromolecules.

A variety of divalent cations have been found to be involved in enzymatic catalysis, e.g. Fe^{2+} in nonheme iron enzymes (oxygenases and demethylases) (Lange & Que, 1998), Zn^{2+} in deacetylases and proteases (Hernick & Fierke, 2005; Kim & Mobashery, 2001), Ni^{2+} in urease (Jabri et al., 1995), and the Mg^{2+} ion is most frequently associated with nucleic acid enzymes (Cowan, 2002). This frequent use of Mg^{2+} is perhaps because of its abundance, solubility, redox stability when compared with Mn^{2+}, Fe^{2+} and Cu^{2+}, its small size relative to Ca^{2+}, and its rigid coordination geometry compared to the transition metals Fe^{2+}, Cu^{2+}, Ni^{2+} and Zn^{2+} (Maguire & Cowan, 2002). The ligand bond of the Mg^{2+} ion is empirically determined to be 2.07Å (Harding, 1999). The coordination geometry of Mg^{2+} is far more stringent than hydrogen bonds. The unusual hydration property of Mg^{2+} ions may also be a factor for its catalytic role. Mg^{2+} ions exhibit extremely slow exchange rates of inner shell water molecules (Diebler et al., 1969; Maguire & Cowan, 2002) and often retain a couple of water ligands when coordinated by organic or macro molecules (Harding, 1999). It is energetically very costly to replace water ligands of Mg2+ with macromolecular ligands. The pKa value of a water molecule is reduced from 16.0 in free solution to 11.4 when associated with Mg^{2+} (Pontius et al., 1997).

5. Three major classes divided by metal-ion dependence

An overwhelming majority of nucleases of diverse function and structure belong to one of the three classes, requiring none, one or two metal ions for catalysis. Three Zn^{2+} ions have been found in the active site of two nucleases: nuclease P1 and *E. coli* Endo IV (Garcin et al., 2008; Ivanov et al., 2007; Romier et al., 1998). They are treated as a variation of the two-metal-ion mechaism in this review. The metal-independent RNases and DNases are grouped in different chapters because there is nothing in common.

5.1 Two-metal-ion catalysis

Two-metal-ion catalysis was first proposed after observing two metal ions in the active site of 3′ to 5′ exonuclease (DnaQ-like) active site of Klenow fragment and alkaline phosphatase (Beese & Steitz, 1991; Freemont et al., 1988; Kim & Wyckoff, 1991). It was further suggested to be a general mechanism for ribozymes catalyzing RNA splicing, which have no chemical groups that have pKa's near neutrality to serve as general base and acid for the phosphoryl transfer reaction (Steitz & Steitz, 1993). Over the years, the two-metal-ion mechanism has been proven to be utilized by all DNA and RNA polymerases (Steitz, 1998) and many nucleases including self-splicing ribozymes (Stahley & Strobel, 2005; Toor et al., 2008).

In all cases, the metal-ion dependent reaction products are 5′-phosphate and 3′-OH groups. The two metal ions (A and B) are ~ 4Å apart in the ground state and coordinated between a non-bridging oxygen of the scissile phosphate and an absolutely conserved Asp or a phosphate backbone in the case of ribozymes (Fig. 5a). The A metal ion is on the nucleophile side and the B on the 3′-O leaving-group side. Additional carboxylates or polar groups help to coordinate the metal ions and exclude water molecules from metal ion B.

Two-metal ion catalysis is fully compatible with the native double-helix structure and requires no phosphosugar distortion, base unstacking or flipping out. The advantages of incorporating two metal ions into catalysis are high substrate specificity and efficient product release (Yang et al., 2006). In addition, two symmetrically placed metal ion in the cut-and-paste recombinases and group I and II introns (ribozymes) allow multiple reactions to be catalyzed consecutively in one active site (Kennedy et al., 2000; Steitz & Steitz, 1993).

In most cases, Mg^{2+} is the choice for two-metal ion catalysis, and Ca^{2+} inhibits phosphoryl transfer (Yang et al., 2006). Some enzymes, e.g Mre11, require Mn^{2+} for in vitro nuclease activity (Hopfner et al., 2001; Paull & Gellert, 1998). Because of the stringent coordination geometry and charge requirements of Mg^{2+}, binding of two such metal ions is most often substrate dependent and highly selective. A number of crystal structures have captured metal ions in non-canonical configurations, which can be correlated with mutated meta-ion coordinated ligands and displacement of the scissile phosphate (Devos et al., 2007; Horton & Perona, 2004; Nowotny et al., 2007). In comparison, Mn^{2+} tends to relax substrate specificity and can rescue defective enzymes (Yang et al., 2006) and references therein). This “relaxing” and broadening of substrate specificity by Mn^{2+} is widely observed in metalloenzymes perhaps due to Mn^{2+} being a transitional element with less stringent coordination requirements than Mg^{2+}. Many enzymes are active in mixed metal ion experiments as long as a trace of Mg^{2+} or Mn^{2+} are present (Brautigam & Steitz, 1998; Pingoud et al., 2009). It has been shown that the A site can accept various metal ions but the B site is more selective for Mg^{2+} for catalysis (Brautigam et al., 1999).

Although metal ion A was proposed to drive the reaction by deprotonating the nucleophile, the similar pH profile of phosphoryl transfer reaction in the presence of Mg^{2+} or Mn^{2+} (Sam & Perona, 1999), which would result in different pKa’s of their ligands, is inconsistent with the metal ion being the general base and simply deprotonating the nucleophilic water. Hydrolytic reactions can occur without a general base, and catalytic rate may be reduced by 3 to 5 orders of magnitude (Mildvan et al., 2005). The current interpretation is that metal ion B is at least as important as metal ion A in two-metal ion catalysis. In addition to the proposed role of stabilizing the penta-covalent transition state, metal ion B appears to destabilize the ground state of a scissile phosphate for cleavage (Yang et al., 2006). Structural studies of an RNase H reaction intermediate and product indicate that the two metal ions likely move closer than 3.5Å and together stabilize the transition state (Nowotny & Yang, 2006).

5.2 One-metal-ion catalysis

An alternative to the two-metal-ion mechanism is one-metal-ion catalysis, in which metal ion B is retained and metal ion A is absent (Yang, 2008) (Fig. 5b). Two major classes of endonucleases are confirmed to use one-metal ion for catalysis: ββα-Me and HUH (Friedhoff et al., 1999; Koonin & Ilyina, 1993; Kuhlmann et al., 1999; Monzingo et al., 2007). Although sharing little tertiary structural similarity, both classes of nucleases use at least one His sidechain to coordinate the metal ion, and the reaction coordinates (arrangement of the metal ion, scissile phosphate and nucleophile) are nearly superimposable. Like the two-metal-ion mechanism, the active site configuration of ββα-Me

and HuH nucleases is compatible with the double-helix structure and produces 5′-phosphate and 3′-OH groups (Fig. 5b). The ββα-Me nucleases most often contain a His as a general base to deprotonate and activate a nucleophilic water, whereas the HUH nucleases invariably use Tyr as the nucleophile to cleave DNA substrates (Yang, 2008). Metal ion selection by one-metal-ion dependent nucleases is often less stringent, and substrate specificity is concomitantly less discriminating than for two-metal-ion enzymes (Yang, 2008). A number of the ββα-Me nucleases are equally capable of hydrolyzing RNA and DNA (sugar nonspecific) with little sequence specificity (Hsia et al., 2005). Sequence-specific DNases in the ββα-Me family, for example homing endonuclease I-PpoI and the type II restriction endonuclease KpnI, depend on additional DNA-binding domains to achieve their specificity (Sokolowska et al., 2009; Stoddard, 2005).

5.3 Metal-independent catalysis

Both RNases and DNases can be metal independent. To date, RNases that don't require metal ions all use a 2′-OH as the nucleophile to generate 2′,3′ cyclic phosphate intermediates. These enzymes therefore require phosphoribose distortion and base unstacking and unpairing surrounding a scissile phosphate for catalysis to proceed (Fig. 3b-c) (Buckle & Fersht, 1994; Calvin & Li, 2008; Cochrane & Strobel, 2008; Correll et al., 2004). The DNases that have been shown to cleave DNA without metal ions form phosphoenzyme covalent intermediates via Tyr, Ser or His sidechains (Champoux, 2001; Gottlin et al., 1998; Grindley et al., 2006; Sasnauskas et al., 2007). The active site and mechanisms for metal ion-independent cleavage by RNases and ribozymes in particular have been extensively characterized by X-ray crystallography (Cochrane & Strobel, 2008; Deshpande & Shankar, 2002; Raines, 1998; Xue et al., 2006; Yoshida, 2001). The mechanism for DNA cleavage without metal ions has also been revealed by combined biochemical analysis and atomic resolution structures (Grindley et al., 2006; Schoeffler & Berger, 2008; Stuckey & Dixon, 1999). Despite variations in structures and active site components, some common features emerge from metal-independent RNases and DNases. Water appears to be excluded from the active site, a 2′-OH of RNA or a protein sidechain serves as the nucleophile, and the highly negatively charged pentacovalent intermediate is neutralized by positively charged sidechains.

6. Two-metal-ion dependent nuclease Superfamilies

This is by far the largest class of nucleases. It includes protein enzymes and ribozymes, sequence specific and non-specific nucleases, endo and exonucleases with the 5′ to 3′ or 3′ to 5′ polarity, RNases and DNases. Based on the tertiary fold and catalytic motifs, they are divided into more than a dozen superfamilies and families as listed below.

6.1 DnaQ-like 3′ - 5′ exonucleases with the DEDD motif

DnaQ-like nucleases share the absolutely conserved sequence motif of DEDD and all carry out 3′ to 5′ exonucleolytic degradation of DNA or RNA. The topology of the catalytic core, after removing the non-conservative parts, is β1-β2-β3-αA-β4-αB-β5-αC, of which the five strands form a central mixed β-sheet (54123,↑↑↑↓↑) (Fig. 6a). The first two conserved carboxylates (DE) are one residue apart on the β1 strand, and the remaining two (DD) are

located on αB and αC on either side of the β-sheet. The two metal ions are coordinated between the first Asp of the DEDD motif and the pro-Sp non-bridging oxygen of the scissile phosphate. Each of the remaining three carboxylates coordinates one of the two metal ions. The nucleophilic water may be oriented and activated by the highly conserved Tyr or His 4 or 5 residues proceeding the last D of DEDD, which give rise to the name of DEDDy or DEDDh exonucleases. Interestingly, the difference in the sequence motif appears to result in little difference in function. For example, both DEDDy and DEDDh are found in the proofreading exonucleases (see below). Several members of this family form dimers (Fig. 6b) but with vastly different dimeric interfaces. Curiously, most dimeric 3′ exonucleases of the DnaQ superfamily have the DEDDh motif (see below).

6.1.1 DnaQ—DnaQ, also known as MutD or epsilon subunit of *E. coli* DNA polymerase III holoenzyme, encodes the 3′ to 5′ exonuclease (DEDDh) that performs proofreading in DNA replication (McHenry, 1985). The 3′ to 5′ exonuclease can exist as a domain of DNA polymerase or a separate polypeptide chain in the replisome. As a domain of the Klenow fragment, the 3′—5′ exonuclease (DEDDy) was one of the earliest crystal structures of nucleic acid enzymes determined (Ollis et al., 1985) and the structures of Klenow-oligonucleotide complexes led to the proposal of the two-metal ion mechanism (Beese & Steitz, 1991; Freemont et al., 1988). The structure of epsilon subunit is homologous to the 3′ to 5′ exonuclease domain of Klenow fragment, and only one metal ion was detected in the absence of ssDNA (Hamdan et al., 2002). The structure of Klenow fragment complexed with ssDNA substrate reveals the coordination of two metal ions (Fig. 6a). Although the substrate DNA is single stranded, its conformaiton is highly similar to a strand in a double helix (Brautigam & Steitz, 1998; Brautigam et al., 1999). These observations indicate that proper binding of two metal ions requires the presence of a cognate DNA substrate. The importance of the scissile phosphate in metal ion coordination is revealed by the sulfur substitution experiments. Replacement of the pro-Sp oxygen with sulfur essentially abolishes the metal-ion binding and the nuclease activity, and replacement of the 3′ bridging oxygen (leaving group) affects the metal ion binding, particularly in the B site, whereas replacement of pro-Rp oxygen moderately affects the metal ions, active site configuration and nuclease activity (Brautigam & Steitz, 1998; Brautigam et al., 1999).

6.1.2 *E. coli* ExoI and ExoX—The 3′ ExoI is the first deoxyribonuclease purified and characterized in *E. coli* (Lehman & Nussbaum, 1964). It specifically degrades single-stranded DNA from the 3′end and is implicated in various DNA repair pathways. The crystal structure of ExoI reveals a C-shaped monomer (PDB: 1FXX) (Breyer & Matthews, 2000). The DEDDh catalytic core is followed by a C-terminal SH3-like domain and surrounded by α-helices. The structure suggests a mechanism for processive digestion of ssDNA. *E. coli* ExoX is highly similar to ExoI in the catalytic domain and ssDNA preference. But, without the C-terminal domain, ExoX is about a half of ExoI in size (Viswanathan & Lovett, 1999). Homologues of *E. coli* ExoI and X are widely spread in bacteria.

6.1.3 TREX1 and TREX2—TREX1 and TREX2 are the major mammalian 3′—5′ exonucleases and also prefer single stranded DNA substrate. They can perform proofreading function for polymerases that lack an intrinsic 3′—5′ exonuclease activity (Shevelev et al.,

2002). Defective TREX1 (aka DNase III) causes Aicardi-Goutieres syndrome in humans, a severe neurological brain disease, and systemic lupus erythematosus probably due to abnormal innate immune responses to accumulation of intracellular nucleic acids (Crow et al., 2006a). Mice lacking TREX1 develop inflammatory myocarditis (Morita et al., 2004). It has recently been shown that TREX1 removes DNA of endogeneous retroelements to prevent induction of type I interferons and auto-immunnity (Stetson et al., 2008). TREX1 is also a part of SET complex and degrades DNA during granzyme A-mediated caspase-independent cell death (Chowdhury et al., 2006). Structures of TREX1 and TREX2 have been determined and are highly similar to that of DnaQ (PDB: 2OA8, 2IOC, 2O4I, 1Y97) (Brucet et al., 2007; de Silva et al., 2007; Perrino et al., 2005). TREX1 and TREX2 differ from DnaQ in being obligatory dimers, and the conserved residue in addition to DEDD in the active site is His rather than Tyr (Fig. 6b).

6.1.4 WRN exonuclease—Defective WRN protein is responsible for the Werner Syndrome, or premature aging (Muftuoglu et al., 2008). WRN contains both a DNA helicase and 3′—5′ exonuclease activity. The isolated WRN exonuclease domain is monomeric and can degrade the 3′-ends of dsDNA with a 5′ overhang (Perry et al., 2006a). The structure of the WRN exonuclease domain contains the DEDDy motif and is similar to other members of the DnaQ family. Two divalent ions were found in the active site in the presence of 50 mM metal ions even without DNA substrate (Perry et al., 2006a).

6.1.5 RNase T and Orn—Bacterial RNase T and Orn (oligoribonuclease) are homodimeric 3′—5′ exonucleases with the DEDDh motif. Both prefer ssRNA (Zuo et al., 2007) (PDB: 2F96, 2IS3, 1YTA, 2IGI, 2GBZ, 1J9A). RNase T is essential for 5S and 23S rRNA maturation and for processing of precursor tRNAs (Deutscher & Li, 2001). Orn can also hydrolyze DNA in the 3′—5′ direction (Fiedler et al., 2004). In the absence of Orn, *E. coli* cells grow slowly. Curiously the two active sites of the dimeric RNase T and Orn are on opposite surfaces.

6.1.6 RNase D and Rrp6—RNase D has the DEDDy motif and processes the 3′ end of structured RNAs (Zuo et al., 2005). It contains 2 HRDC nucleic acid binding domains in addition to the DnaQ-like catalytic domain. The circular substrate-binding tunnel suggests processsivity of RNase D (PDB: 1YT3). One Zn^{2+} ion is tightly bound in the active site, and the second Zn^{2+} ion has low occupancy (Zuo et al., 2005). The yeast homologue of RNase D, Rrp6p, is a component of the nuclear exosome for degradation of unstable mRNA transcripts and maturation of rRNA, snRNA and snoRNAs (for review, see (Houseley et al., 2006)). In the presence of 10 mM $MnCl_2$, two metal ions are also found in the active site of yeast Rrp6 (PDB: 2HBK) (Midtgaard et al., 2006).

6.1.7 PARN, Pan2 and Pop2—Poly A-specific ribonuclease (PARN) is a dimeric processive 3′exonuclease with the DEDDh motif. In addition to the DnaQ-like catalytic domain, PARN has RNA binding domains (PDB: 2A1S) (Wu et al., 2005). Related to PARN, Pop2 is a component of the Ccr4-NOT complex and functions in mRNA degradation. Pop2 likely participates in mRNA deadenylation both directly with its 3′- 5 ′exonuclease activity and indirectly by facilitating the Ccr4 nuclease activity (Parker &

Song, 2004). Curiously, although the DEDDh motif is replaced by SEDQt, yeast Pop2 (yPop2) still has the RNase activity (Thore et al., 2003). It is a puzzle whether the active site still uses two-metal-ion catalysis. Fission Yeast Pop2p, however, has the normal DEDDh motifs, and its structure has been determined at high resolution and two metal ions are found in the active site (Andersen et al., 2009; Jonstrup et al., 2007). Pan2 (poly-A nuclease), which is a component of the third 3′—5′ exoribonuclease complex for mRNA degradation and maturation, is also predicted to have a DnaQ-like exonuclease domain with the DEDDh motif.

6.1.8 ERI-1, 3′hExo and CRN-4 exonucleases—Eukaryotic ERI-1 (stands for exoribonuclease 1), human 3′-Exo (3′hExo) and *C. elegans* CRN-4 nucleaes share the conserved catalytic domain and the DEDDh motif. However, they are not functional orthologs perhaps owing to different additional structural domains. 3′hExo is responsible for histone mRNA degradation (Cheng & Patel, 2004), ERI-1 is implicated in 5.8S rRNA processing and production of small RNAs for RNA interference (Gabel & Ruvkun, 2008), whereas CRN-4 is implicated in apoptotic DNA degradation (Parrish & Xue, 2006). The crystal structure of the full-length *C. elegans* CRN-4 has been reported (Hsiao et al., 2009). It is a dimeric nuclease with the DEDDh motif and cleaves both RNA and DNA. A C-terminal Zn-domain is appended to the catalytic core and may influence CRN-4's preference to exonucleolytically degrade dsDNA over ssDNA.

6.2 RNase H-like endonucleases

The RNase H fold has the same topology as DnaQ and consists of a five-stranded mixed β-sheet (54123, ↑↑↑↓↑) surrounded by α-helices. However, the catalytic residues are different, and instead of exonucleases only endonucleolytic RNases and DNases are found in this superfamily. The catalytic residues are more varied in composition (Asp. Glu or His) and location than those in the DnaQ family. Only the first Asp in β1 is conserved in all members and likely coordinates both metal ions (Nowotny et al., 2005). The Asp located at the end of adjacent β4 is the second most conserved, but it is replaced by Glu in the Holliday junction resolvase RuvC and Ydc2 (Yang & Steitz, 1995b). This RNase H superfamily has been recently reviewed by M. Nowotny (Nowotny, 2009), and readers are referred to it for in-depth descriptions. The representative families and their characteristic are summarized below.

6.2.1 RNase H1—RNase H1 (also referred to as RNase H) is the founding member of this large eclectic superfamily of endonucleases. It is conserved from bacteria, retroviruses to humans and cleaves an RNA strand when it is hybridized to DNA. Cellular RNase H1 primarily degrades RNA primers in DNA replication and RNAs in random RNA-DNA hybrids (R loops)(Cerritelli & Crouch, 2009; Tadokoro & Kanaya, 2009). RNase H activity is essential for retroviral reverse transcription (Champoux & Schultz, 2009). Although not sequence specific, RNase H1 requires a minimum of four ribonucleotides forming RNA/DNA hybrid for cleavage to occur (Tadokoro & Kanaya, 2009). Substrate binding and specificity can be further strengthened by one or two RNA/DNA hybrid-binding domains (HBD) found in many cellular RNases H1 and by the DNA polymerase domain in retroviral reverse transcriptase (Champoux & Schultz, 2009; Nowotny et al., 2008).

RNase H catalysis by the two-metal-ion mechanism has been established in a series of enzyme-nucleic acid complexes along the reaction pathway by X-ray crystallography (Nowotny et al., 2005; Nowotny & Yang, 2006). Four carboxylates (D10, E48, D70 and D134 acoording to *E. coli* RNase H) form the catalytic core (Fig. 7a). The first and third carboxylates coordinate the two metal ions (Fig. 7b). The second carboxylate, Glu located on helix αA, is unique to RNases H1 and binds both the 2′-OH of RNA substrate and metal ion B, thereby enhancing the catalysis specificity (Nowotny et al., 2005). The fourth carboxylate coordinates metal ion A only. Although its replacement by Asn significantly reduces catalytic activity, it can be restored by substitution of Mn^{2+} for Mg^{2+} (Nowotny et al., 2005; Nowotny & Yang, 2006). In addition, the substrate actively participates in cleavage. The pro-Sp oxygen of the scissie phosphate coordinates both metal ions and, the pro-Rp oxygen of the 3′ neighboring phosphate participates in nucleophile formation (Haruki et al., 2000; Nowotny et al., 2005).

6.2.2 Transposase and retroviral integrase with the DDE motif—When the structure of HIV integrase and bacterial Mu transposase were determined, it was a surprise to find that these DNA endonucleases bear clear similarity to RNase H1 (Dyda et al., 1994; Rice & Mizuuchi, 1995). Sequence alignment predicts that many cellular and retroviral enzymes catalyzing cut-and-paste sequence-specific transposition/recombination have the RNase H fold and a DDE motif, which is approximately equivalent to the 1st, 3rd and 4th carboxylates of RNase H1 (Fig. 7a-c). They include the human RAG1 and RAG2 proteins essential for immunoglobulin gene rearrangement (Kim et al., 1999; Landree et al., 1999), and eukaryotic Mariner and Hermes transposases (Hickman et al., 2005; Richardson et al., 2009). Integrases and transposases are at least dimeric when associated with two donor-DNA ends and engaged in recombination. As revealed by the Tn5 transposase-DNA complex structures, the three carboxylates in these integrases and transposases are arranged symmetrically around the two metal ions (Davies et al., 2000; Steiniger-White et al., 2004). The first Asp coordinates both, and the remaining two coordinate one metal ion each (Fig. 7c). The recently reported structure of a retroviral integrase complexed with two donor DNA ends, which are nearly perpendicular to each other rather than antiparallel as in the case of Tn5, confirms the active site configuration (Hare et al.). The symmetry surrounding the two metal ions has implications for the DNA transposition reaction. These integrase and transposase often catalyze two or more consecutive phosphoryltransfer reactions and the 3′-OH product of the first cleavage reaction can be used as a nucleophile for the second strand transfer reaction (Kennedy et al., 2000). It has thus been proposed that the two metal ions switch their roles in coordinating the nucleophile and the leaving group in the two consecutive steps (Nowotny, 2009; Nowotny et al., 2005; Steitz & Steitz, 1993).

6.2.3 RNase H2—RNase H2 is the second cellular RNase H found from bacteria to humans (Cerritelli & Crouch, 2009). Eukaryotic RNase H2 consists of two auxiliary subunits, and all three subunits of human RNase H2 have been implicated in Aicardi-Goutieres syndrome, a heretable auto-immune disease caused by either TREX1 or RNase H2 deficiency due to accumulation of residual RNA and DNA (Crow et al., 2006b; Crow & Rehwinkel, 2009). RNase H2 differs from RNase H1 in that it can cleave a single ribonucleotide embedded in a DNA duplex. Crystal structures of bacterial RNase H2 reveal

an RNase H1-like structure with altered locations of catalytic carboxylates (Fig. 7d). Only the first and third of the four catalytic carboxylates are superimposable with those of RNase H1. The second carboxylate (E) is located immediately next to the first one (D) instead of 40 residues away. The reaction coordinate is yet to be determined.

6.2.4 Argonaute and PIWI—Argonautes (Ago) and PIWI are the key players in the RNA interference (RNAi) pathway and the RNase activity cleaves target mRNAs when it forms base pairs with guide RNAs (Joshua-Tor, 2006; Nowotny & Yang, 2009). But the catalytic residues are not always conserved, and some Ago and PIWI without catalytic activity function in RNAi pathways by binding complementary guide and target RNA duplexes (Farazi et al., 2008; Joshua-Tor, 2006). For those having the RNase activity, the three catalytic residues, either DDD or DDH, are approximately equivalent to the DDE in the integrase family and the 1st, 3rd and 4th carboxylates of RNase H1 (Joshua-Tor, 2006). The catalytic mechanism is revealed in a series of elegant crystallographic studies of Ago-dsRNA complexes (Wang et al., 2008; Wang et al., 2009). Similar to transposases, the first carboxylate coordinate the two metal ions and the remaining two coordinate one metal ion each (Fig. 7e).

6.2.5 RuvC and Ydc2—Bacterial RuvC and mitochondrial Cce1/Ydc2 are the Holliday Junction resolvases that have the RNase H fold (Ariyoshi et al., 1994; Ceschini et al., 2001; Iwasaki et al., 1991; West & Connolly, 1992; White & Lilley, 1997). These proteins are obligatory dimers (Bennett et al., 1993). The active site consists of four carboxylates, and the first two appear to be equivalent to the 1st, and 3rd carboxylates of RNase H1, but the carboxylate at the end of β4 is Glu instead of Asp (Fig. 7f). The last two carboxylates are located on the C-terminal α-helix two residues apart. Based on biochemical analyses, a protein-DNA complex model has been proposed (Fogg et al., 2001; Yoshikawa et al., 2001). How these carboxylates together with the DNA substrate coordinate the metal ions is yet to be elucidated.

6.2.6 UvrC (C-terminal domain)—UvrC is a bacterial endonuclease involved in nucleotide excision repair. It makes two incisions one on each side of a lesion (Verhoeven et al., 2000). UvrC has two nuclease domains in one polypeptide chain, one for each incision. The C-terminal domain of UvrC, which makes the incision 5′ to a lesion, is homologous to RNase H and shares two catalytic carboxylates with RNase H1 (1st and 3rd) (Karakas et al., 2007). But the third catalytic residue in UvrC may be a His that participates in single metal-ion coordination in the absence of DNA substrate (Fig. 7g). Interestingly, replacement of this conserved His with Ala only moderately reduces the enzymatic activity (Karakas et al., 2007). How the active site is formed upon substrate binding and whether the conserved Asp adjacent to the His is involved in catalysis awaits future analysis.

6.2.7 Structural roles and the ATPase catalytic core of Hsp70—The RNase H-like fold has been found in many proteins, where it plays a structural role, e.g. in T7 DNA polymerase and mismatch recognition protein MutS (Obmolova et al., 2000) and RNase E (Callaghan et al., 2005). Intriguingly it is found in pre-mRNA splicing protein Prp8 (Pena et al., 2008; Ritchie et al., 2008), where the first carboxylate is conserved and may play an

essential structural rather than catalytic role (Yang et al., 2008). Finally, two RNase H-like domains are found in actin and Hsp70 proteins and form the ATPase catalytic core (Flaherty et al., 1991). Most interestingly, a conserved Asp is found in the first β strand of each RNase H domain in Hsp70 (D10 and D199) just as in the nucleases of the RNase H superfamily and both are esential for cation binding (K^+ and Mg^{2+}) and the ATPase activity (Johnson & McKay, 1999) (Fig. 7h).

6.3 The major REase fold with the D-(D/E)XK motif

Many commonly used type II restriction endonucleases (REases) share the conserved motif PD-(D/E)XK, or shortened as DEK (Ban & Yang, 1998; Orlowski & Bujnicki, 2008). The three catalytic residues are located close to each other on an uneven β-hairpin (Fig. 8a). The first D is located at the beginning of the first and shorter strand, and the E and K, separated by a hydrophobic residue x, are located in the middle of the second and longer strand. The first D is most conserved and coordinates both metal ions, whereas the second E can be replaced by Q, D, N, H or S, and the third K can be replaced E, Q, D, S, N or T (Lee et al., 2005; Orlowski & Bujnicki, 2008). For instance, the third catalytic residue in BamHI is Glu (E113) rather than Lys (Fig. 8a). Members of this superfamily have very diverse primary sequence and thus different structures surrounding the catalytic core. They can be monomeric, dimeric or even tetrameric and are involved in diverse processes, from restriction digestion, DNA repair, homologous recombination to resolution of Holliday junctions. In addition to endonucleases, members in this superfamily can also be 5′ or 3′ exonucleases. Although not every member with crystal structure determined is shown to bind two metal ions, the two-metal ion mechanism is consistent with all biochemical and structural observations (Horton & Perona, 2004; Lee et al., 2005; Newman et al., 1998; Pingoud et al., 2005; Viadiu & Aggarwal, 1998; Viadiu & Aggarwal, 2000).

6.3.1 Restriction endonucleases (BamHI, HincII, MutH, EcoR124I and etc.)—

Nearly 70% REases belong to this superfamily (Orlowski & Bujnicki, 2008). Many REases in this family have a Pro immediately before the conserved Asp making the PD-EXK motif and a conserved N-terminal Glu, which contributes to the metal ion coordination as observed in EcoRV, BglI, BamHI, and MutH of type II REase family (Horton & Perona, 2004; Lee et al., 2005; Newman et al., 1998; Viadiu & Aggarwal, 1998; Winkler et al., 1993). These REases are most often dimeric (Bitinaite et al., 1998), but monomeric REase also exist (Lee et al., 2005; Sokolowska et al., 2007; Xu et al., 2005). By varying dimeric interfaces and thus the relative positions of the two catalytic centers, dimeric REases can cleave DNA to generate blunt ends or staggered ends with various 5′ or 3′ overhangs (Fig. 8b-c) (Ban & Yang, 1998; Newman et al., 1998). The catalytic module invariably approaches DNA from the minor groove side, and the sequence-specific binding is conducted by a separate module/subdomain in the major groove (Fig. 8d). The first two carboxylates of the DEK motif coordinate the metal ions. The third, which usually is hydrogen bonded with both the nucleophilic water and the DNA-binding module in the major groove (Fig. 8d), has been attributed to couple DNA sequence recognition with the cleavage reaction (Lee et al., 2005).

Type I and type III restriction/modification systems differ from type II in the requirement of nucleotide triphosphate and DNA translocation (Dryden et al., 2001; Murray, 2000), but

their endonucleases have a similar active site composed of D and EXK motifs (Niv et al., 2007). The crystal structure of EcoR124I of type I motor-endonuclease subunit shows that the conserved DEK motif indeed forms the catalytic center although the Pro before the first conserved D is absent (Lapkouski et al., 2009).

6.3.2 Phage λ and RecE 5´- 3´exonuclease—The active site of the PD-(D/E)XK motif is found among bacterial and phage 5´ - 3´ exonucleases, which act on dsDNA and produce a protruding 3´ ssDNA for strand annealing or invasion in homologous recombination (Kolodner et al., 1994; Stahl et al., 1997). RecE together with the ssDNA annealing protein RecT has been exploited for enhanced homologous recombination for in vivo gene manipulation (Muyrers et al., 2000; Zhang et al., 1998). Phage λ exonuclease (aka Red recombinase) and *E. coli* RecE are trimeric and tetrameric, respectively, and both form a toroidal structure, whose central hole is proposed to bind DNA for processive degradation (Kovall & Matthews, 1997; Zhang et al., 2009) (Fig. 8e). A conserved Glu precedes the DEK motif in Phage λ exonuclease (Fig. 8f). In RecE the DEK motif becomes DDK and it is preceeded by a conserved His (Fig. 8g). Whether the multiple active sites in these highly processive exonucleases work sequentially or stochastically are not known yet.

6.3.3 RecB and AdnAB ssDNA nuclease—The nuclease domains of the bacterial motor-nuclease machines RecBCD and AdnAB are closely related to RecE and REases (Singleton et al., 2004; Sinha et al., 2009). They have both exo- and endo-nuclease activity on ssDNA (Yu et al., 1998). Although RecB contains a single nuclease domain, it is one of the three subunits in the helicase/nuclease RecBCD complex. RecBCD forms a cylindrical molecule, and DNA threads through the central hole similar to the cases of RecE and phage λ exonuclease. But the DNA becomes unwound by the helicase activity carried by RecB and RecD of RecBCD or by AdnA and AdnB (Unciuleac & Shuman). The nucleases then nick the ssDNA and ultimately generate 3´ ssDNA overhangs for homologous recombination (Dillingham & Kowalczykowski, 2008; Sinha et al., 2009). Deviating from the canonical DEK motif, the Glu is replaced by Asp in RecB as in RecE. RecB doesn't have the Pro preceding the DDK motif. A conserved His N-terminal to the DDK likely participates in catalysis (Fig. 8h).

Dna2 ubiquitous in all eukaryotes has a helicase domain and a RecB-like nuclease domain containing the DEK motif (Budd et al., 2000). Dna2 works with ssDNA binding protein during DNA replication and removes excessively long primers (Kim et al., 2006; Masuda-Sasa et al., 2006).

6.3.4 HJ resolvase: T7 endonuclease I—Phage T7 endonculease I and archaeal Hjc are Holliday Junction (HJ) resolvases, whose active sites contain the REase-like (E)-PD-EXK motif (Lilley & White, 2001). These HJ resolvases are homodimeric and recognize four-way junctions in a distorted stacked-X form as shown in the crystal structures of enzyme-DNA complexes (PDB: 2PFJ and 2WJ0) (Hadden et al., 2007). Recognition and resolution of Holliday junctions are recently reviewed (Declais & Lilley, 2008). T7 endonuclease I cleaves DNA by the two-metal-ion mechanism with the two most conserved carboxylates coordinating two metal ions (Hadden et al., 2007) (Fig. 8i).

6.3.5 Structure-specific endonuclease: XPF, Hef, Rad1 and Mus81—The archaeal and eukaryotic structure-specific nucleases, Hef, Rad1, XPF and Mus81 all share the conserved nuclease domain, known as ERCC4 domain. The catalytic motif of D-ERK is homologous to that of REases (Chang et al., 2008; Newman et al., 2005; Nishino et al., 2003) (Fig. 8j). These nucleases are required for DNA repair, processing of a stalled replication fork, and repair-associated recombination (for in depth review, read (Ciccia et al., 2008)). In addition to the DEK motif, two cosnerved carboxylates, Asp and Glu, N-terminal to it are located in the active site (Fig. 8j). DNA substrates can vary from a 3′ flap, replication fork, to Holliday junction, all of which have the common feature of a 3′ flap, and cleavage occurs at the single- and double-strand junction. Although archaeal Hef nuclease is homodimeric, all eukaryotic nucleases in this family, for example Rad1, XPF and Mus81, form heterodimers (Rad1/Rad10, XPF/ERCC1 and Mus81/Eme1, Mus81/Eme2, or Mus81/Mms4) with only one active subunit. Interestingly, even with homodimeric nucleases it is likely that only one subunit is engaged in catalysis at a given time (Newman et al., 2005). Based on the conservation of the active site, two-metal ion catalysis is predicted.

6.3.6 DNA mismatch-repair endonuclease Vsr—*E. coli* Vsr (very short-patch repair) endonuclease specifically cleave 5′ to the T of mismatched T:G base pair, which results from deamination of 5-methyl-cytosine in a specific sequence (Hennecke et al., 1991). The crystal structures of Vsr complexed with DNA cleavage products reveal the REase fold in spite of the absence of the last two conserved catalytic residues of the DEK motif (Bunting et al., 2003; Tsutakawa et al., 1999). A conserved Glu preceding the central uneven β-hairpin and, two His residues C-terminal to it are in the catalytic center and may be involved in metal-ion coordination and nucleophile activation (Fig. 8k). In addition to the absolutely conserved Asp at the beginning of the uneven β-hairpin, a backbone carbonyl oxygen in the second β strand also contributes to the metal ion coordination in the Vsr-DNA cleavage product complex (Fig. 8k). The presence of two Mg^{2+} ions in the enzyme-product complex structure is highly suggestive of the two-metal ion mechanism as observed for the other members of this superfamily.

6.3.7 Rai1/Dom3Z for mRNA degradation and processing—Human Dom3Z and yeast Rai1 are the newest enzymes found to have the conserved REase fold and the (E)-D-EXK motif (Xiang et al., 2009) (Fig. 8l). Before the crystal structure of Rat1-Rai1 complex was determined, Rai1 was thought to activate the 5′ to 3′ exo-ribonuclease Rat1 in processing of RNAs (Xue et al., 2000). But the structure reveals a divalent cation-binding site in Rai1. The authors proceed to show that the Rai1 homologue Dom3Z binds GDP, possesses a pyrophosphatase activity and can remove pyrophosphate from a 5′ triphosphorylated RNA. However, the GDP in the crystal structure is too far from the (E)-D-EXK motif to be either a substrate or product (Fig. 8l). Whether Rai1 has nuclease activity is yet to be determined.

6.4 FEN1-like 5′ exo- and endo-nucleases

The nucleases in this family share a conserved βα Rossmann-like fold consisting of a central parallel five-stranded β sheet (in the order of 54123) surrounded by α-helices. The catalytic residues are located between the ends of the strands (β1, β2, β3 and β4) and beginning of

the following helices. They are almost exclusively Asp and Glu residues, and the number of conserved carboxylates ranges from five to eight, four of which may directly participate in phosphodiester bond cleavage (Fig. 9a). Although the crystal structures of *A. fulgidus* FEN1 and T4 RNase H were determined in complex with DNA (Chapados et al., 2004; Devos et al., 2007), the DNA is either far away from the active site (Fig. 9c) or approximately in the active site but with the scissile phosphpate displaced in the absence of metal ions (Fig. 9b). However, two divalent cations have been observed in several apo-FEN1 structures and biochemical analyses suggest that these nucleases use the two-metal ion mechanism like other nucleases containing an absolutely conserved Asp ((Liu et al., 2004; Tomlinson et al., 2010) and reference therein). Many members of this superfamily have dual 5′-exo and endo-nuclease activities.

6.4.1 5′ flap endonucleases: T4 RNase H, yeast Rad27 and human FEN1—The 5′ — 3′ exonuclease intrinsic to *E. coli* DNA Pol I is the founding member of the superfamily (Klett et al., 1968; Setlow & Kornberg, 1972), which includes Phage T4 RNase H, yeast Rad27 and human FEN1. The exonuclease is active on either RNA or DNA and its main function is to remove RNA primers in lagging strand synthesis (Bhagwat et al., 1997; Liu et al., 2004). These nucleases also contain the structure-specific endonuclease activity and can cleave the 5′ displaced ssDNA flap, such as the displaced primers in lagging strand DNA synthesis. The latter activity gives rise to the name of flap endonculease, FEN1 (Harrington & Lieber, 1994). In bacteriophages, archaea and mammals, the 5′ - 3′ exo and flap endonucleases can exist as an independent protein, for example, T4 RNase H (a mis-nomenclature (Bhagwat et al., 1997)). In fact, T4 RNase H has the same activities and structure as the 5′ - 3′ exonuclease of *E. coli* Pol I (Fig. 9a-b). To avoid the confusion, phage T4 RNase H has been renamed as T4FEN (Tomlinson et al., 2010). FEN activity is not only involved in DNA replication, but also in long-patch base excision and double-strand break repair (Shen et al., 2005).

To date, crystal structures of several apo-nucleases in this family and phage T4 and archaeal FEN in complex with DNA have been determined (Ceska et al., 1996; Chapados et al., 2004; Devos et al., 2007; Hwang et al., 1998; Kim et al., 1995). The catalytic center often contains 6–7 highly conserved Asp and Glu residues (Fig. 9a-c). The four most conserved carboxylates located after β1, β3 and β4 are reminiscent of the catalytic carboxylates in RNase H (Fig. 7a). The remaining negatively charged residues in the catalytic center is likely involved in binding of a third metal ion, which may contribute to the catalysis indirectly by coordinating substrate binding (Syson et al., 2008). However, in the absence of knowledge of the active site complete with scissile phosphate and metal ions, the reaction coordinates and chemistry for bond breakage remain uncertain.

6.4.2 XPG and HJ resolvases Gen1 and Yen1—XPG is required for nucleotide excision repair to incise at the 3′ side of a lesion (Habraken et al., 1993; O'Donovan et al., 1994; Scherly et al., 1993). Recently isolated eukaryotic Holliday junction resolvases Gen1 and Yen1 are also found to be homologous to XPG and FEN1 (Ip et al., 2008). Interestingly, like FEN1, human XPG and its yeast homolog Rad2 both exhibit 5′-exonuclease activity (Habraken et al., 1994). Although no crystal structure has been reported for these

endonucleases, the conserved active site residues and functional assay indicate that they all recognize a 5′ flap or branch structure and cleave DNA endonucleolytically at or adjacent to a branch point (including a ss-ds junction), likely by the two metal ion mechanism.

6.4.3 Human and yeast 5′ exonuclease 1 (Exo1)—It is perhaps not surprising to find that human and yeast 5′ exonuclease I, which are implicated in mismatch and double-strand break repair (Genschel et al., 2002; Szankasi & Smith, 1995), are homologous to FEN1 and XPG and share the same conserved active site. Like its homologues, Exo1 also has the flap endonuclease activity (Lee & Wilson, 1999; Tran et al., 2002). This FEN activity of ExoI is reported to be stimulated by Wrn protein (Sharma et al., 2003). Exo1 likely also uses the two-metal ion mechanism.

6.4.4 5′ exoribonuclease Rat1 (XRN2) and XRN1—Recently the structure of mouse Rat1 or XRN2, the 5′ exoribonuclease for RNA processing, has been reported (Xiang et al., 2009). Rat1 is highly similar to the structure of archaeal FEN1 with a large N-terminal loop wrapping around the protein and a helical tower (Fig. 9c-d). The highly conserved carboxylate-rich active site implicates a metal-ion-dependent mechanism of catalysis by these XRNs. It is unclear what makes them specific for RNA degradation and whether XRNs may have endonuclease activities if a proper substrate-binding partner is present. Eukaryotic XRN1, the major 5′—3′ exonuclease of RNAs, shares the conserved catalytic residues of XRN2 (Szankasi & Smith, 1996) and is predicted to have a FEN1-like structure and active site.

6.4.5 PIN domain RNA exonuclease—PIN (PilT N-terminal domain) nuclease is a recent addition to the FEN1 superfamily. It is a component of the exosome for RNA turnover and is also involved in non-sense mediated mRNA decay (Arcus et al., 2004; Clissold & Ponting, 2000; Eberle et al., 2009). Crystal structures of PIN nucleases reveal a stripped down minimal core of FEN1 (Glavan et al., 2006) (Fig. 9e). Like many members of this superfamily, PIN has both 5′-exo and endonucleolytic activities (Eberle et al., 2009; Schneider et al., 2009). Three Asp residues after β1, β3 and β4 are highly conserved among PIN nucleases as well as all FEN1 and XPG superfamily members. The fourth (two residues away from the third) can be Asp, Glu, Asn, or His (Arcus et al., 2004; Glavan et al., 2006). These four are superimposable with the core catalytic residues of all nucleases in the FEN1 superfamily (Fig. 9).

6.5 RecJ and DHH family

RecJ is a 5′—3′ single-strand exonuclease involved in DNA repair and recombination (Kowalczykowski et al., 1994). It contains the DHH motif as does the drosophila prune nuclease (Aravind & Koonin, 1998). Like the FEN1 superfamily, the nuclease core domain of RecJ consists of βα repeats with a central parallel β sheet surrounded by α helices. However, the order of β strands is 54312 in RecJ instead of 54123 as in FEN1 (Fig. 10a-b). The catalytically essential residues are located between the end of central three adjacent parallel β strands (β1, β3 and β4) and the beginning of the following α helices (Yamagata et al., 2002) (Fig. 10a). The consecutive DHH residues, which give rise to the name of this nuclease family (Aravind & Koonin, 1998), is located at the end of the 4th strand just like the

last two catalytically essential Asp residues in FEN1 (Fig. 9 and 10b). A Mn^{2+} is found in the active site coordinated by the two conserved His residues. In addition to the DHH, four conserved carboxylates are located in the active site and are likely involved in metal-ion binding and catalysis (Fig. 10b).

6.6 TOPRIM nucleases: RNase M5

TOPRIM is a metal-binding module found among TOpoisomerases (type IA and type II) as well as DnaG-like PRIMases (Aravind et al., 1998), giving rise to the name of this superfamily. In addition to the topoisomerases and primases, 5S rRNA maturases RNase M5 (Allemand et al., 2005), and bacterial ATP-dependent OLD-family nucleases also contain TOPRIM and are thus members of this superfamily (Aravind et al., 1998). The TOPRIM module has a Rossmann-like βα fold quite similar to the nuclease core domain of RecJ. It consists of a central parallel four-stranded β sheet in the order of 4312 surrounded by α helices (Fig. 10c-d). TOPRIM is also marked by two conserved sequence motifs, E and DXD at the end of 1^{st} and 3^{rd} β strand, respectively, which are proposed to coordinate divalent cations. Not all TOPRIM domains are involved in phosphoryl transfer reactions. RecR, which is an essential component of RecFOR for recombination, has the TOPRIM structure but is devoid of the metal-binding motifs and nuclease activity (Lee et al., 2004).

Bacterial RNase M5 cleaves precursors of 5S rRNA endonucleolytically in the double stranded region and produces the mature form in the context of ribosome (Condon et al., 2001). The cleavage products are 5′-phosphate and 3′-OH. The crystal structure of RNase M5 has been determined (PDB:1T6T) by the Midwest Structure Genomic group (Fig. 10c). In addition to the conserved E and DXD common to the TOPRIM, RNase M5 also contains an additional conserved Asp located 3 residues after the first E (Fig. 10d). These four carboxylates are conserved in the catalytic center of primases (Keck et al., 2000). All DNA and RNA polymerases known to date use the two-metal ion mechanism (Steitz, 1998; Yang et al., 2006). Consistant with the two-metal-ion mechanism, three partially occupied metal ion sites are found in the active site of *E. coli* primase in the absence of nucleic acid substrate (Keck et al., 2000). Even though RNase M5 is a nuclease and catalyzes the reverse reaction of polymerization, its close relationship to primase and its similarities to RecJ and FEN1 suggest that RNase M5 and related OLD nucleases probably catalyze DNA and RNA cleavage by the two-metal ion mechanism.

Interestingly, the fourth carboxylate is absent in the topoisomerases containing the TOPRIM module. The missing carboxylate and usage of a Tyr as the nucleophile may lead DNA cleavage by topoisomerases to depend on a single metal ion for catalysis (see section 7.3).

6.7 DNase I-like endo and 3′ exo-nucleases

Pancreatic DNase I is among the first nucleases discovered and characterized (Hoard & Goad, 1968; Kunitz, 1950; Suck et al., 1984). This family of nucleases now encompasses DNases and possibly RNases, and their functions vary greatly from DNA digestion, base excision repair, to RNA processing (Table 1). Most of the members in this superfamily are endonucleases, but 3′—5′ exonuclease activity of APE1 has also been reported and is essential for the DNA repair functions (Castillo-Acosta et al., 2009; Chen et al., 1991). The

catalytic core of the DNase I superfamily is a four-layered αββα structure (Fig. 11a-b). The two mixed β sheets in the center share a similar but permutated folding topology (Suck et al., 1984), and the tertiary structures are related by a pseudodyad axis roughly parallel to the β strands (Mol et al., 1995). The active site is composed of conserved Asp, Glu and His residues located at the end of the central β sheets (Fig. 11a).

6.7.1 DNase I—DNase I is most prevalent in mammals and is also found in bacteria, but not in low eukaryotes or plants. DNase I functions in apoptosis and has been implicated in the autoimmune disease SLE (systemic lupus erythematosus) (Martinez Valle et al., 2008). The crystal structure of bovine pancreatic DNase I - DNA complex was determined nearly 20 years ago (Weston et al., 1992). In the crystal structures of DNase I without DNA, two Ca^{2+} ions were observed at a distance from the active site and thought to play structural and substrate binding roles (Chen & Liao, 2006). DNase I is most active in the presence of mixed Ca^{2+} and Mg^{2+} (Pan & Lazarus, 1999). All the catalytic residues (four Asp and Glu, two His and one Asn) are located at the end of the central 4 β strands (↓↑↑↓) of both β sheets (Fig. 11a-c). Two conserved His residues surrounding the scissile phosphate have been shown to be important for the general acid-and-base catalysis, and the His mutations can be rescued by imidazole (Chen et al., 2007a). The scissile phosphate is distorted, and both pro-Rp and pro-Sp oxygens interact with DNase I (Fig. 11c, 5c). Although divalent cation is chelated away by 20 mM EDTA and thus absent in the crystal structure of enzyme-substrate complexes (Weston et al., 1992), the requirement of two Asp residues (D168 and D212) and Mg^{2+} for DNA cleavage suggests that metal ions are likely essential for catalysis (Jones et al., 1996).

6.7.2 AP endonuclease Exo III and APE1—Exonuclease III (Exo III), which is the major Apurinic/Apyrimidinic endonuclease in *E. coli*, and its eukaryotic homologue APE1, share the conserved tertiary structure and active site with DNase I (Gorman et al., 1997; Mol et al., 1995). These nucleases cleave the phosphodiester bond 5′ to an abasic (apurinic/apyrimidinic) site endonucleolytically and also cleave exonucleolytically to remove a 3’-dRP (dRP = phosphoglycolate, phosphate, or α,β-unsaturated aldehyde) (Demple & Harrison, 1994). Crystal structures of Exo III and APE1 alone (Gorman et al., 1997; Mol et al., 1995), and APE1 complexed with an abasic DNA substrate without divalent cation and complexed with metal ion and cleavage product have been determined (Mol et al., 2000). The active site is highly similar to that of DNase I, except for the replacement of the H134 and E78 by Y171 on the 3′ leaving group side (Fig. 11c-d). Two Asp and the C-terminal His surrounding the scissile phosphate are superimposable between DNase I and APE1.

In the APE1-DNA complex structure, the abasic nucleotide is flipped out of the DNA double helix. Concomitantly the backbone phosphate turns as well and the pro-Sp non-bridging oxygen points inwards instead of outwards (Fig. 11d). The distortion of the scissile phosphate is identical to that in the DNase I complex, where the pro-Sp oxygen rotates towards the minor groove (Fig. 11c-d). In RNase H and many other two-metal-ion dependent nucleases, the pro-Sp oxygen coordinates both metal ions (Fig. 5). Here the pro-Sp oxygen is stabilized by the C-terminal His in APE1 and DNase I. Instead, it is likely the pro-Rp oxygen that coordinates two metal ions for the nucleophilic attack (see additional

discussion in section 6.16). Consistent with this prediction, sulfur replacement of pro-Sp or pro-Rp oxygen of the scissile phosphate eliminates endonucleolytic cleavage by Exo III (Takeuchi et al., 1994).

6.7.3 RNase E and G—RNase E is an endoribonuclease participating in degradation of messanger and regulatory RNAs and processing of tRNA, rRNA and tmRNA precursors (Worrall & Luisi, 2007). In bacteria it often functions in a multienzyme assembly known as the RNA degradosome, which contains RNA helicase, enolase and exoribonuclease PNPase. RNase G and RNase E are paralogs and share the conserved active site. RNase E forms a homotetramer with D2 symmetry (Callaghan et al., 2003). Each active site is composite and composed of two polypeptide chains, each of which contributes a two-layered αβ structure (Fig. 11e) (Callaghan et al., 2005). The catalytic domain of a single RNase E subunit (one αβ structure) is similar to a half of DNase I (Fig. 11f). The dyad axis that relates the two RNase E subunits that form a composite active site, however, is approximately perpendicular to the β sheet instead of parallel to it as in DNase I structure (Fig. 11a, e). Dimerization of RNase E actually results in a cluster of conserved carboxylates on either end of the β sheets and thus two active sites instead of one as in DNase I (Callaghan et al., 2005). The catalytic residues of the RNase E and their arrangment bear similarity to DnaQ and RNase H (Fig. 6–7). The mechanism for RNase E catalysis is likely two-metal-ion dependent with details yet to be revealed.

6.8 β-CASP nucleases with the metallo-β-lactamase fold

The β-CASP nucleases are named after representative members (CPSF-73, Artemis, Snm1 and Pso2) adopting the metalllo-β-lactmase fold (Aravind, 1999; Callebaut et al., 2002; Daiyasu et al., 2001; Dominski, 2007), which is a four-layer αββα structure with a pseudodyad axis relating the two halves. Metallo-β-lactamase hydrolyzes β-lactams in a group of powerful antibiotics that inhibit bacterial cell wall biogenesis (Wang et al., 1999), whereas β-CASP nucleases hydrolyze the phosphodiester bond in RNA or DNA. The nuclease activity can be either endo or 5′ exo. The β-lactamase fold is reminiscent of the DNase I fold (Callebaut et al., 2002) (Fig. 12a), but each β sheet contains 7 strands instead of 6 and the strand polarities (↓↑↓↑↑↑↑) are different from those in DNase I and APE1 (↑↓↑↑↓↑). The catalytic residues are at one end of the β sheets (Fig. 12a), which is again reminiscent of DNase I and APE1. The β-lactamase family enzymes are unique in their tight binding of two Zn^{2+} ions independent of substrate. The many His residues in the catalytic center may contribute to the selectivity for Zn^{2+} (Baldwin et al., 1979).

6.8.1 RNase Z for tRNA maturation—RNase Z is an endonuclease that processes the 3′ end of tRNA precursors (pre-tRNA) and is also known as the 3′ tRNase. It is widely spread from bacteria, archaea to eukaryotes (Schiffer et al., 2002). RNase Z cleaves 3′ to the discriminator base, which is the last in the acceptor stem and primes the CCA addition. If CCA is already present, RNase Z can cleave after CCA, but cleavage before CCA is severely inhibited thereby avoiding futile cycles of CCA addition (Minagawa et al., 2004). The crystal structure of RNase Z (de la Sierra-Gallay et al., 2005; Ishii et al., 2005; Kostelecky et al., 2006) confirms the sequence-based prediction of its resemblance to β lactamase (Schiffer et al., 2002) and the two Zn^{2+}-based catalytic mechanism (Minagawa et al., 2004).

Five conserved His and two conserved Asp residues are involved in metal ion coordination (Fig. 12b).

6.8.2 CPSF-73 and RNase J1—Mammalian CPSF-73 (Cleavage and Polyadenylation Specificity Factor) was predicted to have the metallo-β-lactamase fold and endonculease activity (Aravind, 1999). Mutagenesis of the yeast CPSF-73 homolog, Ysh1p, confirms the predicted catalytic nuclease activity and its in vivo function (Ryan et al., 2004). CPSF-73 has both an endo and 5′-exo nuclease activity and is essential for processing the 3′ end of mRNA precursors (Chanfreau et al., 1996; Jenny et al., 1996; Marzluff et al., 2008; Yang et al., 2009). Crystal structures of the human CPSF-73 (Mandel et al., 2006) show that the catalytic domain is essentially identical to RNase Z. Like RNase Z, two Zn^{2+} ions are coordinated by five His and two Asp residues.

B. subtilis RNase J1 is a 5′ exonuclease and functions in pre-rRNA maturation and mRNA decay (Bechhofer, 2009; Mathy et al., 2007). RNase J1 also has the metallo-β-lactamase fold and shares the conserved catalytic residues of CPSF-73.

6.8.3 Artemis, Snm1 and Pso2—Artemis, which is required to open DNA hairpins in V(D)J recombination, also belongs to the metallo-β-lactamase nuclease family (Moshous et al., 2001). Mutations in Artemis are linked to defective V(D)J recombination and immune deficiency SCID. Like CPSF-73, Artemis has both endonuclease and 5′ exonuclease activities. In addition, the DNA crosslink repair nucleases Snm1 and Pso2 have similar nuclease domains (Callebaut et al., 2002; Dominski, 2007). These related RNase and DNases share an additional conserved structural domain, called the β-CASP domain, which is inserted near the C-terminus of the nuclease domain (Mandel et al., 2006). Although crystal structures of Artemis, Snm1 and Pso2 are not yet determined, based on the sequence homology these nucleases are likely to bind two Zn^{2+} ions in the active site and catalyze DNA cleavage by the two-metal-ion mechanism.

6.9 Mre11 and protein phosphatase 2B fold

Mre11 is an essential component of Mre11-Rad50-Nbs1 complex (MRN), which detects double-strand breaks (DSBs) and promotes repair (Mimitou & Symington, 2009). Similar to APE1, Mre11 has both the 3′ to 5′ exonuclease activity and endonuclease activity (Paull & Gellert, 1998; Paull & Gellert, 1999). Structurally Mre11 is homologous to protein phosphatases 1, 2A and 2B, for example, calcinurin A (Griffith et al., 1995; Hopfner et al., 2001; Reiter et al., 2002) (Fig. 12c-f). Like the Ser/Thr phosphatases, Mre11 binds two Mn^{2+} tightly in its active site even in the absence of a DNA substrate (Hopfner et al., 2001).

The crystal structures of archaeal Mre11 alone and in complex with DNA reveal a homodimer with the tertiary structure and active sites not unlike that of β-CASP nucleases (Hopfner et al., 2001; Williams et al., 2008) (Fig. 12). The core of each β sheet is composed of 6 strands with the polarity of (↑↓↑↑↑↑), and the active site consists of multiple conserved His residues in addition to conserved carboxylates. The two manganese ions in the active site are also reminiscent of the Zn^{2+} ions in the β-CASP nucleases. Although the DNA in the co-crystal structure is located outside of the active site, structural and mutagenic analyses indicate that one conserved His residue specifically orients DNA substrate for the

exonuclease cleavage and the second His residue is involved in either metal ion binding or catalysis directly (Williams et al., 2008).

The similarities in the tertiary structure, active site composition, and tight binding of metal ions in addition to the shared exo- and endo-nuclease activities among Mre11 and the β-CASP family Snm1 and Pso2 may explain why their functions partially overlap (Lam et al., 2008). The high degree of homology between Mre11 and the Ser/Thr phosphatases (Voegtli et al., 2000) (Fig. 12c-f) raises the possibility that Mre11 may function as a phosphatase in addition to being a nuclease during DSB repair.

6.10 LAGLIDADG homing endonucleases

Homing endonucleases are encoded by introns or inteins and recognize long DNA sequences for specific cleavage (for a comprehensive review see (Stoddard, 2005)). They are found in single cell organisms, fungal and protozoan mitochondria and chroloplasts and cleave dsDNA to enhance the mobility of introns and inteins, to which they belong. LAGLIDADG is one of four families of homing endonucleases, which is named after the conserved sequence motif. Despite the name, the sequence motif has many variations including the last D (Asp) that is critical for coordinating the metal ions (Spiegel et al., 2006). The LAGLIDADG motif can occur once per subunit if a homing endonuclease is a homodimer, for example, I-CeuI (Spiegel et al., 2006) (Fig. 13a). Alternatively, an internal sequence duplication allows monomeric LAGLIDADG nucleases to function as a pseudodimer, for example, I-SceI (Duan et al., 1997; Moure et al., 2008) (Fig. 13b). The two active sites of a LAGLIDADG nuclease are fused together. Each contributes a conserved Asp and the two together coordinate three Mg^{2+} ions, which form two pairs. Each Mg^{2+} pair forms the catalytic center to cleave one DNA strand (Stoddard, 2005) (Fig. 13c). Yeast mating type switch endonuclease (HO) is also a member of this family (Jin et al., 1997).

6.11 RNase II and Rrp44

Bacterial RNase II and its eukaryotic homolog Rrp44 (also called Dis3 and the catalytic subunit of exosome) are 3′ exoribonucleases for ssRNA processing and degradation (Andrade et al., 2009; Lykke-Andersen et al., 2009). RNase R is a paralog of RNase II capable of degrading dsRNA. The active site of this conserved RNase family is composed of four closely spaced Asp residues situated on the loop (inner end) of an uneven β-hairpin structure (Fig. 14). The β-hairpin structure is reminiscent of the active site of the REases, but the DEK motif of the REase family is located at the outer end of the uneven β hairpin (Fig. 8). The active site of RNase II is invariably embedded near the end of a narrow channel, which may prevent RNA substrate from dissociation and promote processivity (Frazao et al., 2006; Lorentzen et al., 2008; Zuo et al., 2006) (Fig. 14a). A divalent metal ion is observed in the active site of RNase II and Rrp44 complexed with a ssRNA substrate (Fig. 14b). Its position is close to the leaving group (3′-OH) and thus similar to the metal ion B. RNA cleavage by RNase II is most likely by the two-metal-ion mechanism. The absence of the second metal ion in the crystal structures may be due to the mutations of Asp to Asn, a metal ion ligand (Frazao et al., 2006; Lorentzen et al., 2008) (Fig. 14b).

6.12 RNase III and Dicer

Bacterial RNase III and eukaryotic Dicer and Drosha are homologous dsRNA endonucleases, and Dicer and Drosha generate guide RNAs in the processes of RNA interference (Ji, 2008; MacRae & Doudna, 2007; Nowotny, 2009). These enzymes are either homodimers or pseudodimeric monomers that have two active sites for dsRNA cleavage. Crystal structures of a bacterial RNase III and eukaryotic dicer have been determined (Gan et al., 2006; MacRae & Doudna, 2007). The active sites are situated such that they cleave dsRNA symmetrically and produce a 2-nt 3′ overhang on each cleaved end (Fig. 15a-b). Each active site is composed of two Asp and Glu pairs located on two closely placed α-helices, one pair of carboxylates a piece (Fig. 15c). RNase III has a dsRNA-binding domain C-terminal to the catalytic domain (Fig. 15a) to facilitate substrate binding and sequence-nonspecific cleavage. Eukaryotic dicers generate dsRNA of defined length, often ~ 20 bp in length. This is because they contain additional dsRNA and 3′ end binding domains to confer the length and structure specificity (MacRae et al., 2007; MacRae et al., 2006). Kinetic analysis of RNase III clearly shows that two closely placed metal ions are required for the catalysis of cleavage (Sun et al., 2005). The crystal structures of RNase III complexed with dsRNA substrate and product provide atomic details of the binding of two metal ions and a catalytic mechanism similar to that of RNase H (Fig. 15c) (Gan et al., 2008; Gan et al., 2006).

6.13 RNase PH, PNPase and exosome

Bacterial RNase PH is a 3′ phosphorolytic exoribonuclease that carries out RNA processing and degradation (Deutscher & Li, 2001) (Fig. 2f). It uses inorganic phosphate as the nucleophile and releases nucleotide diphosphate as cleavage products. Its functional form is a hexameric ring formed as a trimer of dimers (Fig. 16a). Bacterial polynucleotide phosphorylase (PNPase) is a paralog of RNase PH and turns over mRNA and processes tRNA by phosphorolysis. PNPases are ring-shaped homo-trimers. Each subunit containing two RNase PH domains, but only one such domain is catalytically active. Archaeal exosomes are homologous to PNPases and contain six RNase PH-like chains, three Rrp41 and three Rrp42 (Buttner et al., 2005; Lorentzen et al., 2005). Only Rrp41 subunits have the catalytic activity. Interestingly in eukaryotic exosomes, RNase PH homologues form the hexameric ring-shaped structure as well, but have no catalytic activity for RNA degradation (Dziembowski et al., 2007; Liu et al., 2006).

A single RNase PH domain is a four-layered βαβα structure, (Fig. 16b). The active site, composed of both basic residues and carboxylates, is located at one end of the βαβ sandwich. Two such domains tightly associate to form a dimer, and ssRNA substrate is bound at the dimer interface. A Cl^- ion in the co-crystal structure of archaeal exosome-ssRNA complex is suggested to mimic the phosphate for nucleophilic attack (Fig. 16c). The locations of two conserved carboxylates resemble many two-metal-ion dependent nucleases. However, a metal ion is found outside of the active site of the archeal exosome and shown to play a structural role (Lorentzen et al., 2007). Although a catalytic metal-ion binding site is not evident in the crystal structures, it was reported that the phosphorolytic activity of RNase PH and PNPase is Mg^{2+} dependent (Deutscher et al., 1988; Gorchakova, 1981). Whether

and how many Mg^{2+} ions are needed for phosphorolysis by RNase PH and PNPase are yet to be determined.

6.14 RusA

RusA is a Holliday junction resolvase encoded by a defective prophage in *E. coli*, and its homologues are found in many bacteria (Sharples et al., 1994). RusA is a homodimer in solution and each active site appears to be composite and consists of two Asp from one subunit and a third Asp from the second subunit (Fig. 17) (Macmaster et al., 2006). DNA-junction cleavage by RusA is Mg^{2+} dependent (Sharples et al., 1994), and the carboxylate-rich active site is suggestive of the two-metal ion mechanism. The crystal structures of RusA alone and RusA-DNA duplex complex have been determined. However, the required Mg^{2+} has not been located (Macmaster et al., 2006; Rafferty et al., 2003). One possible reason for the absence of metal ions is that the DNA co-crystallized with RusA is a duplex rather than a four-way junction and hence not a true substrate. The other possible reason is that a RusA mutant D70N was used in DNA co-crystallization and the mutation likely reduces Mg^{2+} binding (Fig. 17b).

6.15 Ribozymes

To date, two types of ribozymes are confirmed to cleave RNA in a metal-ion-dependent manner. They are self-splicing group I and group II introns (Kruger et al., 1982; Peebles et al., 1986) and the universal tRNA 5′-processing RNase P (Guerrier-Takada et al., 1983; Kirsebom, 2007). These metal-ion dependent ribozyme nucleases generate 5′-phosphate and 3′-OH cleavage products. In fact, the two-metal-ion mechanism was first proposed to explain how group I and II introns catalyze RNA cleavage (Steitz & Steitz, 1993).

6.15.1 Group I intron—Self-splicing Group I introns catalyze two consecutive phosphoryl transfer reactions (Fig. 18a) and are the best characterized example of two Mg^{2+}-dependent ribozymes (Stahley & Strobel, 2006). The nucleophile in the first step (cleavage reaction of the 5′ exon-intron juction) is the 3′-OH of a free guanosine (or GMP, GTP); which becomes covalently linked to the 5′-end of the intron. In the second step, the 3′-OH of the cleaved exon (product of the first cleavage reaction) serves as the nucleophile and attacks the 3′ intron-exon junction to produce the ligated exons and a free intron (Vicens & Cech, 2006) (Fig. 18a). Cleavage substrates, the intron-exon junctions, are structured and the bases surrounding each scissile phosphate are paired and stacked in a double helix (Fig. 18b) (Adams et al., 2004). Two divalent cations are coordinated between a non-bridging oxygen (pro-Sp) of the scissile phosphate and a backbone phosphate of the ribozyme, which acts exactly like the most conserved Asp in the active site of many two-metal ion dependent protein enzymes (Yang et al., 2006). The two metal ions likely switch their roles of activating nucleophiles in the consecutive reaction steps, similar to DNA transposition by retroviral integrase and bacterial transposases (section 6.2.2, Fig. 7c) (Nowotny et al., 2005; Steitz & Steitz, 1993).

6.15.2 Group II intron—Group II introns also catalyze their own excision and function in retro-transposition in addition (Aizawa et al., 2003; Peebles et al., 1986). The splicing reaction consists of two steps like Group I introns, but Group II introns use the 2′-OH of an

internal Ade to initiate self-splicing (Doudna & Cech, 2002). The intron is excised in a lariat form of a 2′−5′ cyclic diester bond (Fig. 18c), which is similar to mRNA splicing by spliceosomes in eukaryotes (Michel et al., 2009). The crystal structure of the product form of a Group II intron was recently determined, and two metal ions are found in the catalytic center (Toor et al., 2008) (Fig. 18d). A two-metal ion dependent catalysis mechanism similar to that of Group I introns has been postulated for self-splicing group II introns and spliceosomes in general for mRNA splicing (Toor et al., 2009).

6.15.3 RNase P—RNase P is one of the first ribozymes identified and the universally conserved nuclease that endonucleolytically cleaves pre-tRNA to generate the mature 5′ end (Guerrier-Takada et al., 1983). In addition to the catalytic RNA subunit, RNase P also includes a variable number of protein subunits (Kirsebom, 2007). Crystal structures of two types of bacterial RNase P have been determined (Torres-Larios et al., 2006). These structures reveal a conserved architecture of the catalytic core. But, in the absence of an RNase P-tRNA ribozyme-substrate complex, details of the active site are uncertain. The catalytic mechanism is likely to be similar to that of Group I introns in spite of the uncertainty of which ribonucleotide coordinates the Mg^{2+} ions.

6.16 Three-Zn^{2+}-dependent nucleases

Three metal ions, more specifically three Zn^{2+}, have been found in the active site of two structurally unrelated endonucleases: AP endonculease IV (Endo IV) and nuclease P1/S1 (Garcin et al., 2008; Romier et al., 1998). Both result in 5′ phosphate and 3′ hydroxyl cleavage products. Nuclease P1 cleaves ssDNA. Although Endo IV cleaves dsDNA endonucleolytically or as a 3′ exonuclease (Demple & Harrison, 1994), the nucleotide carrying the scissile phosphate (apurine or apyrimidine) is not base paired and thereby effectively single-stranded with large backbone distortions. The crystal structures of Endo IV complexed with DNA substrate and product reveal that one Zn^{2+} is located in the minor groove of the unpaired scissile phosphate and two remaining Zn^{2+} are coordinated similarly to the two metal ions in RNase H1 and DnaQ (Fig. 19, 6 and 7) (Garcin et al., 2008). Therefore, two out of the three metal ions are likely involved in catalysis. This is reminiscent of the case of three metal ions in alkaline phosphatase with two participating in actual catalysis and the third for alignment of the nucleophile relative to the scissile phosphate (Coleman, 1992; Kim & Wyckoff, 1991; Stec et al., 2000; Steitz & Steitz, 1993; Zalatan et al., 2008).

6.16.1 *E. coli* Endo IV (AP endonuclease)—Endo IV is the class II and minor AP endonuclease in *E. coli* (second to Exo III, see section 6.7.2) and is known for its EDTA-resistant activity (Demple & Harrison, 1994). Its yeast homologue is known as Apn1. Endo IV has the TIM-barrel fold, and the active site is located at one end of the β barrel, where the three Zn^{2+} ions bind (Fig. 19a). The crystal structures of the enzyme complexed with substrate and product were also determined at high resolutions (Garcin et al., 2008) (Fig. 19b). Two out of three metal ions, Zn2 and Zn3, are reminiscent of the metal ions A and B, respectively, in the two-metal ion mechanism (Fig. 19c). However, instead of the pro-Sp non-bridging oxygen of the scissile phosphate jointly coordinating these two metal ions, the scissile phosphate in the Endo IV complex turns towards the minor groove and the pro-Rp

oxygen coordinates Zn2 and Zn3. This is very similar to the cases of DNase I and APE1 (Fig. 11c-d). In Endo IV Zn1 (instead of a His as in APE1 and DNase I) stabilizes the pro-Sp oxygen and facilitates the distortion of the scissile phosphate (Fig. 19c).

In Endo IV the Zn3 metal ion is coordinated by both the pro-Rp and the 3′ leaving oxygens just like the B site ion in the two-metal ion mechanism (Fig. 5a, c). Mutational studies also confirm that coordination of Zn3 is more sensitive to amino acid substitution than the other two metal ion-binding sites and that the Zn3 metal ion plays a more important role in catalysis (Garcin et al., 2008). Moreover, for Endo IV to be active the Zn3 site also has a strong preference for Mn^{2+} over Zn^{2+} (Demple & Harrison, 1994; Garcin et al., 2008). Supporting the crystallographic observation, sulfur replacement of the pro-Sp oxygens at the scissile phosphate reduces the Endo IV cleavage activity, but sulfur substitution of the pro-Rp oxygen eliminates the nuclease activity (Takeuchi et al., 1994). Five His and four carboxylates contribute to tight binding of the three metal ions (Fig. 19c), which may explain why Endo IV is EDTA resistant. E261, which coordinates the Zn2 ion (equivalent to metal ion A), is suggested to be essential for nucleophile activation and cleavage (Garcin et al., 2008).

6.16.2 Nuclease P1 and S1—Nuclease P1 and S1 are single-strand specific nucleases that degrade DNA or RNA either endonucleotically or as a 3′ exonuclease (Desai & Shankar, 2003). P1 nuclease is all α helical and resembles bacterial phospholipase C (Hough et al., 1989; Romier et al., 1998) (Fig. 19d). Although P1 nuclease and Endo IV are unrelated in amino acid sequence or tertiary structure, they both use carboxylates and histidines to bind 3 Zn^{2+} ions tightly even in the absence of substrate (Fig. 19). In P1 nuclease, two Zn^{2+} ions are jointly coordinated by two conserved Asp (Fig. 19e). Similar to Endo IV, the pro-Rp rather than the pro-Sp non-bridging oxygen of the scissile phosphate is intolerant of thio-replacement (Romier et al., 1998). Although a P1-substrate complex structure is not available, the sulfur replacement experiment is in agreement with the metal ion coordination observed in Endo IV. It is likely that the pro-Rp oxygen of the scissile phosphate together with the two conserved Asp residues coordinates the two catalytic metal ions.

6.17 Nucleases that may use two metal ions for catalysis

6.17.1 Staphylococcal nuclease—Staphylococcal nuclease (SNase) is a Ca^{2+} dependent extracellular phosphodiesterase that cleaves single-stranded RNA and DNA to 3′ phosphomono and dinucleotides (Tucker et al., 1978). The enzyme contains two antiparallel β sheets and three α helices (Fig. 20a). The active site is composed of four carboxylates at the end of the large β sheet. High-resolution crystal structures of its complex with nucleotide analog/inhibitor pdTp and with Ca^{2+} or with Co^{2+} (inhibitor) reveal a single but mobile metal ion (Loll et al., 1995). In light of the lack of a confirmed general base, the metal ion is postulated to deprotonate and activate the nucleophilic water (Hale et al., 1993; Loll et al., 1995). In the absence of an enzyme-substrate complex, the catalytic mechanism remains undefined. It is possible that SNase uses a single metal ion as observed in the crystal structure, or the two-metal-ion mechanism given the carboxylate-rich active site, or even three metal ions similar to Endo IV and DNase P1/S1 because SNase prefers ssDNA and

ssRNA. Since the cleavage product of SNase is 3′-phosphate, which is radically different from all the confirmed two-metal-ion dependent nucleases, it is likely that it has a different catalytic mechanism.

6.17.2 Cas1—CRISPR (clustered regularly interspaced short palindromic repeats) is a bacterial and archaeal adaptive immune system to resist phage infection (Sorek et al., 2008). Phage DNA is cleaved to short oligonucleotides and incorporated into host CRISPR between repetitive DNA sequences and, the transcription products are used for target degradation if the same phage infection is encountered again. Cas1 and Cas2 are CRISPR-associated proteins essential for CRISPR (Brouns et al., 2008). Cas1 is the universally conserved protein in CRISPRs and is a dimeric metal-dependent DNA endonuclease. The crystal structure reveals a novel fold and a bound Mn^{2+} in the absence of DNA substrate (Wiedenheft et al., 2009). The structure contains a helical catalytic domain (Fig. 20c) and an αβ dimerization domain. The helical structure of the Cas1 catalytic domain is reminiscent of DNase P1/S1. With the active site composed of EHDD residues and at least one conserved Asp indispensable for the nuclease activity (Wiedenheft et al., 2009), it is possible that DNA cleavage by Cas1 is by the two-metal ion mechanism.

6.17.3 Cas2—Cas2 is ferredoxin-like and metal-dependent single-strand endoribonuclease (Beloglazova et al., 2008). It is dimeric, prefers U-rich regions and produces 3′ -OH and 5′-phosphate oligonucleotides. Given its metal ion dependence and requirement for a conserved Asp residue, a two-metal-ion dependent catalysis mechanism has been proposed. Interestingly, in the crystal structure of Cas2 protein, the catalytically essential Asp (D10) is situated at the dimeric interface and two symmetry-related Asp residues are 6.5Å apart (Beloglazova et al., 2008). These two Asp sidechains may belong to a single active site (Fig. 20d).

7. One-metal-ion dependent nuclease Superfamilies

The one-metal-ion mechanism can be viewed as a variation on the two-metal-ion theme as the location and function of the single metal ion is equivalent to the B-site metal ion in the two-metal-ion mechanism (Yang, 2008) (Fig. 5b). The role of this single metal ion appears to be destabilizing the scissile phosphodiester bond and neutralizing the highly negatively charged transition state. A large variety of endonucleases belonging to the ββα-Me and HUH superfamilies, (see detailed description below) have been unequivocally shown to cleave DNA or RNA using the one-metal-ion mechanism. The A metal ion in the two-metal-ion mechanism appears to be replaced by positively charged protein sidechains. Dependence on the metal ion to activate the nucleophie is alleviated by using His as the general base, or using Tyr as a nucleophile, which is more readily deprotonated than a water molecule at the neutral pH. All nucleases using the one-metal-ion mechanism generate 5′ phosphate and 3′ OH products.

7.1 The ββα-Me superfamily

All nucleases in this superfamily share the conserved structural motif, a β hairpin followed by an α helix (Fig. 21a). Within the consecutive ββα structures, an invariable His at the end

of the first β strand serves as the general base to deprotonate and activate the nucleophilic water molecule (Fig. 21). Additional conserved His (H) and Asn (N) in the active site are most often involved in coordinating the single metal ion (Me). Nucleases in the ββα-Me family have very diverse functions. The HNH and His-Cys homing endonucleases, DNases involved in cell death, many non-sequence and non-sugar specific nucleases, colicin E nucleases, certain restriction endonucleases, and a Holliday junction resolvase, all belong to this superfamily (Hsia et al., 2005; Stoddard, 2005). Not surprisingly, the overall structures and DNA binding modes are as varied as the functions. A number of nucleases have large helical insertions between the β and β elements. Nevertheless, the catalytic core structure and the metal ion-binding sites are superimposable.

7.1.1 HNH and His-Cys homing endonucleases—Although HNH and His-Cys were initially classified into two separate families of homing endonucleases based on conserved sequence motifs, close scrutiny of amino acid sequences has led to the proposal that they derived from a common ancestor and share the same ββα-Me catalytic core (Friedhoff et al., 1999; Kuhlmann et al., 1999). The HNH motif is involved in the catalytic metal coordination, whereas the His-Cys motif coordinates additional metal ions to stabilize the tertiary structure (Fig. 21a) (Stoddard, 2005). The catalytic metal ion can be Mg^{2+}, Zn^{2+}, Ca^{2+} or other divalent cations, which are often coordinated by His, Asn and Asp (Fig. 21b). Most noticeably, the ββα-Me motif is nearly a stand-alone domain and separate from the DNA sequence-specific binding domains (Fig. 21a). In the His-Cys homing endonuclease I-PpoI, two structural metal ions (Zn) tie the DNA-binding and ββα-Me catalytic domains together in each subunit (Flick et al., 1998).

7.1.2 HJ resolvase: Phage T4 endonuclease VII—T4 endo VII is the only Holliday junction resolvase that contains the ββα-Me motif for catalysis. It forms a homodimer and recognizes an H-shaped four-way junction (Biertümpfel et al., 2007) (Fig. 21c-d). The two strands that make a U-turn (aka exchanged strands) in the four-way junction are cleaved. Mg^{2+} is the preferred metal ion for DNA cleavage. Like His-Cys homing endonuclease, a Zn^{2+} is also tightly bound by each T4 endo VII subunit and stabilizes the tertiary structure. Relative to T7 endonuclease I, which has the REase-type active site and uses the two-metal-ion mechanism, T4 endo VII is not as specific for four-way junctions and can cleave 3-way junctions and mismatched DNA heteroduplexes, all of which are characterized by distorted double-helix structures (Jensch & Kemper, 1986; Solaro et al., 1993).

7.1.3 Type II restriction endonucleases—Several Type II restriction endonucleases also contain the ββα-Me motif for DNA cleavage. They include HphI (Cymerman et al., 2006), Eco311 (Jakubauskas et al., 2007), KpnI (Chatterjee et al., 1991; Vasu et al., 2008), and Hpy99I (Sokolowska et al., 2009). The active site of these sequence-specific endonucleases contains the conserved DH and N residues just like T4 endo VII (Fig. 21d-e). Additional DNA-binding domains in these restriction enzymes target cleavage to a specific sequence. The crystal structure of Hpy99I complexed with its cognate DNA substrate reveals an interlocked homodimer, which bears remarkable similarity to T4 endo VII (Fig. 21c, e). In addition to the catalytic motifs approaching the cognate DNA from the minor groove side, Hpy99I embraces the DNA with sequence-specific binding in the major groove. Different

from I-PpoI (Fig. 21a), the catalytic motifs, DNA binding modules and the dimeric interface in Hpy99I are rolled into one. Concommitantly, the recognition sequence of Hpy99I is much shorter (5 bp) than I-PpoI (14 bp) and the cleavage sites border the major-groove recognition rather than being at a distance as with I-PpoI (Fig. 21 a, e).

7.1.4 Sugar-nonspecific endonucleases—Sugar-nonspecific nucleases degrade single- or double-stranded DNA and RNA in a sequence-independent manner (Friedhoff et al., 1996). Members of this family have very diverse functions and can take part in bacterial defense, invasion, nutrient scavenging, and eukaryotic programmed cell death. Periplasmic Vvn (Hsia et al., 2005) defends host cells by degrading foreign nucleic acids. The secreted serratia and cyanobacterium NucA (Muro-Pastor et al., 1992) nucleases may be regulated depending on growth phases (Chen et al., 1992). The other secreted nucleases, colicins E7 and E9 (Hsia et al., 2005), kill non-self target cells and thereby enhance the chance of host cell survival under stress. Eukaryotic mitochondrial endonuclease G also belongs to this family and is a key enzyme in cell death (Buttner et al., 2007). These nonspecific nucleases are very efficient and non-discriminative in nucleic acid degradation. Host cells often have specific inhibitors, known as immunity proteins, to avoid self-destruction.

7.1.4.1 Serratia, NucA and Endo G: The Serratia family of nucleases includes bacteria nucleases (NucA) and eukaryotic mitochondrial endonuclease G (Endo G), which is also known as Nuc1p in yeast. The nuclease from *Serratia marcescens* encoded by the nucA gene is the first example described in the family (Benedik & Strych, 1998). Its possible role is scavenging for nutrients. Other bacterial NucA may act as virulence factors in invasion or establishment of a colony. Bacterial hosts, which secrete the nuclease, often have an inhibitor to protect themselves. In eukaryotes, mitochondrial Endo G may play a role in mitochondrial DNA metabolism. Endo G, however, can migrate to the nucleus and function in Caspase-independent cell death (Buttner et al., 2007).

These nucleases are structurally very similar. The catalytic ββα motif forms a structural subdomain and is packed against one face of a 6-stranded antiparallel β sheet (Fig. 21g). The active site is marked by a conserved sequence motif RG immediately preceding the general base H in the first β strand of the ββα motif (Ghosh et al., 2007b). They usually prefer Mg^{2+} for catalysis, and the metal ion is coordinated by the conserved N and E on the α helix. The catalytic metal ion may be directly chelated by an immunity protein and prevented from substrate binding (Ghosh et al., 2007b).

7.1.4.2 Vvn and periplasmic nucleases: Vvn (from *Vibrio vulnificus*) represents the bacterial periplasmic endonuclease I family and likely serves a defensive role against uptake of foreign DNA (Wu et al., 2001). Its tertiary structure is unique and has long helical insertions between the β strand of the ββa-Me motif, but the active site is conserved (Hsia et al., 2005) (Fig. 21h). Homologous proteins are found in bacteria only, which include endonuclease I from *Vibrio cholerae* and *Vibrio Salmonicida* (Altermark et al., 2006; Niiranen et al., 2008). The residues for Mg^{2+} coordination are (W)EH and N(GDRG)N within the ββα-Me motif.

7.1.4.3 Colicins E7 and E9: Colicins are toxins produced by *E. coli* and other enterobacteriaceae to kill unprotected competitive organisms as part of the SOS response. Colicins E2, E7, E8 and E9 are E-group toxins containing the ββα-Me motif, which kills by the highly efficient and non-specific DNase activity (James et al., 1996). *E. coli* and host cells protect themselves by immunity proteins, which bind and inhibit the DNases (Kolade et al., 2002). Crystal structures of colicins E7 and E9 in complex with DNA substrate and their respective immunity protein have been determined (Kleanthous et al., 1999; Ko et al., 1999; Mate & Kleanthous, 2004; Wang et al., 2007). The active site of Colicins E7 and E9 consists of four conserved His. Three appear to coordinate a single matal ion, for which Mg^{2+} and Zn^{2+} are preferred (Mate & Kleanthous, 2004; Wang et al., 2007). The remaining His (the second in sequence and also most conserved) functions as the general base to deprotonate and activate the nucleophile water (Wang et al., 2007) (H545Q in Fig. 21i).

7.1.4.4 Cell death and caspase-activated nuclease (CAD): Caspase-activated DNase (CAD), also known as DFF40 (DNA fragmentation factor 40kDa), is responsible for degradation of genomic DNA in apoptosis when its specific inhibitor ICAD (or DFF45) is removed (Enari et al., 1998; Liu et al., 1997; Widlak & Garrard, 2005). The crystal structure of the CAD reveals a Zn^{2+}-dependent dimer shaped like a pair of scissors (Woo et al., 2004) (Fig. 21j). The active site consists of the ββα-Me motif and is very similar to the nuclease domain of colicin E7 and E9. CAD requires Mg^{2+} for the DNase activity (Widlak, 2000). The putative Mg^{2+} in the active site is coordinated by two His and one Asp (Fig. 21i).

7.2 GIY-YIG endonucleases

GIY-YIG endonucleases are named after their conserved sequence motifs first found among homing endonucleases (Paquin et al., 1995; Van Roey et al., 2002). The family also includes the DNA repair endonculease UvrC (the N-terminal domain), phage T4 EndoII and type II restriction endonucleases (Kaminska et al., 2008; Lagerback et al., 2009; Orlowski & Bujnicki, 2008; Truglio et al., 2005). Recognition of a specific sequence or DNA lesion is usually accomplished by DNA-binding modules outside of the nuclease core (Stoddard, 2005). To date no nuclease-substrate complex structure has been determined for the GIY-YIG nucleases. The structures of the conserved GIY-YIG catalytic core of a homing endonculease I-TevI and UvrC have been reported (Truglio et al., 2005; Van Roey et al., 2002). The catalytic core consists of a three-stranded anti-parallel β sheet, which is surrounded by helices on either side (Fig. 22a). The active site is composed of two Tyr residues of the GIY-YIG motif. The GIY-YIG motif is located on a β-hairpin structure, which is followed by an α helix (Fig. 22b). Thus, the structure of GIY-YIG motif is reminiscent of the ββα module. However, the active site is composed of residues (Arg, His or Tyr, Glu and Asn) outside of the GIY-YIG motif (Fic. 22a, c). A divalent metal ion is found in the UvrC-N structure and is bound to the conserved Glu (Fig. 22c). The catalysis is metal ion dependent and likely by the one-metal-ion mechanism.

7.3 The HUH superfamily

HUH, which stands for His, hydrophobic residue and His, is the motif shared among endonucleolytic DNases involved in rolling-circle replication. Initiation of rolling-circle replication (RCR) of circular DNA requires a free 3′-OH generated by an endonculease.

HUH endonucleases were initially divided to two families, “rep” indicating the association with DNA replication and “mob” indicating the association with DNA mobility via conjugation or transposition (Koonin & Ilyina, 1993). Recently, the HUH motif has been found in ssDNA transposases of the ISHp608 family (Ton-Hoang et al., 2005). The two conserved His residues are involved in the metal ion (most often Mg^{2+}) binding. All HUH endonucleases use a Tyr as the nucleophile to catalyze the DNA cleavage and ligation reactions via a 5′-phosphotyrosyl covalent intermediate. DNA cleavage by these nucleases is necessarily rejoined and the phosphotyrosyl bond reverts to a phosphodiester bond after DNA replication or rearrangement. This process of cleavage-religation is similar to the process of topoisomerization and site-specific recombination.

7.3.1 Rep nucleases—Members of the rep family are found in ss and dsDNA bacterial phages, plasmids, plant geminiviruses and animal parvoviruses, such as Adeno-associated virus (Aav) (Hickman et al., 2002). By forming 5′-phosphotyrosyl linkage, these nucleases generate a free 3′-OH to initiate DNA synthesis. In addition to the HUH motif for metal-ion coordination, this superfamily also contains the YxxxY motif with two conserved Tyr residues. The crystal structure of Aav5 Rep reveals a nuclease core consisting of a five-stranded antiparallel β sheet and a number of surrounding α helices (Hickman et al., 2004) (Fig. 23a). Most catalytic residues including HUH are located on a pair of adjacent central β strands, and the nucleophile Tyr is on a nearby α helix (Fig. 23a). As predicted, a Mg^{2+} is coordinated by the two absolutely conserved His and a conserved Glu (Fig 23a). The catalytic mechanism has not been verified by a crystal structure of enzyme-substrate, but the nuclease alone structure resembles that of mob nucleases (see below) and hence the catalysis is likely by the one-metal-ion mechanism.

7.3.2 Mob nucleases (TraI and TrwC)—Mobility of bacterial integrative conjugative elements (ICEs, including conjugative F plasmids and integrative transposons) and ssDNA phage (φx174) depends on DNA nicking by mob nucleases, which are also known as relaxases (Khan, 2005; Llosa et al., 2002). Even though some mob nucleases recognize ssDNA and make a single stranded nick, the DNA substrate is actually folded into a base paired hairpin structure and the scissile phosphate bond is embedded in the double helix. TraI encoded by *E. coli* F plasmid and TrwC by R388 conjugation plasmid are characterized by two consecutive Tyr residues near the very N-terminus in addition to the HUH motif (Gomis-Ruth & Coll, 2006; Larkin et al., 2007). The first Tyr serves as the nucleophile. Because the cleavage-ligation reactions catalyzed by these nucleases relax supercoiled DNA, they are called relaxases, very much like topoisomerases (Fekete & Frost, 2000). In the crystal structure of TraI, the nucleophile Tyr is mutated to Phe and the relaxase is co-crytallized with its specific DNA substrate (Fig. 23b) (Datta et al., 2003; Larkin et al., 2005). Several positively charged Lys and Arg sidechains facilitate substrate DNA binding. The catalytically essential Mg^{2+} is coordinated by the scissile phosphate, the two absolutely conserved His, and a third His only conserved within the mob family (Fig. 23c). The active site is superimposable with the metal ion center in colicin E7 (Yang, 2008), indicating the conserved metal-ion function and catalytic mechanism.

7.3.3 TnpA DNA transposase of IS200/IS605 family—Nucleases with the HUH motif are also involved in DNA transposition of IS elements (Ton-Hoang et al., 2005). They differ from rep and mob nucleases by possessing only one instead of two conserved Tyr residues besides the HUH motif. These small and dimeric nucleases (less than 200 aa) are represented by the IS200/IS605 family of DNA transposases (Tnp). The ssDNA transposase (TnpA) from transposon ISHp608 is the best-studied example. TnpA recognizes specific ssDNA sequence and utilizes it for substrate recognition by forming basepaired duplex structures for cleavage (Barabas et al., 2008). The tertiary structure and catalytic mechanims of TnpA is reminiscent of TraI and TrwC relaxases (Fig. 23) but the nucleophile Tyr is permutated to be near the C-terminus. Each active site is composite with two metal-chelating His residues from one subunit and the nucleophile Tyr from the second subunit by domain swapping (Fig. 23d-e). A third metal ion ligand, Gln, is located near the Tyr and supplied in trans as well. Interestingly, the domain swapping and subsequent active site formation, are entirely dependent on the DNA substrate binding, which induces a gross conformational change (Barabas et al., 2008).

8. TOPRIM topoisomerase and Ser recombinase: Partial metal ion dependence

TOPRIM topoisomerases and Ser recombinases both cleave DNA by forming 5′ phospho-protein covalent bonds (via Tyr and Ser, respectively) and, after topological change or rearrangement of DNA they catalyze DNA religation and restore phosphodiester bonds (Grindley et al., 2006; Schoeffler & Berger, 2008). In both cases, the strand cleavage step may be metal ion independent but is stimulated by Mg^{2+} ion, whereas the religation step is metal ion dependent (Bhat et al., 2009; Domanico & Tse-Dinh, 1991; Reed, 1981; Zhu & Tse-Dinh, 2000). When complexed with either a type II topoisomerase or Ser recombinase for the cleavage reaction, the DNA substrate is severely bent around the scissile phosphate, suggesting that distortion and stretching of phosphodiester bonds may facilitate the bond breakage. The number, location and mechanism of metal ions involved in the topoisomerization and recombination are still unclear.

8.1 TOPRIM topoisomerases

Type IA, IIA and IIB topoisomerases are members of the TOPRIM superfamily, an established metal-ion-binding module (Aravind et al., 1998). Three conserved carboxylates are found in every member of the TOPRIM family. Two differences divide nucleases containing a TOPRIM domain. The OLD nucleases and RNase M5 (like primases) have an additional carboxylate in the first sequence motif (EGxxD or EGxxE) (see section 6.6), whereas in topoisomerases it is a Lys instead (EK or ESxxK). Secondly, the topoisomerases use a Tyr instead of a water molecule as the nucleophile for DNA cleavage and form a phosphotyrosyl covalent intermediate. These differences may divide the TOPRIM nucleases and topoisomerases into families that use different numbers of metal ions for the DNA cleavage reaction. Spo11 nucleases, which introduce double-strand breaks to initiate meiotic DNA recombination, are highly homologous to Type IIB topoisomerases and likewise have three instead of four conserved carboxylates (Keeney, 2001). Mutation of the carboxylates in the TOPRIM domain abolishes the nuclease activity of Spo11 (Diaz et al., 2002). The

cleavage products of TOPRIM topoisomerases and Spo11 are 5′-phosphate and 3′-OH as for the other TOPRIM nucleases.

8.1.1 Type II topoisomerases—Type II topoisomerases are divided to distinct IIA and IIB families, both of which cleave dsDNA (Wang, 2002). It is uncertain how Mg^{2+} influences the strand cleavage reaction because Type II topoisomerases are also Mg^{2+}-dependent ATPases and Mg^{2+} cannot be omitted from the reaction. These enzymes are dimeric or hetero-tetrameric. Each active site is composite and consists of the nucleophile Tyr on the WHD domain of one subunit and carboxylates on the TOPRIM domain of another subunit (Schoeffler & Berger, 2008). A single Mg^{2+} coordinated by the conserved E and DxD motifs of TOPRIM was first found in the crystal structure of an archaeal type IIB topoisomerase in the absence of DNA substrate (Nichols et al., 1999). A Mg^{2+} ion was later found in the active site of yeast Topo II co-crystallized with a nicked DNA substrate (Dong & Berger, 2007) (Fig. 24a).

The location of this metal ion is close to the leaving group and is reminiscent of the B metal ion in RNase H1 and the single metal ion in TraI (Fig. 7 and 23). The absence of the second metal ion (equivalent to metal ion A on the nucleophile side) is not a proof of a one-metal-ion mechanism because the second metal ion may have escaped detection due to a crystallographic artefact. The arrangement of the Tyr and the metal ion relative to the DNA substrate in Topo II is rather similar to the mob nucleases, suggesting that the one-metal ion mechanism may be applicable here. The absence of the fourth carboxylate and the presence of the Arg adjacent to the nucleophile Tyr to stabilize the scissile phosphate (Fig. 24a) also lend support to the one-metal-ion mechanism.

8.1.2 Type IA topoisomerases—Type IA topoisomerases are monomeric and nick one strand of DNA (Schoeffler & Berger, 2008). In addition, unlike type II topoisomerases, type IA enzymes are ATP-independent and relax negative supercoils only. Interestingly, the ssDNA co-crystallized with *E. coli* Topo III (type IA) adopts the double-helix-like conformation (Changela et al., 2001) (Fig. 24b). Similar to Topo II, the active site of monomeric Type IA is assembled between two domains and composed of ExxK and DxD from the TOPRIM domain (aka domain I) and the nucleophile Tyr from domain III (equivalent to the WHD of Topo II) (Fg. 24b-c). It was controversial as to whether metal ion is required for Topo IA. It is now clear that efficient DNA cleavage in addition to the religation by type IA topoisomerases requires Mg^{2+}(Domanico & Tse-Dinh, 1991). In support of the metal-ion requirement, amino-acid substitutions of the conserved carboxylates in TOPRIM render the mutant topoisomerases defective in DNA supercoil relaxation (Bhat et al., 2009; Zhu & Tse-Dinh, 2000).

The crystal structure of a type IA topoisomerase (Topo III) with the nucleophile Tyr replaced by Phe and in complex with ssDNA substrate provides the highest-resolution view of the active site of TOPRIM topoisomerases (Changela et al., 2001). Relative to the scissile phosphate, the carboxylates and the Tyr of Topo III occupy positions similar to those in Topo II. In addition to the Arg next to the Tyr, a Lys conserved in type IA stabilizes the scissile phosphate (Fig. 24c). But due to the high salt concentration in the crystallization buffer (1.3M $(NH_4)_2SO_4$), soaking in 10 mM $MgCl_2$ was not successful in detecting metal ion

binding (Changela et al., 2001). Superposition of the catalytic residues of *E. coli* Topo III and yeast Topo II show that the metal ion observed in the Topo II falls right between the conserved carboxylates and scissile phosphate in Topo III (Fig. 24d).

The striking similarities of metal ion coordination and nucleophilic attack of the scissile phosphate between TOPRIM topoisomerases and HUH nucleases TraI and TnpA imply a similar catalytic mechanism. The nuclease activity of Topo IA in the absence of Mg^{2+} may be explained by the conserved Lys and Arg in the active site, which can neutralize the developing negative charge on the scissile phosphate (Fig. 24c). A divalent cation on the leaving group side may not be necessary but, in the strand ligation step, the metal ion is on the 3′-OH nucleophile side and may become essential for its deprotonation. It is most likely that type II and type IA topoisomerases with so much in common use the same metal-ion dependent cleavage mechanisms.

The M5 and OLD family nucleases and type IA and type II topoisomerases of the TOPRIM superfamily share the conserved TOPRIM domain yet may use a two- versus one-metal-ion dependent mechanism for DNA cleavage. The divergence appears to originate from different nucleophiles and different environments surrounding the respective scissile phosphate in their cleavage reactions. They may represent an early divergence from a primordial sequence motif and structural domain.

8.2 Ser recombinases

The Ser-recombinase family consists of a large number of bacterial and archaeal resolvases/invertases, transposases and DNA partitioning enzymes, which use the conserved Ser as a nucleophile to cleave and ligate DNA by forming a 5′-phosphoserine covalent intermdiate (Grindley et al., 2006). A pair of long DNA recognition sites is required for DNA recombination, and DNA rearrangement takes place between the steps of cleavage and re-ligation of both sites. Although Ser recombinases are usually compared with DNA recombinases rather than topoisomerases, they can relax negative supercoils like topoisomerases if cleavage of four strands (two duplexes) are incomplete and recombination of DNA is prevented (Falvey et al., 1988).

Ser recombinases are bi-lobal and contain an N-terminal catalytic domain and a C-terminal sequence-specific DNA-binding domain (Yang & Steitz, 1995a) (Fig. 25a). Dimerization is mandatory for binding to a pseudo-palindromic recognition site and for double strand cleavage (Salvo & Grindley, 1988). In order for recombination between two specific sites to take place, Ser recombinases have to form a synaptic dimer of dimers (Fig. 25a-b). After cleavage of both recombination sites, protein and DNA undergo dramatic conformational changes (Li et al., 2005). Unlike the Tyr recombinases (see section 9.2.2), the recombination intermediate of Ser recombinases is not a Holliday junction. The DNA rearrangement catalyzed by a Ser recombinase is rather similar to the topological change catalyzed by type II topoisomerases (Fig. 2d) except for that two dsDNA cleavages are required reather than one.

The catalytic domain of Ser recombinases is composed of ~120 N-terminal residues, which form a mixed five-stranded central β sheet (54312, ↓↑↑↑↑) surrounded by α helices (Fig.

25c). The nucleophile Ser is at the end of the 1st β strand. A number of conserved basic residues are essential for DNA cleavage and religation. The catalytic domain of γδ resolvase was first suggested to be similar to T5-FEN because they share the first four parallel strands (Artymiuk et al., 1997). But γδ resolvase appears even more similar to RecJ than FEN (Fig. 25 c-d). Structural superposition of RecJ and resolvase reveals an uncanny similarity and sheds light on catalytic mechanisms of both nucleases. The Ser nucleophile of resolvase overlays with the two conserved carboxylates in RecJ, which are likely to coordinate a metal ion (A site) in the presence of the DNA substrate for the two-metal-ion dependent hydrolysis. The metal ion observed in the RecJ structure, which is coordinated by two His residues of the DHH motif, overlays with the catalytically essential Arg (R68) in γδ resolvase. The overlay suggests that this metal ion may occupy the B site in RecJ and stabilize the transition state. The similarity is consistent with a catalytic mechanism in which Ser attacks the scissile phosphate and Arg68 stabilize the pentacovalent intermediate. How the metal ion comes into play in DNA religation awaits elucidation by future studies.

Interestingly, Ser recombinases bear structural and functional similarity to TOPRIM topoisomerases because of the connection between RecJ and TOPRIM OLD nucleases (Fig. 10). The passage of one DNA duplex through another in site-specific recombination by a Ser recombinase is not dissimilar to the dsDNA passing in topological changes by type II topoisomerases. Ser recombinases may represent the transition from metal-independent to metal-dependent nucleic acid enzymes. Metal ion-dependent mechanisms have been associated with (1) high specificity, (2) high efficiency and (3) reversibility of forward and reverse reactions (Yang et al., 2006). Ser recombinases achieve their specificity through DNA sequence recognition by the C-terminal domain and reaction efficiency is not a concern as recombination is a rare event in the life of cells. The metal ion is indeed required for the reverse reaction of cleavage (ligation) by Ser recombinases. For topoisomerases, the efficiency of DNA cleavage and religation is in the center of topological change. Correlated with the demands of reaction efficiency and two consecutive phosphoryl transfer reactions, TOPRIM domain, a metal ion-binding module, comes to its being and plays a central role during topoisomerization. In contrast to the metal-independent type IB toposiomerases (see section 10.2), Type IA and type II topoisomerases have little preferences for specific DNA sequences. The requirement for metal ion may also contribute to the cleavage specificity and coupling of DNA cleavage with topological changes in the cases of type IA and type II topoisomerases.

9. Metal-independent RNases

A large number of RNases catalyze phosphodiester bond breakage wihtout metal ions. This is largely owing to the 2′-OH of ribose, which readily makes intra-molecular nucleophilic attack on the adjacent 3′-phosphate, thus breaking the RNA backbone (Fig. 2e, 3b-c). RNase A, T1 and T2 are three large RNase families in this class (Deshpande & Shankar, 2002; Raines, 1998; Yoshida, 2001). Endonucleases for tRNA splicing, colicin D and E5, ferredoxin-like Cas6 and CasE and IRE1 are additional metal-independent RNases. Metal-independent RNases, whether protein enzymes or ribozymes, produce 5′-OH and 2′,3′-cyclic phosphate, which is subsequently converted to 3′ phosphate and occasionally to 2′

phosphate by the phosphodiesterase activity of tRNA ligase during tRNA splicing (Abelson et al., 1998).

These RNases expose and distort the scissile phosphate by splaying the bases surrounding the scissile phosphate far apart (Fig. 3b-c). Despite secondary structures recognized by some of these RNases, the nucleotides placed in the active site are inevitably single stranded and unpaired. For example, when bound to barnase (1BRN) the RNA substrate is in an extended conformation with the bases surrounding the scissile phosphate more than 9Å apart as compared with the 3.2–3.4 Å in a double helix (Fig. 26a) (Buckle & Fersht, 1994). The active site residues facilitate the splay of bases in the substrate and distortion of the scissile phosphate for the 2′-O to attack it. An efficient cleavage reaction requires a general base to deprotonate the 2′-OH, positive charges to neutralize the penta-covalent transition state, and a general acid to protonate the 5′-O leaving group. When a general base and acid with pKa close to neutral pH are absent such as in ribozymes, the catalytic rate is slow (Cochrane & Strobel, 2008; Zamel et al., 2004). In contrast, many protein RNases have excellent general bases and acids and are thus highly active (Deshpande & Shankar, 2002; Raines, 1998; Yoshida, 2001) and usually acquire special inhibitors known as immunity proteins for host protection (Kobe & Deisenhofer, 1996; Kolade et al., 2002; Lee et al., 1989).

9.1 RNase T1, Barnase and microbial RNases

Members of RNase T1 family are found in bacteria and fungi only. Related are the restrictocin/sarcin and colicins E3, E4, and E6. The active site consists of a Glu-His pair as general base and acid.

9.1.1 Barnase—Barnase, an extracellular ribonuclease of *Bacillus amyloliquefaciens*, has been extensively studied for its folding properties, interaction with its intracellular protein inhibitor barstar, and its substrate recognition (Fersht & Daggett, 2002; Urakubo et al., 2008). Homologous RNases are found in other bacillus species, e.g. Binase from *Bacillus intermedius* (Schulga et al., 1992). Barnase has a characteristically twisted five-stranded contiguous antiparallel β sheet with long loops surrounding it and short helices covering one side (Fig. 26a). The exposed face of the β sheet binds nucleic acid substrate. Most of the catalytically essential residues are located on the loops except for the central Glu. The crystal structure of Barnase bound to a tetradeoxynucleotide (instead of RNA to prevent cleavage) reveals the mode of substrate recognition and a possible catalytic mechanism (Buckle & Fersht, 1994). Barnase cleaves 3′ to a Gua, which is sandwiched between an Arg and Phe and forms double hydrogen bonds with a Glu (Fig. 26a). The scissile phosphate is neutralized by two Arg and one Lys. The catalytic residues Glu (E73) on the central β strand and His (H102) on a long loop are on either side of the scissile phosphate and function as the general base and acid, respectively. The conformation of the deoxyribose linked to the scissile phosphate, however, is not in position for the in-line attack in this crystal structure, probably because of the absence of 2′ -OH (Buckle & Fersht, 1994). Y103, which stacks against the (deoxy)ribose, together with the Arg and Lys residues, may align and distort the substrate for the nucleophilic attack.

9.1.2 RNase T1—RNase T1, RNase Sa and fungal RNases U2, F1 and Ms belong to RNase T1 family and are homologous to Barnase in sequence and tertiary structures (Yoshida, 2001). They too cleave ssRNA after Gua. The general base and acid pair, Glu and His, are conserved in these RNases. Several crystal structures of RNase T1 bound to various substrate analogs have been reported (Arni et al., 1999), and the complex with a cyclic thiophosphate substrate is particularly revealing (Zegers et al., 1998). RNase T1 can cleave the cyclic phosphodiester to 3′ phosphate, which is the second half of the normal hydrolysis reaction. The sulfur replacement (thiophosphate) greatly reduces the reaction rate. In the crystal structure, the cyclic phosphate is placed between the conserved Glu (E58) and His (H92) and hydrogen bonded to both (Fig. 26b). The ribose is flipped compared to that in Barnase (Fig. 26a) and well placed for the general acid-base catalysis. In addition, positively charged H40 and R77 interact and orient the scissile phosphate. The guanine base preceding the scissile phosphate is sandwiched between two Tyr residues and forms bifurcated hydrogen bonds with a glutamate (E46) in addition.

9.1.3 Restrictocin—The homologous restrictocin and sarcin are ribotoxins and specifically cleave 28S ribosome RNA (Olmo et al., 2001). Structurally these ribotoxins are related to Barnase and RNase T1 (Yang et al., 2001), yet they specifically recognize a well-folded hairpin loop (sarcin/ricin loop) in the 28S rRNA. Because of the modified 2′-groups used in co-crystallization of restrictocin-RNA to prevent cleavage (Yang et al., 2001), the RNA substrate is out of register by one nucleotide and the scissile-phosphate mimic is displaced from the catalytic residues. Nevertheless, the structure reveals a dramatically deformed hairpin RNA substrate and the unpaired and flipped-out base 5′ to the scissile phosphate (Correll et al., 2004) (Fig. 26c). Such distortions are necessary to align the 2′-OH nucleophile for the in-line attack. The bases surrounding the scissile phosphate are thus splayed much like in the cases of Barnase and RNase T1. The catalytic Glu-His pair is E95 and H136 in Ristrictocin. Like RNsae T1, restrictocin also depends on aromatic and positively charged residues to bind and orient the scissile phosphate for the cleavage reaction (Fig. 26c).

9.1.4 Colicin E3, E4 and E6—Colincin E3, E4 and E6 are homologous and specifically cleave 16S rRNA. Bacteriocin Cloacin DF13 is a ribonuclease homologous to E3 and E6 colicins and it again cleaves 16S rRNA (Akutsu et al., 1989). The crystal structure of E3 complexed with its inhibitor reveals the similarity to that of Barnase and RNase T1 (Carr et al., 2000) (Fig. 26d). The conserved E62 and H71 assume comparable positions as the catalytic Glu-His pair found in the T1 superfamily. But mutagenic studies show that H58 instead of H71 is critical for catalysis and that E62 and H58 are likely the general base and acid pair (Walker et al., 2004). Additional charged residues Asp, Glu, Lys and Arg align the active site. Mutagenesis suggests that R40, D55, E60, Y64 and R90 are essential for catalysis (Walker et al., 2004). How these RNases recognize their substrate remains unsettled in the absence of a co-crystal structure and additional biochemical studies.

9.2 Colicin D and E5

Colicin D cleaves the anticodon loop of all four Arg tRNAs (Kolade et al., 2002). The crystal structure of Colicin D complexed with its immunity protein has been determined

(Graille et al., 2004). Although colicin D consists of a contiguous anti-paralle β sheet supported by long α helix on one side as does RNase T1, the topology is different with the strands (1234) going from right to left instead of left to right (Fig. 26e). The crystal structure also reveals that its active site lacks the Glu-His pair. Instead colicin D has a single His (H611), which is suspected to be the general base. In addition, the active site is marked by aromatic residues, which may determine the base specificity, and by positively charged residues, which may orient and neutralize the scissile phosphate (Graille et al., 2004).

Colicin E5 is similar to colicin D and is also a tRNase. It recognizes the GU sequence in the anticodon loop of *E. coli* Tyr, His, Asn and Asp tRNAs (James et al., 1996). The crystal structure of Colicin E5 complexed with a substrate mimic (dGpdUp) reveals that GU bases are specified by hydrogen bonds mainly with the backbone atoms of the protein (Yajima et al., 2006) (Fig. 26f). This structure reveals a near-active reaction coordination, where the scissile phosphate and the preceding (deoxy)ribose (to which the 2′ OH would belong to if present) are perfectly aligned for the nucleophile attack (compared with the reaction product of 2′,3′ cyclicphosphate shown in 25b). Colicin E5 has no Glu or His in its active site (Fig. 26f). Three basic residues (K25, R33 and K60) provide charge neutralization of the scissile phosphate. These positively charged residues may serve as the general acid and base for catalysis at high pH as proposed (Yajima et al., 2006). Interestingly, two Gln (Q29 and Q93) are located near the scissile phosphate and are potentially involved in the cleavage reaction.

9.3 RNase A

Bovine pancreatic RNase A is perhaps the most studied ribonuclease, which has culminated in four Nobel prizes (Raines, 1998). It is the protein that Chris Anfinsen used to show that information for disulfide formation and tertiary folding is intrisically stored in the amino acid sequene (Anfinsen, 1973). Homologs of RNase A are widespread among animals. There are eight versions of RNase A in the human genome, six expressed in pancreas (RNase 1 to 6) and two in skin (7 to 8). Genes encoding these RNases tend to be in a cluster on one chromosome. Only homologues of RNase 5 have been reported outside the mammals. Crystal structures of pancreatic RNase A (Avey et al., 1967; Kartha et al., 1967; Wyckoff et al., 1970) and homologous seminal (Mazzarella et al., 1993; Merlino et al., 2008) and eggwhite ribonucleases (PDB: 2ZPO) have been determined. Like Barnase, RNase A contains a central antiparallel β sheet, but it is much more extended and twisted (Fig. 27a). The catalytic triad, two His (H12 and H119) and one Lys (K41) surround a central substrate-binding groove (Fig. 27a).

Pancreatic RNases recognize U or C for endonucleolytic cleavage to produce 3′-Up or 3′-Cp. The apo-protein structure of RNase A was among the first protein crystal structures determined (Kartha et al., 1967; Wyckoff et al., 1967), and the RNase complexed with ssDNA substrate mimics were determined in 1990s (Raines, 1998). The structure of RNaseA complexed with d(ATAAG) with the dT mimicking a U is most revealing (Fontecilla-Camps et al., 1994). The preference for cleaving after a pyrimidine is due to steric exclusion of purines. The reaction coordinate is rather similar to the other known metal-independent RNases (Fig. 26, 27a). The conserved H12 (potentially the general base) is hydrogen bonded with the scissile phosphate on the 3′-O side (2′-OH is replaced by H), and H119 (potentially

the general acid) is hydrogen bonded with the leaving group O5′. Studies by chemical perturbation of the catalytic triad and pH profiling indicate that indeed H12 is the general base, H119 the general acid and K41 specifically neutralizes the transition state (Raines, 1998).

9.4 RNase T2

Members of RNase T2 family are widespread from *E. coli* (RNase I), fungi (Rd, DdI), plants (LE, NT) and mammals (Deshpande & Shankar, 2002; Irie & Ohgi, 2001). RNases T2 are seqeunce non-specific. The structure of RNase T2 consists of a central 4-stranded antiparallel β sheet surrounded by short strands and long helices on one face. The topology and tertiary structure, however, are different from RNase A and T1 (Fig. 27b). The active site is located on the exposed face of the β sheet. The conserved Glu, Lys and three His residues in the active site are essential for the catalytic activity. Interestingly, mutation of individual amino acids only reduces, but not eliminates, the RNase activity (Tanaka et al., 2000). The crystal structure of tobacco RNase T2 (NT) complexed with two 5′ GMP in the active site may mimic the enzyme-substrate complex (Kawano et al., 2006). Each guanine bases is sandwiched by two aromatic sidechains. The catalytic residues are within hydrogen bonding distance to the scissile phosphate mimics (Fig. 27c), a His and Lys coordinating the attacking nucleophile 2′-OH, and the remaining three coordinating the phosphate.

9.5 tRNA splicing endonuclease

About 5–25% of archaeal and eukaryotic tRNAs contain introns, which are recognized and excised by the tRNA splicing endonuclease (Abelson et al., 1998). The tRNA splicing endonucleases vary from homodimeric (archaea) to hetero-tetrameric (eukarya), but the overall structures are identical. Regardless of the number of peptides, each active molecule contains two catalytic and two structural units, all of which are structurally similar (Calvin & Li, 2008). All tRNA splicing endonucleases recognize the bulge-helix-bulge (BHB) structure in pre-tRNAs. The crystal structure of an archaeal homodimeric tRNA endonuclease complexed with RNA substrate with two bulges reveals two composite active sites (Xue et al., 2006) (Fig. 27d). One active site is bound to a non-cleavable 2′-deoxy substrate, and the other is bound to the cleaved product (Fig. 27e-f).

The pre-tRNA substrate is mostly base paired except for the cleavage sites in the 3-nt bulges. The bases flanking the scissile phosphate are unpaired and splayed as in substrate complexes of other metal-independent RNases. Each active site is composite. The catalytic residues are from one subunit, while the other subunit donates the Arg residues that sandwich the flipped out base flanking the scissile phosphate by the cation-π interactions (Fig. 27e-f). The catalytic unit contains a five-stranded mixed β sheet not unlike metal-independent RNases. The conserved Tyr, His and Lys in the active site are confirmed to play catalytic roles. Double mutation of the Tyr and His eliminates the nuclease activity (Calvin et al., 2008). This Tyr-His pair appears to replace the Glu-His in Barnase and the His-His pair in RNase A and acts as the general acid and base in the RNA cleavage reaction. Interestingly, replacing the conserved Lys in the active site by Glu, Gln or Arg abolishes the cleavge activity too, but the K to E mutant enzyme alone can be rescued by a specific divalent cation (Calvin et al.,

2008). This may be an in-testtube mimic of the evolution from metal-independent to metal-dependent nucleases.

Ligation of the cleavage products 5′-OH and 2′,3′- cyclic phosphate in tRNA splicing is rather baroque (Abelson et al., 1998). It requires the 5′ end to be phosphorylated and the 2′, 3′ cyclic phosphate to be converted to the 3′-OH and 2′-phosphate by a special phosphodiesterase (Wang & Shuman, 2005). After the standard ligation, the 2′-phosphate needs to be removed by another enzyme. The archaic processing of such metal ion independent RNA cleavage products may suggest an ancient origin. The simpler metal-dependent 3′-OH and 5′-phosphate splicing and cleavage intermediates ready for ligation and replication may arise in parallel to this or after, and they are clearly favored by evolution as shown by their abundance in today's world.

9.6 Ferredoxin-fold Cas6

Cas6 (for CRISPR associated) and CasE (Cse3) are related endoribonucleases that specifically recognize and cleave CRISPR RNA repeats to generate guide RNA for antiviral defense in prokaryotes (Brouns et al., 2008). The cleavage by Cas6 occurs 21 or 22 nucloetide downstream of the first repeat nucleotide. It is metal ion independent and presumably generates 5′-OH and 2′,3′-cyclic phosphate (Carte et al., 2008). Cas6 and CasE belong to one of the repeat-associated mysterious protein (RAMP) families (Makarova et al., 2006). The crystal structure of Cas6 reveals that it is composed of two ferredoxin domains in a direct repeat (Fig. 28a). Ferredoxin-like domains are often found as RNA-binding modules. In addition to Cas6, Cas2 is also an RNase with a ferredoxin fold, but Cas2 is metal-ion dependent and generates 5′-phosphate and 3′-OH products (section 6.17.3).

The two Ferredoxin-domains in Cas6 are arranged approximately side-by-side and a G(Gly)-rich region fills the gap between the domains (Carte et al., 2008) (Fig. 28a). The active site of Cas6 consists of highly conserved Tyr, His, and Lys in the first ferredoxin domain and a conserved Lys in the G-rich region. The Tyr-His pair is reminiscent of the catalytic residues of tRNA endonucleases. The structure of archaeal protein TTHB192, a homolog of CasE (Cse3), was reported before its function was identified (Ebihara et al., 2006). Whether CasE is an RNase has not been confirmed. Interestingly, His, Glu and Arg from the first ferredoxin domain and Lys from the G-rich region of CasE occupy the same positions as the catalytic residues in Cas6 (Fig. 28a-b). A His-Glu pair may replace the Tyr-His pair for catalysis if CasE is an RNase.

9.7 XendoU

Xenopus laevis RNA endonuclease is involved in processing of the intron-encoded boxC/D U16 snoRNA (small nucleolar RNA) for ribosome biogenesis (Laneve et al., 2003). Cleavage is poly(U) specific and homologues of XendoU are found in most metazoa (Laneve et al., 2008). Although initially it was thought that its catalysis is metal ion dependent, metal ion cannot be found in the active site in the crystal structure (Renzi et al., 2006). Considering the cleavage products are 3′-phosphate and 5′-OH, the required metal ion was suggested to facilitate RNA substrate binding. The tertiary structure of XendoU is unique. It contains a bunch of α helices at the N-terminus and a duplication of an α-helix

and three-stranded β sheet unit at the C-terminus (Fig. 28c). The catalytic residues are concentrated in the first repeat of the α/ β structure and include two His, one Lys and one Arg (Renzi et al., 2006).

9.8 IRE1 and RNase L

IRE1 is an ancient transmembrane sensor of ER stress and is conserved in all eukaryotes (Sidrauski & Walter, 1997). In addition to the N-terminal ER luminal domain (receptor of unfolded protein) and a transmembrane segment, IRE1 has both a C-terminal cytoplasmic kinase domain and a kinase-extension nuclease (KEN) domain. IRE1 catalyzes splicing of target mRNAs in a splicesome-independent manner. The cleavage products are 2′,3′ cyclic phosphate and 5′ -OH, and the cleavage mechanism is proposed to be similar to RNase A. Dimerization and auto-phosphorylation of IRE1 activate its ribonuclease activity, and binding ADP/ATP in the kinase domain enhances dimerization of the KEN and thereby the nuclease activity (Sidrauski & Walter, 1997). The crystal structure of the kinase and KEN domain has been recently determined (Lee et al., 2008) (Fig. 28d-e). The KEN nuclease is rather unusual and is entirely α helical without any β strand. The active site residues are concentrated along an α helix at the dimer interface, including His, Asn, Tyr and several Arg side chains.

The kinase and KEN domains are also found in mammalian RNase L (Bork & Sander, 1993; Dong et al., 2001), which contains 9 ankarin repeats in addition. In parallel to the nuclease activation of IRE1 by ER stress, RNase L is activated by 2′, 5′ oligoadenylates (whose production is induced by viral infection and mediated by interferon) binding to the ankarin repeats (Silverman, 2007). RNase L cleaves ssRNA at the 3′ of UA or UU sequences and plays an essential role in breaking down viral RNAs in innate immune response. Like all other metal ion-independent RNases, the cleavage products of RNase L are 3′ phosphate and 5′-OH. Reminiscent of the correlated kinase and nuclease activities in IRE1, RNase L activity is dampened by an ATP-binding cassette protein ABCE1 (Silverman, 2007).

9.9 Hammerhead, hairpin, glmS, HDV and VS ribozymes

Metal-independent ribozymes cleave RNA very much like metal-independent protein enzymes by splaying bases surrounding the scissile phosphate and aligning the 2′-OH for inline nucleophilic attack (see the recent comprehensive review (Cochrane & Strobel, 2008)). Because ribozymes lack a general acid and base with pKa close to neutrality, the fastest ribozyme Varkud satellite (VS) RNA has a turnover rate of 10 s^{-1} (Zamel et al., 2004), which is orders of magnitude slower than protein ribonucleases. Three-dimensional structures of the hammerhead, hairpin, glmS, hepatitis delta virus (HDV) and Varkud satellite (VS) ribozymes, which cleave RNA to generate 2′,3′ cyclic phosphate and 5′-OH, have been determined (Chi et al., 2008; Ferre-D'Amare et al., 1998; Klein & Ferre-D'Amare, 2006; MacElrevey et al., 2008; Rupert et al., 2002; Scott et al., 1996). In most cases, the unprotonated N1 of a Gua base is placed adjacent to the 2′-OH nucleophile and may serve as a general base. This is evident in the high-resolution structures of hammerhead in the pre- and post-catalytic states and of the hairpin ribozyme along the reaction pathway (Chi et al., 2008; Rupert et al., 2002) (Fig. 29). The general acid to donate a proton to the 5′ leaving group may also be a nucleobase (Cochrane & Strobel, 2008). Although Mg^{2+} is

critical for the folding of ribozymes and may play a role in substrate binding, there is no evidence that Mg^{2+} directly participates in catalysis.

10. Metal-ion independent DNases

A number of DNases are known to be metal-ion independent. To date these DNases have been shown to catalyze cleavage reactions in two steps and require a phospho-enzyme covalent intermediate. The classic examples are recombinases and topoisomerases, which use Tyr as a nucleophile and form a 3′-phosphotyrosine covalent intermediate (Grindley et al., 2006; Schoeffler & Berger, 2008). In addition, DNase II and BfiI restriction endonuclease represent members of the phospholipase D family and cleave DNA via a phospho-histidine intermediate (Sasnauskas et al., 2010). The cleavage products of DNase II and BfiI are 5′ -phosphate and 3′-OH. The last example of metal-independent DNase is the newly identified halfpipe restriction endonuclease PabI (Miyazono et al., 2007). A conserved Tyr is required for catalysis, but a phospho-Tyr intermediate is yet to be confirmed. The metal ion-independent DNases use positively charged side chains to align the scissile phosphate for nucleophilic attack and to stabilize the penta-covalent intermediate.

10.1 DNases with phospholipase D (PLD) fold

DNases in the PLD superfamily contain the $HXK(X)_4D$ (or HKD in short) motif and cleave DNA via a two-step mechanism by forming an phospho-histidine intermediate (Gottlin et al., 1998). The conserved HKD motif is present twice in each PLD family member either by homodimerization or an internal duplication (Uesugi & Hatanaka, 2009). The His and Lys of the HKD motif are involved in catalysis whereas the Asp appears to stabilize the structure by hydrogen bonding with the mainchain amides. The catalytic mechanism appears to be highly conserved in the PLD family, whether the substrate is phospholipids, DNA or phosphorylated proteins (Davies et al., 2004). The reaction coordinate is examplified by the crystal structure of human tyrosyl-DNA phosphodiesterase (TDP1) complexed with vanadate mimicking the transition state (Davies et al., 2004) (Fig. 30a). One of the two conserved His residues acts as the nucleophile and, the other as the general acid to protonate the leaving group (Fig. 30b).

10.1.1 Nuc and DNase II—Nuc of *Salmonella typhimurium* provided the first glimpse of a PLD family enzyme. It is a homodimer. The conserved His residues from two subunits (H94) align a narrow groove forming one active site and most probably acting as the nucleophile and general acid in the transesterifaciton reaction (Stuckey & Dixon, 1999) (Fig. 30c). The reaction intermediate may be stabilized by the conserved Lys residues (K96) much as in cleavage by RNase A. The structure and metal-ion independent catalysis indicate that the DNA substrate is recognized in the single-stranded form. Like all PLD-like DNases, Nuc generates 5′-phosphate and 3′-OH. Metazoa DNases II are homologs of bacterial Nuc and belong to the PLD family. DNase II in lysosomes of macrophages plays an essential role in degrading DNAs downstream from CAD/DFF40 after engulfment of apoptotic cells (Nagata, 2007). Without DNase II, residual DNA fragments lead to autoimmune diseases. The Nuc and DNase II are non-sequence specific.

10.1.2 BfiI restriction endonuclease—BfiI restriction endonuclease presents the first crystal structure of Mg^{2+} independent type II restriction endoncucleases (Grazulis et al., 2005; Vitkute et al., 1998). It is a homodimer in solution and the two PLD-like domains form one active site (Lagunavicius et al., 2003) (Fig. 30d). Like all PLD-family enzymes, Bfii cleaves DNA via a two-step transesterification mechanism (Sasnauskas et al., 2007). In the first step, it uses the conserved His as a nucleophile to cleave DNA forming a 5′ phosphoenzyme. In the second step, it transfers the phosphodiester bond to a water or alcohol molecule to regenerate the enzyme. The transition intermediate is likely stabilized by the conserved Lys residues as in TDP1 (Davies et al., 2004). Although BfiI cleaves double strand DNA, it cleaves one strand first and then the second (Sasnauskas et al., 2010). Sequence specific recognition is achieved by the DNA-binding domains that are separate from the catalytic domains (Fig. 30d) and occurs several base pairs away from the cleavage site (Grazulis et al., 2005; Vitkute et al., 1998).

10.2 Type IB topoisomerase and Tyr recombinase

Type IB topoisomerase (TopIB) and Tyr recombinases share a conserved catalytic core and similar reaction mechanism (Cheng et al., 1998; Hickman et al., 1997). These recombinases and topoisomerases contain one or more DNA binding domains in addition to the catalytic domain and often have a preference for certain DNA sequences. They all have an absolutely conserved Tyr, which serves as the nucleophile and forms a phosphotyrosyl DNA-protein bond. The cleavage reaction produces a 3′-phosphotyrosine and 5′-OH. The DNA-enzyme covalent bond is cleaved by the 5′-OH of DNA in the religation step of recombination or topoisomerization (Grindley et al., 2006; Schoeffler & Berger, 2008). If Topo IB fails to religate the DNA, the covalently linked DNA and protein intermediate is the substrate of TDP1 (Fig. 30a-b) (Pouliot et al., 1999). In the absence of a DNA substrate, the Tyr is disordered or in a conformation unsuitable for catalysis (Biswas et al., 2005; Cheng et al., 1998; Kwon et al., 1997; Perry et al., 2006b; Yang & Mizuuchi, 1997). In the assembled active site the Tyr is surrounded by a handful of basic residues, which participate in the chemistry of cleavage and religation.

10.2.1 Type IB topoisomerases—Type 1B topoisomerases relax supercoiled DNA. They can be sequence specific like viral topoisomerases (Cheng et al., 1998) or have weak preference for certain DNA sequences like eukaryotic cellular TopIB (Redinbo et al., 1998). Many crystal structures of Topo 1B, from protein alone (Cheng et al., 1998), protein-DNA complexes (Perry et al., 2006b; Redinbo et al., 1998) to a cleavage transition mimic (Davies et al., 2006), have been determined. The active site contains two Arg, one Lys, one His and the nucleophile Tyr (Fig. 31a). The basic residues orient and neutralize the DNA backbone. One conserved Arg that is hydrogen bonded to both scissile phosphate and the nucleophile Tyr (Fig. 31b) is postulated to be the general base to deprotonate the Tyr (Davies et al., 2006; Yakovleva et al., 2008). The remaining Arg is proposed to work together with the Lys to act as the general acid and protonate the 5′ leaving group (Hwang et al., 1998; Yakovleva et al., 2008).

10.2.2 Tyr recombinases: Cre, Flp, Xer and Phage integrase—The representative members of the Tyr recombinase superfamily include phage integrases (λ and

HP1) (Biswas et al., 2005; Hickman et al., 1997), the Cre-loxP recombination system (Baldwin et al., 2003; Guo et al., 1997) widely used in the gene knockout techniques, XerC/D for bacterial DNA segregation (Subramanya et al., 1997), and yeast Flp recombinase (Chen et al., 2000). They are all site-specific recombinases and share the conserved catalytic motif RHR in addition to the Tyr nucleophile. These recombinases are most often bi-lobel with a sequence-specific DNA-binding domain at the N-terminus and catalytic domain at the C-terminus (Fig. 31c). Many crystal structures have been determined along the reaction pathway (Grindley et al., 2006), and the active site and surrounding structure of these recombinases can be superimposed with that of Topo IB (Fig. 31d-e). The Tyr nucleophile is located on the third helix in a three-helix bundle, which resembles a classic HTH domain (Yang & Steitz, 1995a) (Fig. 31d). Positioning the Tyr for nucleophilic attack requires the synapsis of four protein subunits and two palindromic DNA recombination sites (Ghosh et al., 2007a) (Fig. 31c). A Holliday junction is a necessary intermediate in recombination (Voziyanov et al., 1999). A catalytically competent active site may consist of residues from two adjacent subunits (so-called trans configuration) (Chen et al., 2000). The Tyr nucleophile is likely deprotonated by one of the two conserved Arg residues as with human and vaccinia Topo IB (Fig. 31e) (Redinbo et al., 2000; Yakovleva et al., 2008). The other conserved Arg and Lys residues in the active site orient the scissile phosphate, stabilize the transition state, and may also protonate the 5′-O leaving group.

10.3 Halfpipe restriction endonuclease

The last group of metal ion-independent nucleases is represented by the newly identified restriction endonculeases PabI encoded by transposable elements in archaea (Ishikawa et al., 2005). Homologues of PabI possibly exist in bacteria as well. They are called “halfpipe” because the quaternary structure of the homodimeric enzyme resembles a halfpipe with a deep groove in the center (Fig. 32) (Miyazono et al., 2007). The nuclease is highly toxic to cells, presumably because of its nuclease activity. Over-expression was achieved in a cell-free system for the biochemical and structural studies. The crystal structure is determined without DNA substrate, and the catalytic mechanism is unclear. Mutagenesis indicates that the conserved Tyr (Y134), Glu and Arg are indispensable for the catalytic activity (Miyazono et al., 2007). It is not known whether a DNA-tyrosyl covalent bond is formed in the process of DNA cleavage.

11. Concluding remarks and future directions

11.1 Metal ions and nucleases

Classification of nucleases by metal-ion dependence highlights the following general properties. Firstly, when metal ions are not directly involved in catalysis, RNases and DNases do not (and perhaps cannot) use water molecules as nucleophiles to attack a phosphodiester bond. The 2′-OH immediately adjacent to the scissile phosphate is universally used by metal-independent RNases for nucleophilic attack, whereas the hydroxyl group of Tyr or Ser or the imidazole of His is used by metal-independent DNases. Each of these ribose and side-chain nucleophiles has a lower pKa than water and is more readily deprotonated at physiological pH. In these metal-independent nucleolytic reactions, cleavage requires a second step to hydrolyze the cyclic diphosphate or covalent enzyme-substrate

intermediate (Fig. 1b, 2d-e). Incorporation of one or two metal ions into an active site, however, allows water to be a nucleophile and cleavage to occur in one step. Interestingly, the metal-ion site in common between the one and two metal-ion dependent mechanisms is situated on the leaving group side (B site) (Yang, 2008) and is not directly involved in deprotonating and activating the nucleophilic water.

Secondly, metal-ion dependent nucleases cleave nucleic acid in the base-stacked helical conformation whether single- or double-stranded, whereas metal-independent nucleases prefer a base unpaired and unstacked single-stranded substrate, for example, all metal-independent RNases and PLD-like DNases. Type IB topoisomerases and Tyr recombinases are exceptional and cleave a scissile phosphate embedded in the double helix with assistances of Arg and Lys sidechains reaching into the DNA minor groove (Fig. 31a). Interestingly, these DNases cleave one strand only. This is likely because two such active sites cannot be easily configured in the minor groove adjacent to each other

Thirdly, cleavage products of metal-ion dependent reactions are always a 5′-phosphate and 3′-OH groups, and products of metal-ion independent reactions are most often a 5′-OH and 3′-phosphate. This division is observed among all RNases, but among DNases there are a couple of exceptions. Ser recombinases (section 8.2) and DNase II and BfiII of the PLD family (section 10.1) cleave DNA without metal ions and produce 5′-phosphoserine and 5′-phosphohistidine intermediates, respectively.

Fourthly, nucleases that require no or one metal ion for catalysis most often require specific inhibitors to keep their activity in check. This requirement for inhibition is evident for eukaryotic RNase A and homologs (section 9.3), death-associated DNases (Endo G, Nuc, CAD and DNase II, section 7.1.4 and 10.1.1), and microbial colicins (sections 7.1.4.3, 9.1.4 and 9.2). The process of inhibition can be quite cumbersome, and each nuclease often requires a specific inhibitor (Ghosh et al., 2007b; Kolade et al., 2002; Rutkoski & Raines, 2008; Widlak & Garrard, 2005). In contrast, two-metal-ion dependent nucleases rarely require specific inhibitors to regulate their cleavage activity. The most prevalent protection is by DNA methylation in the restriction-modification systems (Bujnicki, 2001). An addition of methyl groups to a DNA recognition sequence is often sufficient to stop nuclease digestion. The reason that restriction-modification systems can work may be a result of the improved coupling between substrate recognition and catalysis of bond cleavage by the two-metal-ion mechanism (Yang et al., 2006). Although one-metal and no-metal dependent nucleases can be sequence specific, substrate recognition and the cleavage reaction are less tightly coupled for these enzymes than for two-metal-ion dependent nucleases, and specificity is achieved by recognition of longer DNA sequences (e.g. homing endonucleases), additional separate DNA binding domains (KpnI and BfiI), and formation of high-order protein-DNA complexes (e.g. site-specific recombination).

11.2 Diversity and convergence

Two themes emerge from analyzing the diversity and convergence of nucleases and their biological functions. At one end of the spectrum, a wide range of nucleases of different structure and catalytic mechanism are employed to catalyze a similar biological reaction. At

the other end of the spectrum, a conserved structural module and catalytic sequence motif may function in divergent or completely unrelated biological pathways.

11.2.1 Diversity of nucleases in a similar cleavage reaction—In the first category, the divergence of restriction endonucleases, Holliday Junction resolvases, site-specific recombinases, homing endonuclease and AP endonucleases stand out. As noted by Darwin, greater variation is found closer to the evolutionary source of a species. This principal is exemplified in the recent genomic sequencing of African Bushmen (Schuster et al., 2010), which reveals that the genetic differences between any two Bushmen is greater than that between a European and an Asian. The diversity of nucleases may indicate that repair of an abasic lesion, homologous and site-specific DNA recombination and restrictive digestion of foreign DNA are ancient processes. The different nucleases that result in a shared outcome may also provide hints of a convergent relationship. For example, two AP endonucleases, Endo IV and Exo III (APE1) (section 6.7.2 and 6.1.6.1), recognize the abasic site in a very similar way and use the pro-Rp oxygen to coordinate the catalytic two metal ions despite their unrelated tertiary structure and catalytic motifs.

Two cases of diverse nucleases for one biological process are worth noting. Holliday junctions (HJ) or four-way DNA junctions are resolved to two duplexes by nucleases with different structure and mechanisms. Even among bacterial and single-cell eukaryotes there are more than four different HJ resolvases (Table 1). In higher eukaryotes, HJ resolvases exhibit additional diversity both in catalytic motifs and nuclease organization (Fekairi et al., 2009; Ip et al., 2008). HJ resolvases in lower organisms are homodimeric regardless of differences in catalytic mechanisms and symmetrically cleave fully base paired four-way junctions in antiparallel or square-planar configurations (Biertümpfel et al., 2007; Hadden et al., 2007; Lilley & White, 2001). Eukaryotic HJ resolvase SLX1-SLX4 and Mus81-Eme1, however, are heterodimeric, and only one subunit contains the active site (Blanco et al.; Ciccia et al., 2008). Instead of symmetric and fully base-paired junctions, eukaryotic HJ resolvases can recognize and cleave asymmetric ssDNA flaps. In bacteria HJs often occur due to localized short palindromic sequences, which can be easily arranged in symmetric antiparallel or open-square conformation to be cleaved by homodimeric HJ resolvases. But in eukaryotes, four-way junctions often arise during homologous recombination between two distal sites or sister chromatids, where a symmetric HJ in antiparallel conformation is not easily achievable The increasing diversity in HJ resolvases may correlate with the increased genomic complexity from bacteria to eukaryotes.

At least four different types of endonucleases are involved in site-specific DNA recombination: two kinds of Tyr recombinases (section 7.3 and 10.2), Ser recombinases (section 8.2), and many two-metal-ion dependent transposases (section 6.2.2). The catalytic mechanisms of these nucleases range from no metal, one-metal to two-metal dependent. Ser and Tyr recombinases are rarely found in eukaryotes and are absent in plants and metazoa. In contrast, two-metal-ion dependent transposases/recombinases are widespread in bacteria, retroviruses, and lower and higher eukaryotes. Usage of two-metal-ion catalysis is also associated with the cut-and-paste mechanism and a widened selection of target DNA for recombination

11.2.2 Adaptation of a catalytic motif in various nucleases—Several catalytic modules of conserved structure and mechanism are found in many DNases and RNases (see section sections 6.1 to 6.4 and 7.1). Wide distribution of a particular catalytic module likely reflects its catalytic efficiency. For example, the DEDD motif is associated with a large number of 3′ exonucleases, regardless of whether the substrate is DNA or RNA, and FEN1-like nucleases containing both a 5′ exo and endonuclease activity are found to remove primers in DNA replication and to cleave nucleic acid in HJ resolution, DNA repair and RNA processing.

Two catalytic motifs have the widest adaptation and are associated with the most diverse functions. They are the REase fold with the DEK motif (section 6.3) and the ββα-Me motif (section 7.1). These two catalytic motifs share the following features, which may allow them to be incorporated into different nucleases and different pathways. Firstly, the conserved catalytic motif is modular and small in size. Both the DEK and ββα-Me motifs are often contained within a stretch of 20–30 residues. The DEK motif occurs in a β-hairpin structure (Fig. 8), and the ββα-Me motif consists of a β-hairpin followed by an α-helix (Fig. 21). Thus, the DEK and ββα-Me motifs are readily incorporated into diverse surrounding tertiary structures and adapted to different nuclease activities and pathways. Secondly, both the DEK and ββα-Me motif are extremely tolerant of amino acid substitutions. Except for the first D in the DEK motif and a His serving as the general base in ββα-Me, other catalytic residues can vary greatly (see section 6.3 and 7.1). Thridly, the REase-like nucleases are further aided by the two-metal-ion mechanism in substrate specificity and catalytic efficiency.

It is worth noting that metal-ion dependent mechanisms appear most adaptable. This observation may be explained by the advantages of specificity, efficiency and diversity endowed by metal ions (Yang et al., 2006). Multiple metal-independent mechanisms and varied catalytic motifs are found among RNases, and this is likely due to efficient catalysis using a 2′-OH as the nucleophile. Adaptation of metal-independent mechanisms among DNases is rather limited and with few alterations, e.g. DNase II versus BfiI and type IB topoisomerases versus Tyr recombinases. The small number of metal-independent DNases may be a result of the limited types of reactions catalyzed and additional requirements for regulation and inhibition of cleavage activity.

11.3 Future directions

Although nucleases are the oldest nucleic acid enzymes characterized, new nucleases are being discovered every year and it is safe to predict that this trend will continue. Among the more recently discovered nucleases, several have novel sequence motifs, and their structures cannot be modeled using existing nucleases. For example, Sae2 in meiotic DNA break repair, SLX1-SLX4 HJ resolvase, and nucleases in CRISPR pathways have unique catalytic motifs and unknown structures. For the well-studied processes of mRNA splicing and processing, the mechanism of the spliceosome and involvement of exon-junction complex and nonsense-mediated decay are still being fleshed out. Furthermore, for many nucleases whose structures are known or are homologous to nucleases of known structure the catalytic mechanism remains unclear without additional atomic structures of functional enzyme-substrate complexes. Last, but not least, many nucleases are linked to genetic or infectious

diseases and are potential therapeutic targets. It is clear that exciting discoveries will continue to expand our understanding of these diverse and essential enzymes

Table. 1 Classification of nucleases by function. DNases and RNases are classified according to biological processes they are involved from DNA replication to cell defense. Each processes is further divided into functional pathways. Enzymes of different catalytic mechanisms or different tertiary structures are separated by semi-colons for each pathway or process. Detailed descriptions of each category are referred to specific chapters and under sections.

Acknowledgment

W. Y. is supported by NIH, NIDDK intramural research fund. The author thanks Dr. C. Biertuempfel for initially collecting nucleases deposited with PDB database, and Drs. R. Craigie and D. Leahy for reading and editing the manuscript.

References

ABELSON J, TROTTA CR & LI H (1998). tRNA splicing. J Biol Chem, 273(21), 12685–12688. [PubMed: 9582290]

ADAMS PL, STAHLEY MR, KOSEK AB, WANG J & STROBEL SA (2004). Crystal structure of a self-splicing group I intron with both exons. Nature, 430(6995), 45–50. [PubMed: 15175762]

AIZAWA Y, XIANG Q, LAMBOWITZ AM & PYLE AM (2003). The pathway for DNA recognition and RNA integration by a group II intron retrotransposon. Mol Cell, 11(3), 795–805. [PubMed: 12667460]

AKUTSU A, MASAKI H & OHTA T (1989). Molecular structure and immunity specificity of colicin E6, an evolutionary intermediate between E-group colicins and cloacin DF13. J Bacteriol, 171(12), 6430–6436. [PubMed: 2687234]

ALLEMAND F, MATHY N, BRECHEMIER-BAEY D & CONDON C (2005). The 5S rRNA maturase, ribonuclease M5, is a Toprim domain family member. Nucleic Acids Res, 33(13), 4368–4376. [PubMed: 16077031]

ALTERMARK B, SMALAS AO, WILLASSEN NP & HELLAND R (2006). The structure of Vibrio cholerae extracellular endonuclease I reveals the presence of a buried chloride ion. Acta Crystallogr D Biol Crystallogr, 62(Pt 11), 1387–1391. [PubMed: 17057343]

ANDERSEN KR, JONSTRUP AT, VAN LB & BRODERSEN DE (2009). The activity and selectivity of fission yeast Pop2p are affected by a high affinity for Zn2+ and Mn2+ in the active site. RNA, 15(5), 850–861. [PubMed: 19307292]

ANDRADE JM, POBRE V, SILVA IJ, DOMINGUES S & ARRAIANO CM (2009). The role of 3'−5' exoribonucleases in RNA degradation. Prog Mol Biol Transl Sci, 85, 187–229. [PubMed: 19215773]

ANFINSEN CB (1973). Principles that govern the folding of protein chains. Science, 181(96), 223–230. [PubMed: 4124164]

ARAVIND L (1999). An evolutionary classification of the metallo-beta-lactamase fold proteins. In Silico Biol, 1(2), 69–91. [PubMed: 11471246]

ARAVIND L & KOONIN EV (1998). A novel family of predicted phosphoesterases includes Drosophila prune protein and bacterial RecJ exonuclease. Trends Biochem Sci, 23(1), 17–19. [PubMed: 9478130]

ARAVIND L, LEIPE DD & KOONIN EV (1998). Toprim--a conserved catalytic domain in type IA and II topoisomerases, DnaG-type primases, OLD family nucleases and RecR proteins. Nucleic Acids Res, 26(18), 4205–4213. [PubMed: 9722641]

ARCUS VL, BACKBRO K, ROOS A, DANIEL EL & BAKER EN (2004). Distant structural homology leads to the functional characterization of an archaeal PIN domain as an exonuclease. J Biol Chem, 279(16), 16471–16478. [PubMed: 14734548]

ARIYOSHI M, VASSYLYEV DG, IWASAKI H, NAKAMURA H, SHINAGAWA H & MORIKAWA K (1994). Atomic structure of the RuvC resolvase: a holliday junction-specific endonuclease from E. coli. Cell, 78(6), 1063–1072. [PubMed: 7923356]

ARNI RK, WATANABE L, WARD RJ, KREITMAN RJ, KUMAR K & WALZ FG, JR. (1999). Three-dimensional structure of ribonuclease T1 complexed with an isosteric phosphonate substrate analogue of GpU: alternate substrate binding modes and catalysis. Biochemistry, 38(8), 2452–2461. [PubMed: 10029539]

ARTYMIUK PJ, CESKA TA, SUCK D & SAYERS JR (1997). Prokaryotic 5'−3' exonucleases share a common core structure with gamma-delta resolvase. Nucleic Acids Res, 25(21), 4224–4229. [PubMed: 9336450]

AVEY HP, BOLES MO, CARLISLE CH, EVANS SA, MORRIS SJ, PALMER RA, WOOLHOUSE BA & SHALL S (1967). Structure of ribonuclease. Nature, 213(5076), 557–562. [PubMed: 6032249]

BALDWIN EP, MARTIN SS, ABEL J, GELATO KA, KIM H, SCHULTZ PG & SANTORO SW (2003). A specificity switch in selected cre recombinase variants is mediated by macromolecular plasticity and water. Chem Biol, 10(11), 1085–1094. [PubMed: 14652076]

BALDWIN GS, WALEY SG & ABRAHAM EP (1979). Identification of histidine residues that act as zinc ligands in beta-lactamase II by differential tritium exchange. Biochem J, 179(3), 459–463. [PubMed: 314287]

BAN C & YANG W (1998). Structural basis for MutH activation in E.coli mismatch repair and relationship of MutH to restriction endonucleases. Embo J, 17(5), 1526–1534. [PubMed: 9482749]

BARABAS O, RONNING DR, GUYNET C, HICKMAN AB, TON-HOANG B, CHANDLER M & DYDA F (2008). Mechanism of IS200/IS605 family DNA transposases: activation and transposon-directed target site selection. Cell, 132(2), 208–220. [PubMed: 18243097]

BECHHOFER DH (2009). Messenger RNA decay and maturation in Bacillus subtilis. Prog Mol Biol Transl Sci, 85, 231–273. [PubMed: 19215774]

BEESE LS & STEITZ TA (1991). Structural basis for the 3'−5' exonuclease activity of Escherichia coli DNA polymerase I: a two metal ion mechanism. Embo J, 10(1), 25–33. [PubMed: 1989886]

BELOGLAZOVA N, BROWN G, ZIMMERMAN MD, PROUDFOOT M, MAKAROVA KS, KUDRITSKA M, KOCHINYAN S, WANG S, CHRUSZCZ M, MINOR W, KOONIN EV, EDWARDS AM, SAVCHENKO A & YAKUNIN AF (2008). A novel family of sequence-specific endoribonucleases associated with the clustered regularly interspaced short palindromic repeats. J Biol Chem, 283(29), 20361–20371. [PubMed: 18482976]

BENEDIK MJ & STRYCH U (1998). Serratia marcescens and its extracellular nuclease. FEMS Microbiol Lett, 165(1), 1–13. [PubMed: 9711834]

BENNETT RJ, DUNDERDALE HJ & WEST SC (1993). Resolution of Holliday junctions by RuvC resolvase: cleavage specificity and DNA distortion. Cell, 74(6), 1021–1031. [PubMed: 8402879]

BHAGWAT M, HOBBS LJ & NOSSAL NG (1997). The 5'-exonuclease activity of bacteriophage T4 RNase H is stimulated by the T4 gene 32 single-stranded DNA-binding protein, but its flap endonuclease is inhibited. J Biol Chem, 272(45), 28523–28530. [PubMed: 9353314]

BHAT AG, LEELARAM MN, HEGDE SM & NAGARAJA V (2009). Deciphering the distinct role for the metal coordination motif in the catalytic activity of Mycobacterium smegmatis topoisomerase I. J Mol Biol, 393(4), 788–802. [PubMed: 19733176]

BIERTÜMPFEL C, YANG W & SUCK D (2007). Crystal structure of T4 endonuclease VII resolving a Holliday junction. Nature, 449(7162), 616–620. [PubMed: 17873859]

BISWAS T, AIHARA H, RADMAN-LIVAJA M, FILMAN D, LANDY A & ELLENBERGER T (2005). A structural basis for allosteric control of DNA recombination by lambda integrase. Nature, 435(7045), 1059–1066. [PubMed: 15973401]

BITINAITE J, WAH DA, AGGARWAL AK & SCHILDKRAUT I (1998). FokI dimerization is required for DNA cleavage. Proc Natl Acad Sci U S A, 95(18), 10570–10575. [PubMed: 9724744]

BLANCO MG, MATOS J, RASS U, IP SC & WEST SC (2010). Functional overlap between the structure-specific nucleases Yen1 and Mus81-Mms4 for DNA-damage repair in S. cerevisiae. DNA Repair (Amst). 9, 394–402. [PubMed: 20106725]

BORK P & SANDER C (1993). A hybrid protein kinase-RNase in an interferon-induced pathway? FEBS Lett, 334(2), 149–152. [PubMed: 7693513]

BRAUTIGAM CA & STEITZ TA (1998). Structural principles for the inhibition of the 3'−5' exonuclease activity of Escherichia coli DNA polymerase I by phosphorothioates. J Mol Biol, 277(2), 363–377. [PubMed: 9514742]

BRAUTIGAM CA, SUN S, PICCIRILLI JA & STEITZ TA (1999). Structures of normal single-stranded DNA and deoxyribo-3'-S-phosphorothiolates bound to the 3'−5' exonucleolytic active site of DNA polymerase I from Escherichia coli. Biochemistry, 38(2), 696–704. [PubMed: 9888810]

BREYER WA & MATTHEWS BW (2000). Structure of Escherichia coli exonuclease I suggests how processivity is achieved. Nat Struct Biol, 7(12), 1125–1128. [PubMed: 11101894]

BROUNS SJ, JORE MM, LUNDGREN M, WESTRA ER, SLIJKHUIS RJ, SNIJDERS AP, DICKMAN MJ, MAKAROVA KS, KOONIN EV & VAN DER OOST J (2008). Small CRISPR RNAs guide antiviral defense in prokaryotes. Science, 321(5891), 960–964. [PubMed: 18703739]

BRUCET M, QUEROL-AUDI J, SERRA M, RAMIREZ-ESPAIN X, BERTLIK K, RUIZ L, LLOBERAS J, MACIAS MJ, FITA I & CELADA A (2007). Structure of the dimeric exonuclease TREX1 in complex with DNA displays a proline-rich binding site for WW Domains. J Biol Chem, 282(19), 14547–14557. [PubMed: 17355961]

BUCKLE AM & FERSHT AR (1994). Subsite binding in an RNase: structure of a barnase-tetranucleotide complex at 1.76-A resolution. Biochemistry, 33(7), 1644–1653. [PubMed: 8110767]

BUDD ME, CHOE W & CAMPBELL JL (2000). The nuclease activity of the yeast DNA2 protein, which is related to the RecB-like nucleases, is essential in vivo. J Biol Chem, 275(22), 16518–16529. [PubMed: 10748138]

BUJNICKI JM (2001). Understanding the evolution of restriction-modification systems: clues from sequence and structure comparisons. Acta Biochim Pol, 48(4), 935–967. [PubMed: 11996004]

BUNTING KA, ROE SM, HEADLEY A, BROWN T, SAVVA R & PEARL LH (2003). Crystal structure of the Escherichia coli dcm very-short-patch DNA repair endonuclease bound to its reaction product-site in a DNA superhelix. Nucleic Acids Res, 31(6), 1633–1639. [PubMed: 12626704]

BUTTNER K, WENIG K & HOPFNER KP (2005). Structural framework for the mechanism of archaeal exosomes in RNA processing. Mol Cell, 20(3), 461–471. [PubMed: 16285927]

BUTTNER S, EISENBERG T, CARMONA-GUTIERREZ D, RULI D, KNAUER H, RUCKENSTUHL C, SIGRIST C, WISSING S, KOLLROSER M, FROHLICH KU, SIGRIST S & MADEO F (2007). Endonuclease G regulates budding yeast life and death. Mol Cell, 25(2), 233–246. [PubMed: 17244531]

CALLAGHAN AJ, GROSSMANN JG, REDKO YU, ILAG LL, MONCRIEFFE MC, SYMMONS MF, ROBINSON CV, MCDOWALL KJ & LUISI BF (2003). Quaternary structure and catalytic activity of the Escherichia coli ribonuclease E amino-terminal catalytic domain. Biochemistry, 42(47), 13848–13855. [PubMed: 14636052]

CALLAGHAN AJ, MARCAIDA MJ, STEAD JA, MCDOWALL KJ, SCOTT WG & LUISI BF (2005). Structure of Escherichia coli RNase E catalytic domain and implications for RNA turnover. Nature, 437(7062), 1187–1191. [PubMed: 16237448]

CALLEBAUT I, MOSHOUS D, MORNON JP & DE VILLARTAY JP (2002). Metallo-beta-lactamase fold within nucleic acids processing enzymes: the beta-CASP family. Nucleic Acids Res, 30(16), 3592–3601. [PubMed: 12177301]

CALVIN K & LI H (2008). RNA-splicing endonuclease structure and function. Cell Mol Life Sci, 65(7–8), 1176–1185. [PubMed: 18217203]

CALVIN K, XUE S, ELLIS C, MITCHELL MH & LI H (2008). Probing the catalytic triad of an archaeal RNA splicing endonuclease. Biochemistry, 47(51), 13659–13665. [PubMed: 19053288]

CARR S, WALKER D, JAMES R, KLEANTHOUS C & HEMMINGS AM (2000). Inhibition of a ribosome-inactivating ribonuclease: the crystal structure of the cytotoxic domain of colicin E3 in complex with its immunity protein. Structure, 8(9), 949–960. [PubMed: 10986462]

CARTE J, WANG R, LI H, TERNS RM & TERNS MP (2008). Cas6 is an endoribonuclease that generates guide RNAs for invader defense in prokaryotes. Genes Dev, 22(24), 3489–3496. [PubMed: 19141480]

CASTILLO-ACOSTA VM, RUIZ-PEREZ LM, YANG W, GONZALEZ-PACANOWSKA D & VIDAL AE (2009). Identification of a residue critical for the excision of 3'-blocking ends in apurinic/apyrimidinic endonucleases of the Xth family. Nucleic Acids Res, 37(6), 1829–1842. [PubMed: 19181704]

CERRITELLI SM & CROUCH RJ (2009). Ribonuclease H: the enzymes in eukaryotes. FEBS J, 276(6), 1494–1505. [PubMed: 19228196]

CESCHINI S, KEELEY A, MCALISTER MS, ORAM M, PHELAN J, PEARL LH, TSANEVA IR & BARRETT TE (2001). Crystal structure of the fission yeast mitochondrial Holliday junction resolvase Ydc2. Embo J, 20(23), 6601–6611. [PubMed: 11726496]

CESKA TA, SAYERS JR, STIER G & SUCK D (1996). A helical arch allowing single-stranded DNA to thread through T5 5'-exonuclease. Nature, 382(6586), 90–93. [PubMed: 8657312]

CHAMPOUX JJ (2001). DNA topoisomerases: structure, function, and mechanism. Annu Rev Biochem, 70, 369–413. [PubMed: 11395412]

CHAMPOUX JJ & SCHULTZ SJ (2009). Ribonuclease H: properties, substrate specificity and roles in retroviral reverse transcription. FEBS J, 276(6), 1506–1516. [PubMed: 19228195]

CHANFREAU G, NOBLE SM & GUTHRIE C (1996). Essential yeast protein with unexpected similarity to subunits of mammalian cleavage and polyadenylation specificity factor (CPSF). Science, 274(5292), 1511–1514. [PubMed: 8929408]

CHANG JH, KIM JJ, CHOI JM, LEE JH & CHO Y (2008). Crystal structure of the Mus81-Eme1 complex. Genes Dev, 22(8), 1093–1106. [PubMed: 18413719]

CHANGELA A, DIGATE RJ & MONDRAGON A (2001). Crystal structure of a complex of a type IA DNA topoisomerase with a single-stranded DNA molecule. Nature, 411(6841), 1077–1081. [PubMed: 11429611]

CHAPADOS BR, HOSFIELD DJ, HAN S, QIU J, YELENT B, SHEN B & TAINER JA (2004). Structural basis for FEN-1 substrate specificity and PCNA-mediated activation in DNA replication and repair. Cell, 116(1), 39–50. [PubMed: 14718165]

CHATTERJEE DK, HAMMOND AW, BLAKESLEY RW, ADAMS SM & GERARD GF (1991). Genetic organization of the KpnI restriction--modification system. Nucleic Acids Res, 19(23), 6505–6509. [PubMed: 1754388]

CHEN DS, HERMAN T & DEMPLE B (1991). Two distinct human DNA diesterases that hydrolyze 3'-blocking deoxyribose fragments from oxidized DNA. Nucleic Acids Res, 19(21), 5907–5914. [PubMed: 1719484]

CHEN WJ, LAI PJ, LAI YS, HUANG PT, LIN CC & LIAO TH (2007a). Probing the catalytic mechanism of bovine pancreatic deoxyribonuclease I by chemical rescue. Biochem Biophys Res Commun, 352(3), 689–696. [PubMed: 17141190]

CHEN WJ & LIAO TH (2006). Structure and function of bovine pancreatic deoxyribonuclease I. Protein Pept Lett, 13(5), 447–453. [PubMed: 16800797]

CHEN X, LI N & ELLINGTON AD (2007b). Ribozyme catalysis of metabolism in the RNA world. Chem Biodivers, 4(4), 633–655. [PubMed: 17443876]

CHEN Y, NARENDRA U, IYPE LE, COX MM & RICE PA (2000). Crystal structure of a Flp recombinase-Holliday junction complex: assembly of an active oligomer by helix swapping. Mol Cell, 6(4), 885–897. [PubMed: 11090626]

CHEN YC, SHIPLEY GL, BALL TK & BENEDIK MJ (1992). Regulatory mutants and transcriptional control of the Serratia marcescens extracellular nuclease gene. Mol Microbiol, 6(5), 643–651. [PubMed: 1372678]

CHENG C, KUSSIE P, PAVLETICH N & SHUMAN S (1998). Conservation of structure and mechanism between eukaryotic topoisomerase I and site-specific recombinases. Cell, 92(6), 841–850. [PubMed: 9529259]

CHENG Y & PATEL DJ (2004). Crystallographic structure of the nuclease domain of 3'hExo, a DEDDh family member, bound to rAMP. J Mol Biol, 343(2), 305–312. [PubMed: 15451662]

CHI YI, MARTICK M, LARES M, KIM R, SCOTT WG & KIM SH (2008). Capturing hammerhead ribozyme structures in action by modulating general base catalysis. PLoS Biol, 6(9), e234. [PubMed: 18834200]

CHOWDHURY D, BERESFORD PJ, ZHU P, ZHANG D, SUNG JS, DEMPLE B, PERRINO FW & LIEBERMAN J (2006). The exonuclease TREX1 is in the SET complex and acts in concert with NM23-H1 to degrade DNA during granzyme A-mediated cell death. Mol Cell, 23(1), 133–142. [PubMed: 16818237]

CHRISTIANSON DW (1991). Structural biology of zinc. Adv Protein Chem, 42, 281–355. [PubMed: 1793007]

CHU CY & RANA TM (2007). Small RNAs: regulators and guardians of the genome. J Cell Physiol, 213(2), 412–419. [PubMed: 17674365]

CICCIA A, MCDONALD N & WEST SC (2008). Structural and functional relationships of the XPF/MUS81 family of proteins. Annu Rev Biochem, 77, 259–287. [PubMed: 18518821]

CLISSOLD PM & PONTING CP (2000). PIN domains in nonsense-mediated mRNA decay and RNAi. Curr Biol, 10(24), R888–890. [PubMed: 11137022]

COCHRANE JC & STROBEL SA (2008). Catalytic strategies of self-cleaving ribozymes. Acc Chem Res, 41(8), 1027–1035. [PubMed: 18652494]

COLEMAN JE (1992). Structure and mechanism of alkaline phosphatase. Annu Rev Biophys Biomol Struct, 21, 441–483. [PubMed: 1525473]

CONDON C, BRECHEMIER-BAEY D, BELTCHEV B, GRUNBERG-MANAGO M & PUTZER H (2001). Identification of the gene encoding the 5S ribosomal RNA maturase in Bacillus subtilis: mature 5S rRNA is dispensable for ribosome function. RNA, 7(2), 242–253. [PubMed: 11233981]

CORRELL CC, YANG X, GERCZEI T, BENEKEN J & PLANTINGA MJ (2004). RNA recognition and base flipping by the toxin sarcin. J Synchrotron Radiat, 11(Pt 1), 93–96. [PubMed: 14646144]

COWAN JA (2002). Structural and catalytic chemistry of magnesium-dependent enzymes. Biometals, 15(3), 225–235. [PubMed: 12206389]

CROW YJ, HAYWARD BE, PARMAR R, ROBINS P, LEITCH A, ALI M, BLACK DN, VAN BOKHOVEN H, BRUNNER HG, HAMEL BC, CORRY PC, COWAN FM, FRINTS SG, KLEPPER J, LIVINGSTON JH, LYNCH SA, MASSEY RF, MERITET JF, MICHAUD JL, PONSOT G, VOIT T, LEBON P, BONTHRON DT, JACKSON AP, BARNES DE & LINDAHL T (2006a). Mutations in the gene encoding the 3'−5' DNA exonuclease TREX1 cause Aicardi-Goutieres syndrome at the AGS1 locus. Nat Genet, 38(8), 917–920. [PubMed: 16845398]

CROW YJ, LEITCH A, HAYWARD BE, GARNER A, PARMAR R, GRIFFITH E, ALI M, SEMPLE C, AICARDI J, BABUL-HIRJI R, BAUMANN C, BAXTER P, BERTINI E, CHANDLER KE, CHITAYAT D, CAU D, DERY C, FAZZI E, GOIZET C, KING MD, KLEPPER J, LACOMBE D, LANZI G, LYALL H, MARTINEZ-FRIAS ML, MATHIEU M, MCKEOWN C, MONIER A, OADE Y, QUARRELL OW, RITTEY CD, ROGERS RC, SANCHIS A, STEPHENSON JB, TACKE U, TILL M, TOLMIE JL, TOMLIN P, VOIT T, WESCHKE B, WOODS CG, LEBON P, BONTHRON DT, PONTING CP & JACKSON AP (2006b). Mutations in genes encoding ribonuclease H2 subunits cause Aicardi-Goutieres syndrome and mimic congenital viral brain infection. Nat Genet, 38(8), 910–916. [PubMed: 16845400]

CROW YJ & REHWINKEL J (2009). Aicardi-Goutieres syndrome and related phenotypes: linking nucleic acid metabolism with autoimmunity. Hum Mol Genet, 18(R2), R130–136. [PubMed: 19808788]

CYMERMAN IA, OBARSKA A, SKOWRONEK KJ, LUBYS A & BUJNICKI JM (2006). Identification of a new subfamily of HNH nucleases and experimental characterization of a representative member, HphI restriction endonuclease. Proteins, 65(4), 867–876. [PubMed: 17029241]

DAIYASU H, OSAKA K, ISHINO Y & TOH H (2001). Expansion of the zinc metallo-hydrolase family of the beta-lactamase fold. FEBS Lett, 503(1), 1–6. [PubMed: 11513844]

DATTA S, LARKIN C & SCHILDBACH JF (2003). Structural insights into single-stranded DNA binding and cleavage by F factor TraI. Structure, 11(11), 1369–1379. [PubMed: 14604527]

DAVIES DR, GORYSHIN IY, REZNIKOFF WS & RAYMENT I (2000). Three-dimensional structure of the Tn5 synaptic complex transposition intermediate. Science, 289(5476), 77–85. [PubMed: 10884228]

DAVIES DR, INTERTHAL H, CHAMPOUX JJ & HOL WG (2004). Explorations of peptide and oligonucleotide binding sites of tyrosyl-DNA phosphodiesterase using vanadate complexes. J Med Chem, 47(4), 829–837. [PubMed: 14761185]

DAVIES DR, MUSHTAQ A, INTERTHAL H, CHAMPOUX JJ & HOL WG (2006). The structure of the transition state of the heterodimeric topoisomerase I of Leishmania donovani as a vanadate complex with nicked DNA. J Mol Biol, 357(4), 1202–1210. [PubMed: 16487540]

DE LA SIERRA-GALLAY IL, PELLEGRINI O & CONDON C (2005). Structural basis for substrate binding, cleavage and allostery in the tRNA maturase RNase Z. Nature, 433(7026), 657–661. [PubMed: 15654328]

DE SILVA U, CHOUDHURY S, BAILEY SL, HARVEY S, PERRINO FW & HOLLIS T (2007). The crystal structure of TREX1 explains the 3' nucleotide specificity and reveals a polyproline II helix for protein partnering. J Biol Chem, 282(14), 10537–10543. [PubMed: 17293595]

DECLAIS AC & LILLEY DM (2008). New insight into the recognition of branched DNA structure by junction-resolving enzymes. Curr Opin Struct Biol, 18(1), 86–95. [PubMed: 18160275]

DEMPLE B & HARRISON L (1994). Repair of oxidative damage to DNA: enzymology and biology. Annu Rev Biochem, 63, 915–948. [PubMed: 7979257]

DESAI NA & SHANKAR V (2003). Single-strand-specific nucleases. FEMS Microbiol Rev, 26(5), 457–491. [PubMed: 12586391]

DESHPANDE RA & SHANKAR V (2002). Ribonucleases from T2 family. Crit Rev Microbiol, 28(2), 79–122. [PubMed: 12109772]

DEUTSCHER MP & LI Z (2001). Exoribonucleases and their multiple roles in RNA metabolism. Prog Nucleic Acid Res Mol Biol, 66, 67–105. [PubMed: 11051762]

DEUTSCHER MP, MARSHALL GT & CUDNY H (1988). RNase PH: an Escherichia coli phosphate-dependent nuclease distinct from polynucleotide phosphorylase. Proc Natl Acad Sci U S A, 85(13), 4710–4714. [PubMed: 2455297]

DEVOS JM, TOMANICEK SJ, JONES CE, NOSSAL NG & MUESER TC (2007). Crystal structure of bacteriophage T4 5' nuclease in complex with a branched DNA reveals how flap endonuclease-1 family nucleases bind their substrates. J Biol Chem, 282(43), 31713–31724. [PubMed: 17693399]

DIAZ RL, ALCID AD, BERGER JM & KEENEY S (2002). Identification of residues in yeast Spo11p critical for meiotic DNA double-strand break formation. Mol Cell Biol, 22(4), 1106–1115. [PubMed: 11809802]

DIEBLER H, EIGEN M, ILGENFRITZ G, MAASS G & WINKLER R (1969). Kinetics and mechanisms of reactions of main group metal ions with biological carriers. Pure Appl. Chem , 20(1), 93–115.

DILLINGHAM MS & KOWALCZYKOWSKI SC (2008). RecBCD enzyme and the repair of double-stranded DNA breaks. Microbiol Mol Biol Rev, 72(4), 642–671, Table of Contents. [PubMed: 19052323]

DOMANICO PL & TSE-DINH YC (1991). Mechanistic studies on E. coli DNA topoisomerase I: divalent ion effects. J Inorg Biochem, 42(2), 87–96. [PubMed: 1649911]

DOMINSKI Z (2007). Nucleases of the metallo-beta-lactamase family and their role in DNA and RNA metabolism. Crit Rev Biochem Mol Biol, 42(2), 67–93. [PubMed: 17453916]

DONG B, NIWA M, WALTER P & SILVERMAN RH (2001). Basis for regulated RNA cleavage by functional analysis of RNase L and Ire1p. RNA, 7(3), 361–373. [PubMed: 11333017]

DONG KC & BERGER JM (2007). Structural basis for gate-DNA recognition and bending by type IIA topoisomerases. Nature, 450(7173), 1201–1205. [PubMed: 18097402]

DOUDNA JA & CECH TR (2002). The chemical repertoire of natural ribozymes. Nature, 418(6894), 222–228. [PubMed: 12110898]

DRYDEN DT, MURRAY NE & RAO DN (2001). Nucleoside triphosphate-dependent restriction enzymes. Nucleic Acids Res, 29(18), 3728–3741. [PubMed: 11557806]

DUAN X, GIMBLE FS & QUIOCHO FA (1997). Crystal structure of PI-SceI, a homing endonuclease with protein splicing activity. Cell, 89(4), 555–564. [PubMed: 9160747]

DYDA F, HICKMAN AB, JENKINS TM, ENGELMAN A, CRAIGIE R & DAVIES DR (1994). Crystal structure of the catalytic domain of HIV-1 integrase: similarity to other polynucleotidyl transferases. Science, 266(5193), 1981–1986. [PubMed: 7801124]

DZIEMBOWSKI A, LORENTZEN E, CONTI E & SERAPHIN B (2007). A single subunit, Dis3, is essentially responsible for yeast exosome core activity. Nat Struct Mol Biol, 14(1), 15–22. [PubMed: 17173052]

EBERLE AB, LYKKE-ANDERSEN S, MUHLEMANN O & JENSEN TH (2009). SMG6 promotes endonucleolytic cleavage of nonsense mRNA in human cells. Nat Struct Mol Biol, 16(1), 49–55. [PubMed: 19060897]

EBIHARA A, YAO M, MASUI R, TANAKA I, YOKOYAMA S & KURAMITSU S (2006). Crystal structure of hypothetical protein TTHB192 from Thermus thermophilus HB8 reveals a new protein family with an RNA recognition motif-like domain. Protein Sci, 15(6), 1494–1499. [PubMed: 16672237]

ECKSTEIN F (1985). Nucleoside phosphorothioates. Annu Rev Biochem, 54, 367–402. [PubMed: 2411211]

ENARI M, SAKAHIRA H, YOKOYAMA H, OKAWA K, IWAMATSU A & NAGATA S (1998). A caspase-activated DNase that degrades DNA during apoptosis, and its inhibitor ICAD. Nature, 391(6662), 43–50. [PubMed: 9422506]

FALVEY E, HATFULL GF & GRINDLEY ND (1988). Uncoupling of the recombination and topoisomerase activities of the gamma delta resolvase by a mutation at the crossover point. Nature, 332(6167), 861–863. [PubMed: 2833710]

FARAZI TA, JURANEK SA & TUSCHL T (2008). The growing catalog of small RNAs and their association with distinct Argonaute/Piwi family members. Development, 135(7), 1201–1214. [PubMed: 18287206]

FEKAIRI S, SCAGLIONE S, CHAHWAN C, TAYLOR ER, TISSIER A, COULON S, DONG MQ, RUSE C, YATES JR, 3RD, RUSSELL P, FUCHS RP, MCGOWAN CH & GAILLARD PH (2009). Human SLX4 is a Holliday junction resolvase subunit that binds multiple DNA repair/recombination endonucleases. Cell, 138(1), 78–89. [PubMed: 19596236]

FEKETE RA & FROST LS (2000). Mobilization of chimeric oriT plasmids by F and R100–1: role of relaxosome formation in defining plasmid specificity. J Bacteriol, 182(14), 4022–4027. [PubMed: 10869081]

FERRE-D'AMARE AR, ZHOU K & DOUDNA JA (1998). Crystal structure of a hepatitis delta virus ribozyme. Nature, 395(6702), 567–574. [PubMed: 9783582]

FERSHT AR & DAGGETT V (2002). Protein folding and unfolding at atomic resolution. Cell, 108(4), 573–582. [PubMed: 11909527]

FIEDLER TJ, VINCENT HA, ZUO Y, GAVRIALOV O & MALHOTRA A (2004). Purification and crystallization of Escherichia coli oligoribonuclease. Acta Crystallogr D Biol Crystallogr, 60(Pt 4), 736–739. [PubMed: 15039570]

FLAHERTY KM, MCKAY DB, KABSCH W & HOLMES KC (1991). Similarity of the three-dimensional structures of actin and the ATPase fragment of a 70-kDa heat shock cognate protein. Proc Natl Acad Sci U S A, 88(11), 5041–5045. [PubMed: 1828889]

FLICK KE, JURICA MS, MONNAT RJ, JR. & STODDARD BL (1998). DNA binding and cleavage by the nuclear intron-encoded homing endonuclease I-PpoI. Nature, 394(6688), 96–101. [PubMed: 9665136]

FOGG JM, KVARATSKHELIA M, WHITE MF & LILLEY DM (2001). Distortion of DNA junctions imposed by the binding of resolving enzymes: a fluorescence study. J Mol Biol, 313(4), 751–764. [PubMed: 11697901]

FONTECILLA-CAMPS JC, DE LLORENS R, LE DU MH & CUCHILLO CM (1994). Crystal structure of ribonuclease A.d(ApTpApApG) complex. Direct evidence for extended substrate recognition. J Biol Chem, 269(34), 21526–21531. [PubMed: 8063789]

FRAZAO C, MCVEY CE, AMBLAR M, BARBAS A, VONRHEIN C, ARRAIANO CM & CARRONDO MA (2006). Unravelling the dynamics of RNA degradation by ribonuclease II and its RNA-bound complex. Nature, 443(7107), 110–114. [PubMed: 16957732]

FREEMONT PS, FRIEDMAN JM, BEESE LS, SANDERSON MR & STEITZ TA (1988). Cocrystal structure of an editing complex of Klenow fragment with DNA. Proc Natl Acad Sci U S A, 85(23), 8924–8928. [PubMed: 3194400]

FRIEDHOFF P, FRANKE I, MEISS G, WENDE W, KRAUSE KL & PINGOUD A (1999). A similar active site for non-specific and specific endonucleases. Nat Struct Biol, 6(2), 112–113. [PubMed: 10048918]

FRIEDHOFF P, KOLMES B, GIMADUTDINOW O, WENDE W, KRAUSE KL & PINGOUD A (1996). Analysis of the mechanism of the Serratia nuclease using site-directed mutagenesis. Nucleic Acids Res, 24(14), 2632–2639. [PubMed: 8758988]

GABEL HW & RUVKUN G (2008). The exonuclease ERI-1 has a conserved dual role in 5.8S rRNA processing and RNAi. Nat Struct Mol Biol, 15(5), 531–533. [PubMed: 18438419]

GAN J, SHAW G, TROPEA JE, WAUGH DS, COURT DL & JI X (2008). A stepwise model for double-stranded RNA processing by ribonuclease III. Mol Microbiol, 67(1), 143–154. [PubMed: 18047582]

GAN J, TROPEA JE, AUSTIN BP, COURT DL, WAUGH DS & JI X (2006). Structural insight into the mechanism of double-stranded RNA processing by ribonuclease III. Cell, 124(2), 355–366. [PubMed: 16439209]

GARCIN ED, HOSFIELD DJ, DESAI SA, HAAS BJ, BJORAS M, CUNNINGHAM RP & TAINER JA (2008). DNA apurinic-apyrimidinic site binding and excision by endonuclease IV. Nat Struct Mol Biol, 15(5), 515–522. [PubMed: 18408731]

GENSCHEL J, BAZEMORE LR & MODRICH P (2002). Human exonuclease I is required for 5' and 3' mismatch repair. J Biol Chem, 277(15), 13302–13311. [PubMed: 11809771]

GERLT JA, CODERRE JA & MEHDI S (1983). Oxygen chiral phosphate esters. Adv Enzymol Relat Areas Mol Biol, 55, 291–380. [PubMed: 6312782]

GHOSH K, GUO F & VAN DUYNE GD (2007a). Synapsis of loxP sites by Cre recombinase. J Biol Chem, 282(33), 24004–24016. [PubMed: 17573343]

GHOSH M, MEISS G, PINGOUD AM, LONDON RE & PEDERSEN LC (2007b). The nuclease a-inhibitor complex is characterized by a novel metal ion bridge. J Biol Chem, 282(8), 5682–5690. [PubMed: 17138564]

GLAVAN F, BEHM-ANSMANT I, IZAURRALDE E & CONTI E (2006). Structures of the PIN domains of SMG6 and SMG5 reveal a nuclease within the mRNA surveillance complex. Embo J, 25(21), 5117–5125. [PubMed: 17053788]

GOMIS-RUTH FX & COLL M (2006). Cut and move: protein machinery for DNA processing in bacterial conjugation. Curr Opin Struct Biol, 16(6), 744–752. [PubMed: 17079132]

GORCHAKOVA GA (1981). [Polynucleotide phosphorylase from rat liver nuclei. Determination of the activity and some properties]. Biokhimiia, 46(5), 797–801. [PubMed: 7295810]

GORMAN MA, MORERA S, ROTHWELL DG, DE LA FORTELLE E, MOL CD, TAINER JA, HICKSON ID & FREEMONT PS (1997). The crystal structure of the human DNA repair endonuclease HAP1 suggests the recognition of extra-helical deoxyribose at DNA abasic sites. Embo J, 16(21), 6548–6558. [PubMed: 9351835]

GOTTLIN EB, RUDOLPH AE, ZHAO Y, MATTHEWS HR & DIXON JE (1998). Catalytic mechanism of the phospholipase D superfamily proceeds via a covalent phosphohistidine intermediate. Proc Natl Acad Sci U S A, 95(16), 9202–9207. [PubMed: 9689058]

GRAILLE M, MORA L, BUCKINGHAM RH, VAN TILBEURGH H & DE ZAMAROCZY M (2004). Structural inhibition of the colicin D tRNase by the tRNA-mimicking immunity protein. Embo J, 23(7), 1474–1482. [PubMed: 15014439]

GRAZULIS S, MANAKOVA E, ROESSLE M, BOCHTLER M, TAMULAITIENE G, HUBER R & SIKSNYS V (2005). Structure of the metal-independent restriction enzyme BfiI reveals fusion of a specific DNA-binding domain with a nonspecific nuclease. Proc Natl Acad Sci U S A, 102(44), 15797–15802. [PubMed: 16247004]

GRIFFITH JP, KIM JL, KIM EE, SINTCHAK MD, THOMSON JA, FITZGIBBON MJ, FLEMING MA, CARON PR, HSIAO K & NAVIA MA (1995). X-ray structure of calcineurin inhibited by the immunophilin-immunosuppressant FKBP12-FK506 complex. Cell, 82(3), 507–522. [PubMed: 7543369]

GRINDLEY ND, WHITESON KL & RICE PA (2006). Mechanisms of site-specific recombination. Annu Rev Biochem, 75, 567–605. [PubMed: 16756503]

GUERRIER-TAKADA C, GARDINER K, MARSH T, PACE N & ALTMAN S (1983). The RNA moiety of ribonuclease P is the catalytic subunit of the enzyme. Cell, 35(3 Pt 2), 849–857. [PubMed: 6197186]

GUO F, GOPAUL DN & VAN DUYNE GD (1997). Structure of Cre recombinase complexed with DNA in a site-specific recombination synapse. Nature, 389(6646), 40–46. [PubMed: 9288963]

HABRAKEN Y, SUNG P, PRAKASH L & PRAKASH S (1993). Yeast excision repair gene RAD2 encodes a single-stranded DNA endonuclease. Nature, 366(6453), 365–368. [PubMed: 8247134]

HABRAKEN Y, SUNG P, PRAKASH L & PRAKASH S (1994). A conserved 5’ to 3’ exonuclease activity in the yeast and human nucleotide excision repair proteins RAD2 and XPG. J Biol Chem, 269(50), 31342–31345. [PubMed: 7989298]

HADDEN JM, DÉCLAIS A-C, CARR SB, LILLEY DMJ & PHILLIPS EV (2007). The structural basis of Holliday junction resolution. Nature 449, 621–624. [PubMed: 17873858]

HALE SP, POOLE LB & GERLT JA (1993). Mechanism of the reaction catalyzed by staphylococcal nuclease: identification of the rate-determining step. Biochemistry, 32(29), 7479–7487. [PubMed: 8338846]

HAMDAN S, CARR PD, BROWN SE, OLLIS DL & DIXON NE (2002). Structural basis for proofreading during replication of the Escherichia coli chromosome. Structure, 10(4), 535–546. [PubMed: 11937058]

HARDING MM (1999). The geometry of metal-ligand interactions relevant to proteins. Acta Crystallogr D Biol Crystallogr, 55 (Pt 8), 1432–1443. [PubMed: 10417412]

HARE S, GUPTA SS, VALKOV E, ENGELMAN A & CHEREPANOV P (2010) Retroviral intasome assembly and inhibition of DNA strand transfer. Nature, 464(7286), 232–236. [PubMed: 20118915]

HARRINGTON JJ & LIEBER MR (1994). The characterization of a mammalian DNA structure-specific endonuclease. Embo J, 13(5), 1235–1246. [PubMed: 8131753]

HARUKI M, TSUNAKA Y, MORIKAWA M, IWAI S & KANAYA S (2000). Catalysis by Escherichia coli ribonuclease HI is facilitated by a phosphate group of the substrate. Biochemistry, 39(45), 13939–13944. [PubMed: 11076536]

HENNECKE F, KOLMAR H, BRUNDL K & FRITZ HJ (1991). The vsr gene product of E. coli K-12 is a strand- and sequence-specific DNA mismatch endonuclease. Nature, 353(6346), 776–778. [PubMed: 1944537]

HERNICK M & FIERKE CA (2005). Zinc hydrolases: the mechanisms of zinc-dependent deacetylases. Arch Biochem Biophys, 433(1), 71–84. [PubMed: 15581567]

HICKMAN AB, PEREZ ZN, ZHOU L, MUSINGARIMI P, GHIRLANDO R, HINSHAW JE, CRAIG NL & DYDA F (2005). Molecular architecture of a eukaryotic DNA transposase. Nat Struct Mol Biol, 12(8), 715–721. [PubMed: 16041385]

HICKMAN AB, RONNING DR, KOTIN RM & DYDA F (2002). Structural unity among viral origin binding proteins: crystal structure of the nuclease domain of adeno-associated virus Rep. Mol Cell, 10(2), 327–337. [PubMed: 12191478]

HICKMAN AB, RONNING DR, PEREZ ZN, KOTIN RM & DYDA F (2004). The nuclease domain of adeno-associated virus rep coordinates replication initiation using two distinct DNA recognition interfaces. Mol Cell, 13(3), 403–414. [PubMed: 14967147]

HICKMAN AB, WANINGER S, SCOCCA JJ & DYDA F (1997). Molecular organization in site-specific recombination: the catalytic domain of bacteriophage HP1 integrase at 2.7 A resolution. Cell, 89(2), 227–237. [PubMed: 9108478]

HOARD DE & GOAD W (1968). Products in the initial stages of digestion of polydeoxynucleotides by pancreatic deoxyribonuclease (DNase I). J Mol Biol, 31(3), 595–606. [PubMed: 4295316]

HOPFNER KP, KARCHER A, CRAIG L, WOO TT, CARNEY JP & TAINER JA (2001). Structural biochemistry and interaction architecture of the DNA double-strand break repair Mre11 nuclease and Rad50-ATPase. Cell, 105(4), 473–485. [PubMed: 11371344]

HORTON NC (2008). DNA Nucleases In Protein-Nucleic Acid Interactions eds. Rice PA and Correll CC), pp. 333–363. Cambridge: Royal Society of Chemistry Publishing.

HORTON NC & PERONA JJ (2004). DNA cleavage by EcoRV endonuclease: two metal ions in three metal ion binding sites. Biochemistry, 43(22), 6841–6857. [PubMed: 15170321]

HOUGH E, HANSEN LK, BIRKNES B, JYNGE K, HANSEN S, HORDVIK A, LITTLE C, DODSON E & DEREWENDA Z (1989). High-resolution (1.5 A) crystal structure of phospholipase C from Bacillus cereus. Nature, 338(6213), 357–360. [PubMed: 2493587]

HOUSELEY J, LACAVA J & TOLLERVEY D (2006). RNA-quality control by the exosome. Nat Rev Mol Cell Biol, 7(7), 529–539. [PubMed: 16829983]

HSIA KC, LI CL & YUAN HS (2005). Structural and functional insight into sugar-nonspecific nucleases in host defense. Curr Opin Struct Biol, 15(1), 126–134. [PubMed: 15718143]

HSIAO YY, NAKAGAWA A, SHI Z, MITANI S, XUE D & YUAN HS (2009). Crystal structure of CRN-4: implications for domain function in apoptotic DNA degradation. Mol Cell Biol, 29(2), 448–457. [PubMed: 18981218]

HWANG KY, BAEK K, KIM HY & CHO Y (1998). The crystal structure of flap endonuclease-1 from Methanococcus jannaschii. Nat Struct Biol, 5(8), 707–713. [PubMed: 9699635]

IP SC, RASS U, BLANCO MG, FLYNN HR, SKEHEL JM & WEST SC (2008). Identification of Holliday junction resolvases from humans and yeast. Nature, 456(7220), 357–361. [PubMed: 19020614]

IRIE M & OHGI K (2001). Ribonuclease T2. Methods Enzymol, 341, 42–55. [PubMed: 11582795]

ISHII R, MINAGAWA A, TAKAKU H, TAKAGI M, NASHIMOTO M & YOKOYAMA S (2005). Crystal structure of the tRNA 3' processing endoribonuclease tRNase Z from Thermotoga maritima. J Biol Chem, 280(14), 14138–14144. [PubMed: 15701599]

ISHIKAWA K, WATANABE M, KUROITA T, UCHIYAMA I, BUJNICKI JM, KAWAKAMI B, TANOKURA M & KOBAYASHI I (2005). Discovery of a novel restriction endonuclease by genome comparison and application of a wheat-germ-based cell-free translation assay: PabI (5'-GTA/C) from the hyperthermophilic archaeon Pyrococcus abyssi. Nucleic Acids Res, 33(13), e112. [PubMed: 16040595]

IVANOV I, TAINER JA & MCCAMMON JA (2007). Unraveling the three-metal-ion catalytic mechanism of the DNA repair enzyme endonuclease IV. Proc Natl Acad Sci U S A, 104(5), 1465–1470. [PubMed: 17242363]

IWASAKI H, TAKAHAGI M, SHIBA T, NAKATA A & SHINAGAWA H (1991). Escherichia coli RuvC protein is an endonuclease that resolves the Holliday structure. Embo J, 10(13), 4381–4389. [PubMed: 1661673]

JABRI E, CARR MB, HAUSINGER RP & KARPLUS PA (1995). The crystal structure of urease from Klebsiella aerogenes. Science, 268(5213), 998–1004. [PubMed: 7754395]

JAKUBAUSKAS A, GIEDRIENE J, BUJNICKI JM & JANULAITIS A (2007). Identification of a single HNH active site in type IIS restriction endonuclease Eco31I. J Mol Biol, 370(1), 157–169. [PubMed: 17499273]

JAMES R, KLEANTHOUS C & MOORE GR (1996). The biology of E colicins: paradigms and paradoxes. Microbiology, 142 (Pt 7), 1569–1580. [PubMed: 8757721]

JENNY A, MINVIELLE-SEBASTIA L, PREKER PJ & KELLER W (1996). Sequence similarity between the 73-kilodalton protein of mammalian CPSF and a subunit of yeast polyadenylation factor I. Science, 274(5292), 1514–1517. [PubMed: 8929409]

JENSCH F & KEMPER B (1986). Endonuclease VII resolves Y-junctions in branched DNA in vitro. Embo J, 5(1), 181–189. [PubMed: 3007114]

JI X (2008). The mechanism of RNase III action: how dicer dices. Curr Top Microbiol Immunol, 320, 99–116. [PubMed: 18268841]

JIN Y, BINKOWSKI G, SIMON LD & NORRIS D (1997). Ho endonuclease cleaves MAT DNA in vitro by an inefficient stoichiometric reaction mechanism. J Biol Chem, 272(11), 7352–7359. [PubMed: 9054434]

JOHNSON ER & MCKAY DB (1999). Mapping the role of active site residues for transducing an ATP-induced conformational change in the bovine 70-kDa heat shock cognate protein. Biochemistry, 38(33), 10823–10830. [PubMed: 10451379]

JONES SJ, WORRALL AF & CONNOLLY BA (1996). Site-directed mutagenesis of the catalytic residues of bovine pancreatic deoxyribonuclease I. J Mol Biol, 264(5), 1154–1163. [PubMed: 9000637]

JONSTRUP AT, ANDERSEN KR, VAN LB & BRODERSEN DE (2007). The 1.4-A crystal structure of the S. pombe Pop2p deadenylase subunit unveils the configuration of an active enzyme. Nucleic Acids Res, 35(9), 3153–3164. [PubMed: 17452359]

JOSHUA-TOR L (2006). The Argonautes. Cold Spring Harb Symp Quant Biol, 71, 67–72. [PubMed: 17381282]

KAMINSKA KH, KAWAI M, BONIECKI M, KOBAYASHI I & BUJNICKI JM (2008). Type II restriction endonuclease R.Hpy188I belongs to the GIY-YIG nuclease superfamily, but exhibits an unusual active site. BMC Struct Biol, 8, 48. [PubMed: 19014591]

KAO HI & BAMBARA RA (2003). The protein components and mechanism of eukaryotic Okazaki fragment maturation. Crit Rev Biochem Mol Biol, 38(5), 433–452. [PubMed: 14693726]

KARAKAS E, TRUGLIO JJ, CROTEAU D, RHAU B, WANG L, VAN HOUTEN B & KISKER C (2007). Structure of the C-terminal half of UvrC reveals an RNase H endonuclease domain with an Argonaute-like catalytic triad. Embo J, 26(2), 613–622. [PubMed: 17245438]

KARTHA G, BELLO J & HARKER D (1967). Tertiary structure of ribonuclease. Nature, 213(5079), 862–865. [PubMed: 6043657]

KAWANO S, KAKUTA Y, NAKASHIMA T & KIMURA M (2006). Crystal structures of the Nicotiana glutinosa ribonuclease NT in complex with nucleoside monophosphates. J Biochem, 140(3), 375–381. [PubMed: 16870673]

KECK JL, ROCHE DD, LYNCH AS & BERGER JM (2000). Structure of the RNA polymerase domain of E. coli primase. Science, 287(5462), 2482–2486. [PubMed: 10741967]

KEENEY S (2001). Mechanism and control of meiotic recombination initiation. Curr Top Dev Biol, 52, 1–53. [PubMed: 11529427]

KENNEDY AK, HANIFORD DB & MIZUUCHI K (2000). Single active site catalysis of the successive phosphoryl transfer steps by DNA transposases: insights from phosphorothioate stereoselectivity. Cell, 101(3), 295–305. [PubMed: 10847684]

KHAN SA (2005). Plasmid rolling-circle replication: highlights of two decades of research. Plasmid, 53(2), 126–136. [PubMed: 15737400]

KIM DH & MOBASHERY S (2001). Mechanism-based inhibition of zinc proteases. Curr Med Chem, 8(8), 959–965. [PubMed: 11375763]

KIM DR, DAI Y, MUNDY CL, YANG W & OETTINGER MA (1999). Mutations of acidic residues in RAG1 define the active site of the V(D)J recombinase. Genes Dev, 13(23), 3070–3080. [PubMed: 10601033]

KIM EE & WYCKOFF HW (1991). Reaction mechanism of alkaline phosphatase based on crystal structures. Two-metal ion catalysis. J Mol Biol, 218(2), 449–464. [PubMed: 2010919]

KIM JH, KIM HD, RYU GH, KIM DH, HURWITZ J & SEO YS (2006). Isolation of human Dna2 endonuclease and characterization of its enzymatic properties. Nucleic Acids Res, 34(6), 1854–1864. [PubMed: 16595799]

KIM Y, EOM SH, WANG J, LEE DS, SUH SW & STEITZ TA (1995). Crystal structure of Thermus aquaticus DNA polymerase. Nature, 376(6541), 612–616. [PubMed: 7637814]

KIRSEBOM LA (2007). RNase P RNA mediated cleavage: substrate recognition and catalysis. Biochimie, 89(10), 1183–1194. [PubMed: 17624654]

KLEANTHOUS C, KUHLMANN UC, POMMER AJ, FERGUSON N, RADFORD SE, MOORE GR, JAMES R & HEMMINGS AM (1999). Structural and mechanistic basis of immunity toward endonuclease colicins. Nat Struct Biol, 6(3), 243–252. [PubMed: 10074943]

KLEIN DJ & FERRE-D'AMARE AR (2006). Structural basis of glmS ribozyme activation by glucosamine-6-phosphate. Science, 313(5794), 1752–1756. [PubMed: 16990543]

KLETT RP, CERAMI A & REICH E (1968). Exonuclease VI, a new nuclease activity associated with E. coli DNA polymerase. Proc Natl Acad Sci U S A, 60(3), 943–950. [PubMed: 4875807]

KO TP, LIAO CC, KU WY, CHAK KF & YUAN HS (1999). The crystal structure of the DNase domain of colicin E7 in complex with its inhibitor Im7 protein. Structure, 7(1), 91–102. [PubMed: 10368275]

KOBE B & DEISENHOFER J (1996). Mechanism of ribonuclease inhibition by ribonuclease inhibitor protein based on the crystal structure of its complex with ribonuclease A. J Mol Biol, 264(5), 1028–1043. [PubMed: 9000628]

KOLADE OO, CARR SB, KUHLMANN UC, POMMER A, KLEANTHOUS C, BOUCHCINSKY CA & HEMMINGS AM (2002). Structural aspects of the inhibition of DNase and rRNase colicins by their immunity proteins. Biochimie, 84(5–6), 439–446. [PubMed: 12423787]

KOLODNER R, HALL SD & LUISI-DELUCA C (1994). Homologous pairing proteins encoded by the Escherichia coli recE and recT genes. Mol Microbiol, 11(1), 23–30. [PubMed: 8145642]

KOONIN EV & ILYINA TV (1993). Computer-assisted dissection of rolling circle DNA replication. Biosystems, 30(1–3), 241–268. [PubMed: 8374079]

KOSTELECKY B, POHL E, VOGEL A, SCHILLING O & MEYER-KLAUCKE W (2006). The crystal structure of the zinc phosphodiesterase from Escherichia coli provides insight into function and cooperativity of tRNase Z-family proteins. J Bacteriol, 188(4), 1607–1614. [PubMed: 16452444]

KOVALL R & MATTHEWS BW (1997). Toroidal structure of lambda-exonuclease. Science, 277(5333), 1824–1827. [PubMed: 9295273]

KOWALCZYKOWSKI SC, DIXON DA, EGGLESTON AK, LAUDER SD & REHRAUER WM (1994). Biochemistry of homologous recombination in Escherichia coli. Microbiol Rev, 58(3), 401–465. [PubMed: 7968921]

KRUGER K, GRABOWSKI PJ, ZAUG AJ, SANDS J, GOTTSCHLING DE & CECH TR (1982). Self-splicing RNA: autoexcision and autocyclization of the ribosomal RNA intervening sequence of Tetrahymena. Cell, 31(1), 147–157. [PubMed: 6297745]

KUHLMANN UC, MOORE GR, JAMES R, KLEANTHOUS C & HEMMINGS AM (1999). Structural parsimony in endonuclease active sites: should the number of homing endonuclease families be redefined? FEBS Lett, 463(1–2), 1–2. [PubMed: 10601625]

KUNITZ M (1950). Crystalline desoxyribonuclease; isolation and general properties; spectrophotometric method for the measurement of desoxyribonuclease activity. J Gen Physiol, 33(4), 349–362. [PubMed: 15406373]

KWON HJ, TIRUMALAI R, LANDY A & ELLENBERGER T (1997). Flexibility in DNA recombination: structure of the lambda integrase catalytic core. Science, 276(5309), 126–131. [PubMed: 9082984]

LAGERBACK P, ANDERSSON E, MALMBERG C & CARLSON K (2009). Bacteriophage T4 endonuclease II, a promiscuous GIY-YIG nuclease, binds as a tetramer to two DNA substrates. Nucleic Acids Res, 37(18), 6174–6183. [PubMed: 19666720]

LAGUNAVICIUS A, SASNAUSKAS G, HALFORD SE & SIKSNYS V (2003). The metal-independent type IIs restriction enzyme BfiI is a dimer that binds two DNA sites but has only one catalytic centre. J Mol Biol, 326(4), 1051–1064. [PubMed: 12589753]

LAM AF, KROGH BO & SYMINGTON LS (2008). Unique and overlapping functions of the Exo1, Mre11 and Pso2 nucleases in DNA repair. DNA Repair (Amst), 7(4), 655–662. [PubMed: 18295552]

LANDREE MA, WIBBENMEYER JA & ROTH DB (1999). Mutational analysis of RAG1 and RAG2 identifies three catalytic amino acids in RAG1 critical for both cleavage steps of V(D)J recombination. Genes Dev, 13(23), 3059–3069. [PubMed: 10601032]

LANEVE P, ALTIERI F, FIORI ME, SCALONI A, BOZZONI I & CAFFARELLI E (2003). Purification, cloning, and characterization of XendoU, a novel endoribonuclease involved in processing of intron-encoded small nucleolar RNAs in Xenopus laevis. J Biol Chem, 278(15), 13026–13032. [PubMed: 12571235]

LANEVE P, GIOIA U, RAGNO R, ALTIERI F, DI FRANCO C, SANTINI T, ARCECI M, BOZZONI I & CAFFARELLI E (2008). The tumor marker human placental protein 11 is an endoribonuclease. J Biol Chem, 283(50), 34712–34719. [PubMed: 18936097]

LANGE SJ & QUE L, JR. (1998). Oxygen activating nonheme iron enzymes. Curr Opin Chem Biol, 2(2), 159–172. [PubMed: 9667935]

LAPKOUSKI M, PANJIKAR S, JANSCAK P, SMATANOVA IK, CAREY J, ETTRICH R & CSEFALVAY E (2009). Structure of the motor subunit of type I restriction-modification complex EcoR124I. Nat Struct Mol Biol, 16(1), 94–95. [PubMed: 19079266]

LARKIN C, DATTA S, HARLEY MJ, ANDERSON BJ, EBIE A, HARGREAVES V & SCHILDBACH JF (2005). Inter- and intramolecular determinants of the specificity of single-stranded DNA binding and cleavage by the F factor relaxase. Structure, 13(10), 1533–1544. [PubMed: 16216584]

LARKIN C, HAFT RJ, HARLEY MJ, TRAXLER B & SCHILDBACH JF (2007). Roles of active site residues and the HUH motif of the F plasmid TraI relaxase. J Biol Chem, 282(46), 33707–33713. [PubMed: 17890221]

LASKOWSKI M, SR. (1985). Nucleases: historical erspectives In Nucleases eds. Linn SM and Roberts RJ), pp. 1–21. Cold Spring Harbor, NY: Cold Spring Harbor Laboratory Press.

LEE BI, KIM KH, PARK SJ, EOM SH, SONG HK & SUH SW (2004). Ring-shaped architecture of RecR: implications for its role in homologous recombinational DNA repair. Embo J, 23(10), 2029–2038. [PubMed: 15116069]

LEE BI & WILSON DM, 3RD. (1999). The RAD2 domain of human exonuclease 1 exhibits 5' to 3' exonuclease and flap structure-specific endonuclease activities. J Biol Chem, 274(53), 37763–37769. [PubMed: 10608837]

LEE FS, AULD DS & VALLEE BL (1989). Tryptophan fluorescence as a probe of placental ribonuclease inhibitor binding to angiogenin. Biochemistry, 28(1), 219–224. [PubMed: 2706245]

LEE JY, CHANG J, JOSEPH N, GHIRLANDO R, RAO DN & YANG W (2005). MutH complexed with Hemi- and unmethylated DNAs: coupling base recognition and DNA cleavage. Mol Cell, 20(1), 155–166. [PubMed: 16209953]

LEE KP, DEY M, NECULAI D, CAO C, DEVER TE & SICHERI F (2008). Structure of the dual enzyme Ire1 reveals the basis for catalysis and regulation in nonconventional RNA splicing. Cell, 132(1), 89–100. [PubMed: 18191223]

LEHMAN IR & NUSSBAUM AL (1964). The Deoxyribonucleases of Escherichia Coli. V. on the Specificity of Exonuclease I (Phosphodiesterase). J Biol Chem, 239, 2628–2636. [PubMed: 14235546]

LI W, KAMTEKAR S, XIONG Y, SARKIS GJ, GRINDLEY ND & STEITZ TA (2005). Structure of a synaptic gammadelta resolvase tetramer covalently linked to two cleaved DNAs. Science, 309(5738), 1210–1215. [PubMed: 15994378]

LILLEY DM (2005). Structure, folding and mechanisms of ribozymes. Curr Opin Struct Biol, 15(3), 313–323. [PubMed: 15919196]

LILLEY DM & WHITE MF (2001). The junction-resolving enzymes. Nat Rev Mol Cell Biol, 2(6), 433–443. [PubMed: 11389467]

LIU Q, GREIMANN JC & LIMA CD (2006). Reconstitution, activities, and structure of the eukaryotic RNA exosome. Cell, 127(6), 1223–1237. [PubMed: 17174896]

LIU X, ZOU H, SLAUGHTER C & WANG X (1997). DFF, a heterodimeric protein that functions downstream of caspase-3 to trigger DNA fragmentation during apoptosis. Cell, 89(2), 175–184. [PubMed: 9108473]

LIU Y, KAO HI & BAMBARA RA (2004). Flap endonuclease 1: a central component of DNA metabolism. Annu Rev Biochem, 73, 589–615. [PubMed: 15189154]

LLOSA M, GOMIS-RUTH FX, COLL M & DE LA CRUZ FD F (2002). Bacterial conjugation: a two-step mechanism for DNA transport. Mol Microbiol, 45(1), 1–8. [PubMed: 12100543]

LOLL PJ, QUIRK S, LATTMAN EE & GARAVITO RM (1995). X-ray crystal structures of staphylococcal nuclease complexed with the competitive inhibitor cobalt(II) and nucleotide. Biochemistry, 34(13), 4316–4324. [PubMed: 7703245]

LORENTZEN E, BASQUIN J, TOMECKI R, DZIEMBOWSKI A & CONTI E (2008). Structure of the active subunit of the yeast exosome core, Rrp44: diverse modes of substrate recruitment in the RNase II nuclease family. Mol Cell, 29(6), 717–728. [PubMed: 18374646]

LORENTZEN E, DZIEMBOWSKI A, LINDNER D, SERAPHIN B & CONTI E (2007). RNA channelling by the archaeal exosome. EMBO Rep, 8(5), 470–476. [PubMed: 17380186]

LORENTZEN E, WALTER P, FRIBOURG S, EVGUENIEVA-HACKENBERG E, KLUG G & CONTI E (2005). The archaeal exosome core is a hexameric ring structure with three catalytic subunits. Nat Struct Mol Biol, 12(7), 575–581. [PubMed: 15951817]

LYAMICHEV V, BROW MA & DAHLBERG JE (1993). Structure-specific endonucleolytic cleavage of nucleic acids by eubacterial DNA polymerases. Science, 260(5109), 778–783. [PubMed: 7683443]

LYKKE-ANDERSEN S, BRODERSEN DE & JENSEN TH (2009). Origins and activities of the eukaryotic exosome. J Cell Sci, 122(Pt 10), 1487–1494. [PubMed: 19420235]

LYONS TJ & EIDE DJ (2006). Transport and storage of metal ions in biology In Biological Inorganic Chemistry: Structure and Reactivity eds. Bertini I, Gray HB, Stiefel EI and Valentine JS), pp. 57–77. Herndon, VA: University Science Books.

MACELREVEY C, SALTER JD, KRUCINSKA J & WEDEKIND JE (2008). Structural effects of nucleobase variations at key active site residue Ade38 in the hairpin ribozyme. RNA, 14(8), 1600–1616. [PubMed: 18596253]

MACMASTER R, SEDELNIKOVA S, BAKER PJ, BOLT EL, LLOYD RG & RAFFERTY JB (2006). RusA Holliday junction resolvase: DNA complex structure--insights into selectivity and specificity. Nucleic Acids Res, 34(19), 5577–5584. [PubMed: 17028102]

MACRAE IJ & DOUDNA JA (2007). Ribonuclease revisited: structural insights into ribonuclease III family enzymes. Curr Opin Struct Biol, 17(1), 138–145. [PubMed: 17194582]

MACRAE IJ, ZHOU K & DOUDNA JA (2007). Structural determinants of RNA recognition and cleavage by Dicer. Nat Struct Mol Biol, 14(10), 934–940. [PubMed: 17873886]

MACRAE IJ, ZHOU K, LI F, REPIC A, BROOKS AN, CANDE WZ, ADAMS PD & DOUDNA JA (2006). Structural basis for double-stranded RNA processing by Dicer. Science, 311(5758), 195–198. [PubMed: 16410517]

MAGUIRE ME & COWAN JA (2002). Magnesium chemistry and biochemistry. Biometals, 15(3), 203–210. [PubMed: 12206387]

MAKAROVA KS, GRISHIN NV, SHABALINA SA, WOLF YI & KOONIN EV (2006). A putative RNA-interference-based immune system in prokaryotes: computational analysis of the predicted enzymatic machinery, functional analogies with eukaryotic RNAi, and hypothetical mechanisms of action. Biol Direct, 1, 7. [PubMed: 16545108]

MANDEL CR, KANEKO S, ZHANG H, GEBAUER D, VETHANTHAM V, MANLEY JL & TONG L (2006). Polyadenylation factor CPSF-73 is the pre-mRNA 3'-end-processing endonuclease. Nature, 444(7121), 953–956. [PubMed: 17128255]

MARTI TM & FLECK O (2004). DNA repair nucleases. Cell Mol Life Sci, 61(3), 336–354. [PubMed: 14770297]

MARTINEZ VALLE F, BALADA E, ORDI-ROS J & VILARDELL-TARRES M (2008). DNase 1 and systemic lupus erythematosus. Autoimmun Rev, 7(5), 359–363. [PubMed: 18486922]

MARZLUFF WF, WAGNER EJ & DURONIO RJ (2008). Metabolism and regulation of canonical histone mRNAs: life without a poly(A) tail. Nat Rev Genet, 9(11), 843–854. [PubMed: 18927579]

MASUDA-SASA T, IMAMURA O & CAMPBELL JL (2006). Biochemical analysis of human Dna2. Nucleic Acids Res, 34(6), 1865–1875. [PubMed: 16595800]

MATE MJ & KLEANTHOUS C (2004). Structure-based analysis of the metal-dependent mechanism of H-N-H endonucleases. J Biol Chem, 279(33), 34763–34769. [PubMed: 15190054]

MATHY N, BENARD L, PELLEGRINI O, DAOU R, WEN T & CONDON C (2007). 5'-to-3' exoribonuclease activity in bacteria: role of RNase J1 in rRNA maturation and 5' stability of mRNA. Cell, 129(4), 681–692. [PubMed: 17512403]

MAZZARELLA L, CAPASSO S, DEMASI D, DI LORENZO G, MATTIA CA & ZAGARI A (1993). Bovine seminal ribonuclease: structure at 1.9 A resolution. Acta Crystallogr D Biol Crystallogr, 49(Pt 4), 389–402. [PubMed: 15299514]

MCHENRY CS (1985). DNA polymerase III holoenzyme of Escherichia coli: components and function of a true replicative complex. Mol Cell Biochem, 66(1), 71–85. [PubMed: 3885002]

MERLINO A, ERCOLE C, PICONE D, PIZZO E, MAZZARELLA L & SICA F (2008). The buried diversity of bovine seminal ribonuclease: shape and cytotoxicity of the swapped non-covalent form of the enzyme. J Mol Biol, 376(2), 427–437. [PubMed: 18164315]

MICHEL F, COSTA M & WESTHOF E (2009). The ribozyme core of group II introns: a structure in want of partners. Trends Biochem Sci, 34(4), 189–199. [PubMed: 19299141]

MIDTGAARD SF, ASSENHOLT J, JONSTRUP AT, VAN LB, JENSEN TH & BRODERSEN DE (2006). Structure of the nuclear exosome component Rrp6p reveals an interplay between the active site and the HRDC domain. Proc Natl Acad Sci U S A, 103(32), 11898–11903. [PubMed: 16882719]

MILDVAN AS, XIA Z, AZURMENDI HF, SARASWAT V, LEGLER PM, MASSIAH MA, GABELLI SB, BIANCHET MA, KANG LW & AMZEL LM (2005). Structures and mechanisms of Nudix hydrolases. Arch Biochem Biophys, 433(1), 129–143. [PubMed: 15581572]

MIMITOU EP & SYMINGTON LS (2009). DNA end resection: many nucleases make light work. DNA Repair (Amst), 8(9), 983–995. [PubMed: 19473888]

MINAGAWA A, TAKAKU H, TAKAGI M & NASHIMOTO M (2004). A novel endonucleolytic mechanism to generate the CCA 3' termini of tRNA molecules in Thermotoga maritima. J Biol Chem, 279(15), 15688–15697. [PubMed: 14749326]

MIYAZONO K, WATANABE M, KOSINSKI J, ISHIKAWA K, KAMO M, SAWASAKI T, NAGATA K, BUJNICKI JM, ENDO Y, TANOKURA M & KOBAYASHI I (2007). Novel protein fold discovered in the PabI family of restriction enzymes. Nucleic Acids Res, 35(6), 1908–1918. [PubMed: 17332011]

MOL CD, IZUMI T, MITRA S & TAINER JA (2000). DNA-bound structures and mutants reveal abasic DNA binding by APE1 and DNA repair coordination [corrected]. Nature, 403(6768), 451–456. [PubMed: 10667800]

MOL CD, KUO CF, THAYER MM, CUNNINGHAM RP & TAINER JA (1995). Structure and function of the multifunctional DNA-repair enzyme exonuclease III. Nature, 374(6520), 381–386. [PubMed: 7885481]

MONZINGO AF, OZBURN A, XIA S, MEYER RJ & ROBERTUS JD (2007). The structure of the minimal relaxase domain of MobA at 2.1 A resolution. J Mol Biol, 366(1), 165–178. [PubMed: 17157875]

MOORE MJ & PROUDFOOT NJ (2009). Pre-mRNA processing reaches back to transcription and ahead to translation. Cell, 136(4), 688–700. [PubMed: 19239889]

MORITA M, STAMP G, ROBINS P, DULIC A, ROSEWELL I, HRIVNAK G, DALY G, LINDAHL T & BARNES DE (2004). Gene-targeted mice lacking the Trex1 (DNase III) 3'-->5' DNA exonuclease develop inflammatory myocarditis. Mol Cell Biol, 24(15), 6719–6727. [PubMed: 15254239]

MOSHOUS D, CALLEBAUT I, DE CHASSEVAL R, CORNEO B, CAVAZZANA-CALVO M, LE DEIST F, TEZCAN I, SANAL O, BERTRAND Y, PHILIPPE N, FISCHER A & DE VILLARTAY JP (2001). Artemis, a novel DNA double-strand break repair/V(D)J recombination protein, is mutated in human severe combined immune deficiency. Cell, 105(2), 177–186. [PubMed: 11336668]

MOURE CM, GIMBLE FS & QUIOCHO FA (2008). Crystal structures of I-SceI complexed to nicked DNA substrates: snapshots of intermediates along the DNA cleavage reaction pathway. Nucleic Acids Res, 36(10), 3287–3296. [PubMed: 18424798]

MUFTUOGLU M, OSHIMA J, VON KOBBE C, CHENG WH, LEISTRITZ DF & BOHR VA (2008). The clinical characteristics of Werner syndrome: molecular and biochemical diagnosis. Hum Genet, 124(4), 369–377. [PubMed: 18810497]

MURO-PASTOR AM, FLORES E, HERRERO A & WOLK CP (1992). Identification, genetic analysis and characterization of a sugar-non-specific nuclease from the cyanobacterium Anabaena sp. PCC 7120. Mol Microbiol, 6(20), 3021–3030. [PubMed: 1343821]

MURRAY NE (2000). Type I restriction systems: sophisticated molecular machines (a legacy of Bertani and Weigle). Microbiol Mol Biol Rev, 64(2), 412–434. [PubMed: 10839821]

MUYRERS JP, ZHANG Y & STEWART AF (2000). ET-cloning: think recombination first. Genet Eng (N Y), 22, 77–98. [PubMed: 11501382]

NAGATA S (2007). Autoimmune diseases caused by defects in clearing dead cells and nuclei expelled from erythroid precursors. Immunol Rev, 220, 237–250. [PubMed: 17979851]

NANDAKUMAR J, SCHWER B, SCHAFFRATH R & SHUMAN S (2008). RNA repair: an antidote to cytotoxic eukaryal RNA damage. Mol Cell, 31(2), 278–286. [PubMed: 18657509]

NEWMAN M, LUNNEN K, WILSON G, GRECI J, SCHILDKRAUT I & PHILLIPS SE (1998). Crystal structure of restriction endonuclease BglI bound to its interrupted DNA recognition sequence. Embo J, 17(18), 5466–5476. [PubMed: 9736624]

NEWMAN M, MURRAY-RUST J, LALLY J, RUDOLF J, FADDEN A, KNOWLES PP, WHITE MF & MCDONALD NQ (2005). Structure of an XPF endonuclease with and without DNA suggests a model for substrate recognition. Embo J, 24(5), 895–905. [PubMed: 15719018]

NICHOLS MD, DEANGELIS K, KECK JL & BERGER JM (1999). Structure and function of an archaeal topoisomerase VI subunit with homology to the meiotic recombination factor Spo11. Embo J, 18(21), 6177–6188. [PubMed: 10545127]

NIIRANEN L, ALTERMARK B, BRANDSDAL BO, LEIROS HK, HELLAND R, SMALAS AO & WILLASSEN NP (2008). Effects of salt on the kinetics and thermodynamic stability of endonuclease I from Vibrio salmonicida and Vibrio cholerae. FEBS J, 275(7), 1593–1605. [PubMed: 18312415]

NISHINO T, KOMORI K, ISHINO Y & MORIKAWA K (2003). X-ray and biochemical anatomy of an archaeal XPF/Rad1/Mus81 family nuclease: similarity between its endonuclease domain and restriction enzymes. Structure, 11(4), 445–457. [PubMed: 12679022]

NIV MY, RIPOLL DR, VILA JA, LIWO A, VANAMEE ES, AGGARWAL AK, WEINSTEIN H & SCHERAGA HA (2007). Topology of Type II REases revisited; structural classes and the common conserved core. Nucleic Acids Res, 35(7), 2227–2237. [PubMed: 17369272]

NOWOTNY M (2009). Retroviral integrase superfamily: the structural perspective. EMBO Rep, 10(2), 144–151. [PubMed: 19165139]

NOWOTNY M, CERRITELLI SM, GHIRLANDO R, GAIDAMAKOV SA, CROUCH RJ & YANG W (2008). Specific recognition of RNA/DNA hybrid and enhancement of human RNase H1 activity by HBD. Embo J, 27(7), 1172–1181. [PubMed: 18337749]

NOWOTNY M, GAIDAMAKOV SA, CROUCH RJ & YANG W (2005). Crystal structures of RNase H bound to an RNA/DNA hybrid: substrate specificity and metal-dependent catalysis. Cell, 121(7), 1005–1016. [PubMed: 15989951]

NOWOTNY M, GAIDAMAKOV SA, GHIRLANDO R, CERRITELLI SM, CROUCH RJ & YANG W (2007). Structure of human RNase H1 complexed with an RNA/DNA hybrid: insight into HIV reverse transcription. Mol Cell, 28(2), 264–276. [PubMed: 17964265]

NOWOTNY M & YANG W (2006). Stepwise analyses of metal ions in RNase H catalysis from substrate destabilization to product release. Embo J, 25(9), 1924–1933. [PubMed: 16601679]

NOWOTNY M & YANG W (2009). Structural and functional modules in RNA interference. Curr Opin Struct Biol, 19(3), 286–293. [PubMed: 19477631]

O'DONOVAN A, DAVIES AA, MOGGS JG, WEST SC & WOOD RD (1994). XPG endonuclease makes the 3' incision in human DNA nucleotide excision repair. Nature, 371(6496), 432–435. [PubMed: 8090225]

OBMOLOVA G, BAN C, HSIEH P & YANG W (2000). Crystal structures of mismatch repair protein MutS and its complex with a substrate DNA. Nature, 407(6805), 703–710. [PubMed: 11048710]

OLLIS DL, BRICK P, HAMLIN R, XUONG NG & STEITZ TA (1985). Structure of large fragment of Escherichia coli DNA polymerase I complexed with dTMP. Nature, 313(6005), 762–766. [PubMed: 3883192]

OLMO N, TURNAY J, GONZALEZ DE BUITRAGO G, LOPEZ DE SILANES I, GAVILANES JG & LIZARBE MA (2001). Cytotoxic mechanism of the ribotoxin alpha-sarcin. Induction of cell death via apoptosis. Eur J Biochem, 268(7), 2113–2123. [PubMed: 11277935]

ORLOWSKI J & BUJNICKI JM (2008). Structural and evolutionary classification of Type II restriction enzymes based on theoretical and experimental analyses. Nucleic Acids Res, 36(11), 3552–3569. [PubMed: 18456708]

PAN CQ & LAZARUS RA (1999). Ca2+-dependent activity of human DNase I and its hyperactive variants. Protein Sci, 8(9), 1780–1788. [PubMed: 10493579]

PAQUIN B, O'KELLY CJ & LANG BF (1995). Intron-encoded open reading frame of the GIY-YIG subclass in a plastid gene. Curr Genet, 28(1), 97–99. [PubMed: 8536320]

PARKER R & SONG H (2004). The enzymes and control of eukaryotic mRNA turnover. Nat Struct Mol Biol, 11(2), 121–127. [PubMed: 14749774]

PARRISH JZ & XUE D (2006). Cuts can kill: the roles of apoptotic nucleases in cell death and animal development. Chromosoma, 115(2), 89–97. [PubMed: 16418867]

PATEL AA & STEITZ JA (2003). Splicing double: insights from the second spliceosome. Nat Rev Mol Cell Biol, 4(12), 960–970. [PubMed: 14685174]

PAULING L (1961). The nature of the chemical bond. Ithaca: Cornell University Press.

PAULL TT & GELLERT M (1998). The 3' to 5' exonuclease activity of Mre 11 facilitates repair of DNA double-strand breaks. Mol Cell, 1(7), 969–979. [PubMed: 9651580]

PAULL TT & GELLERT M (1999). Nbs1 potentiates ATP-driven DNA unwinding and endonuclease cleavage by the Mre11/Rad50 complex. Genes Dev, 13(10), 1276–1288. [PubMed: 10346816]

PEEBLES CL, PERLMAN PS, MECKLENBURG KL, PETRILLO ML, TABOR JH, JARRELL KA & CHENG HL (1986). A self-splicing RNA excises an intron lariat. Cell, 44(2), 213–223. [PubMed: 3510741]

PENA V, ROZOV A, FABRIZIO P, LUHRMANN R & WAHL MC (2008). Structure and function of an RNase H domain at the heart of the spliceosome. Embo J, 27(21), 2929–2940. [PubMed: 18843295]

PERRINO FW, HARVEY S, MCMILLIN S & HOLLIS T (2005). The human TREX2 3' -> 5'-exonuclease structure suggests a mechanism for efficient nonprocessive DNA catalysis. J Biol Chem, 280(15), 15212–15218. [PubMed: 15661738]

PERRY JJ, YANNONE SM, HOLDEN LG, HITOMI C, ASAITHAMBY A, HAN S, COOPER PK, CHEN DJ & TAINER JA (2006a). WRN exonuclease structure and molecular mechanism imply an editing role in DNA end processing. Nat Struct Mol Biol, 13(5), 414–422. [PubMed: 16622405]

PERRY K, HWANG Y, BUSHMAN FD & VAN DUYNE GD (2006b). Structural basis for specificity in the poxvirus topoisomerase. Mol Cell, 23(3), 343–354. [PubMed: 16885024]

PIDCOCK E & MOORE GR (2001). Structural characteristics of protein binding sites for calcium and lanthanide ions. J Biol Inorg Chem, 6(5–6), 479–489. [PubMed: 11472012]

PINGOUD A, FUXREITER M, PINGOUD V & WENDE W (2005). Type II restriction endonucleases: structure and mechanism. Cell Mol Life Sci, 62(6), 685–707. [PubMed: 15770420]

PINGOUD V, WENDE W, FRIEDHOFF P, REUTER M, ALVES J, JELTSCH A, MONES L, FUXREITER M & PINGOUD A (2009). On the divalent metal ion dependence of DNA cleavage by restriction endonucleases of the EcoRI family. J Mol Biol, 393(1), 140–160. [PubMed: 19682999]

PONTIUS BW, LOTT WB & VON HIPPEL PH (1997). Observations on catalysis by hammerhead ribozymes are consistent with a two-divalent-metal-ion mechanism. Proc Natl Acad Sci U S A, 94(6), 2290–2294. [PubMed: 9122187]

POULIOT JJ, YAO KC, ROBERTSON CA & NASH HA (1999). Yeast gene for a Tyr-DNA phosphodiesterase that repairs topoisomerase I complexes. Science, 286(5439), 552–555. [PubMed: 10521354]

RAFFERTY JB, BOLT EL, MURANOVA TA, SEDELNIKOVA SE, LEONARD P, PASQUO A, BAKER PJ, RICE DW, SHARPLES GJ & LLOYD RG (2003). The structure of Escherichia coli RusA endonuclease reveals a new Holliday junction DNA binding fold. Structure, 11(12), 1557–1567. [PubMed: 14656440]

RAINES RT (1998). Ribonuclease A. Chem Rev, 98(3), 1045–1066. [PubMed: 11848924]

RANGARAJAN ES & SHANKAR V (2001). Sugar non-specific endonucleases. FEMS Microbiol Rev, 25(5), 583–613. [PubMed: 11742693]

REDINBO MR, CHAMPOUX JJ & HOL WG (2000). Novel insights into catalytic mechanism from a crystal structure of human topoisomerase I in complex with DNA. Biochemistry, 39(23), 6832–6840. [PubMed: 10841763]

REDINBO MR, STEWART L, KUHN P, CHAMPOUX JJ & HOL WG (1998). Crystal structures of human topoisomerase I in covalent and noncovalent complexes with DNA. Science, 279(5356), 1504–1513. [PubMed: 9488644]

REED RR (1981). Transposon-mediated site-specific recombination: a defined in vitro system. Cell, 25(3), 713–719. [PubMed: 6269755]

REHA-KRANTZ LJ (2010). DNA polymerase proofreading: Multiple roles maintain genome stability. Biochim Biophys Acta. 1804, 1049–1063. [PubMed: 19545649]

REITER TA, REITER NJ & RUSNAK F (2002). Mn2+ is a native metal ion activator for bacteriophage lambda protein phosphatase. Biochemistry, 41(51), 15404–15409. [PubMed: 12484780]

RENZI F, CAFFARELLI E, LANEVE P, BOZZONI I, BRUNORI M & VALLONE B (2006). The structure of the endoribonuclease XendoU: From small nucleolar RNA processing to severe acute respiratory syndrome coronavirus replication. Proc Natl Acad Sci U S A, 103(33), 12365–12370. [PubMed: 16895992]

RICE P & MIZUUCHI K (1995). Structure of the bacteriophage Mu transposase core: a common structural motif for DNA transposition and retroviral integration. Cell, 82(2), 209–220. [PubMed: 7628012]

RICHARDSON JM, COLLOMS SD, FINNEGAN DJ & WALKINSHAW MD (2009). Molecular architecture of the Mos1 paired-end complex: the structural basis of DNA transposition in a eukaryote. Cell, 138(6), 1096–1108. [PubMed: 19766564]

RITCHIE DB, SCHELLENBERG MJ, GESNER EM, RAITHATHA SA, STUART DT & MACMILLAN AM (2008). Structural elucidation of a PRP8 core domain from the heart of the spliceosome. Nat Struct Mol Biol, 15(11), 1199–1205. [PubMed: 18836455]

ROBERTS RJ, VINCZE T, POSFAI J & MACELIS D (2009). REBASE--a database for DNA restriction and modification: enzymes, genes and genomes. Nucleic Acids Res, 38(Database issue), D234–236. [PubMed: 19846593]

ROMANI A & SCARPA A (1992). Regulation of cell magnesium. Arch Biochem Biophys, 298(1), 1–12. [PubMed: 1524417]

ROMIER C, DOMINGUEZ R, LAHM A, DAHL O & SUCK D (1998). Recognition of single-stranded DNA by nuclease P1: high resolution crystal structures of complexes with substrate analogs. Proteins, 32(4), 414–424. [PubMed: 9726413]

RUPERT PB, MASSEY AP, SIGURDSSON ST & FERRE-D'AMARE AR (2002). Transition state stabilization by a catalytic RNA. Science, 298(5597), 1421–1424. [PubMed: 12376595]

RUTKOSKI TJ & RAINES RT (2008). Evasion of ribonuclease inhibitor as a determinant of ribonuclease cytotoxicity. Curr Pharm Biotechnol, 9(3), 185–189. [PubMed: 18673284]

RYAN K, CALVO O & MANLEY JL (2004). Evidence that polyadenylation factor CPSF-73 is the mRNA 3' processing endonuclease. RNA, 10(4), 565–573. [PubMed: 15037765]

SAENGER W (1984). Principles of nucleic acid structure. New York, NY: Springer.

SALVO JJ & GRINDLEY ND (1988). The gamma delta resolvase bends the res site into a recombinogenic complex. Embo J, 7(11), 3609–3616. [PubMed: 2850169]

SAM MD & PERONA JJ (1999). Catalytic roles of divalent metal ions in phosphoryl transfer by EcoRV endonuclease. Biochemistry, 38(20), 6576–6586. [PubMed: 10350476]

SASNAUSKAS G, CONNOLLY BA, HALFORD SE & SIKSNYS V (2007). Site-specific DNA transesterification catalyzed by a restriction enzyme. Proc Natl Acad Sci U S A, 104(7), 2115–2120. [PubMed: 17267608]

SASNAUSKAS G, ZAKRYS L, ZAREMBA M, COSSTICK R, GAYNOR JW, HALFORD SE & SIKSNYS V (2010). A novel mechanism for the scission of double-stranded DNA: BfiI cuts both 3'−5' and 5'−3' strands by rotating a single active site. Nucleic Acids Res. 38, 2399–2410. [PubMed: 20047964]

SCHERLY D, NOUSPIKEL T, CORLET J, UCLA C, BAIROCH A & CLARKSON SG (1993). Complementation of the DNA repair defect in xeroderma pigmentosum group G cells by a human cDNA related to yeast RAD2. Nature, 363(6425), 182–185. [PubMed: 8483504]

SCHIFFER S, ROSCH S & MARCHFELDER A (2002). Assigning a function to a conserved group of proteins: the tRNA 3'-processing enzymes. Embo J, 21(11), 2769–2777. [PubMed: 12032089]

SCHNEIDER C, LEUNG E, BROWN J & TOLLERVEY D (2009). The N-terminal PIN domain of the exosome subunit Rrp44 harbors endonuclease activity and tethers Rrp44 to the yeast core exosome. Nucleic Acids Res, 37(4), 1127–1140. [PubMed: 19129231]

SCHOEFFLER AJ & BERGER JM (2008). DNA topoisomerases: harnessing and constraining energy to govern chromosome topology. Q Rev Biophys, 41(1), 41–101. [PubMed: 18755053]

SCHULGA AA, NURKIYANOVA KM, ZAKHARYEV VM, KIRPICHNIKOV MP & SKRYABIN KG (1992). Cloning of the gene encoding RNase binase from Bacillus intermedius 7P. Nucleic Acids Res, 20(9), 2375. [PubMed: 1594455]

SCHUSTER SC, MILLER W, RATAN A, TOMSHO LP, GIARDINE B, KASSON LR, HARRIS RS, PETERSEN DC, ZHAO F, QI J, ALKAN C, KIDD JM, SUN Y, DRAUTZ DI, BOUFFARD P, MUZNY DM, REID JG, NAZARETH LV, WANG Q, BURHANS R, RIEMER C, WITTEKINDT NE, MOORJANI P, TINDALL EA, DANKO CG, TEO WS, BUBOLTZ AM, ZHANG Z, MA Q, OOSTHUYSEN A, STEENKAMP AW, OOSTUISEN H, VENTER P, GAJEWSKI J, ZHANG Y, PUGH BF, MAKOVA KD, NEKRUTENKO A, MARDIS ER, PATTERSON N, PRINGLE TH, CHIAROMONTE F, MULLIKIN JC, EICHLER EE, HARDISON RC, GIBBS RA, HARKINS TT & HAYES VM (2010). Complete Khoisan and Bantu genomes from southern Africa. Nature, 463(7283), 943–947. [PubMed: 20164927]

SCOTT WG, MURRAY JB, ARNOLD JR, STODDARD BL & KLUG A (1996). Capturing the structure of a catalytic RNA intermediate: the hammerhead ribozyme. Science, 274(5295), 2065–2069. [PubMed: 8953035]

SETLOW P & KORNBERG A (1972). Deoxyribonucleic acid polymerase: two distinct enzymes in one polypeptide. II. A proteolytic fragment containing the 5' leads to 3' exonuclease function. Restoration of intact enzyme functions from the two proteolytic fragments. J Biol Chem, 247(1), 232–240. [PubMed: 4552925]

SHARMA S, SOMMERS JA, DRISCOLL HC, UZDILLA L, WILSON TM & BROSH RM, JR. (2003). The exonucleolytic and endonucleolytic cleavage activities of human exonuclease 1 are stimulated by an interaction with the carboxyl-terminal region of the Werner syndrome protein. J Biol Chem, 278(26), 23487–23496. [PubMed: 12704184]

SHARPLES GJ, CHAN SN, MAHDI AA, WHITBY MC & LLOYD RG (1994). Processing of intermediates in recombination and DNA repair: identification of a new endonuclease that specifically cleaves Holliday junctions. Embo J, 13(24), 6133–6142. [PubMed: 7813450]

SHEN B, SINGH P, LIU R, QIU J, ZHENG L, FINGER LD & ALAS S (2005). Multiple but dissectible functions of FEN-1 nucleases in nucleic acid processing, genome stability and diseases. Bioessays, 27(7), 717–729. [PubMed: 15954100]

SHEVELEV IV, RAMADAN K & HUBSCHER U (2002). The TREX2 3'-->5' exonuclease physically interacts with DNA polymerase delta and increases its accuracy. ScientificWorldJournal, 2, 275–281. [PubMed: 12806015]

SIDRAUSKI C & WALTER P (1997). The transmembrane kinase Ire1p is a site-specific endonuclease that initiates mRNA splicing in the unfolded protein response. Cell, 90(6), 1031–1039. [PubMed: 9323131]

SILVERMAN RH (2007). Viral encounters with 2',5'-oligoadenylate synthetase and RNase L during the interferon antiviral response. J Virol, 81(23), 12720–12729. [PubMed: 17804500]

SINGLETON MR, DILLINGHAM MS, GAUDIER M, KOWALCZYKOWSKI SC & WIGLEY DB (2004). Crystal structure of RecBCD enzyme reveals a machine for processing DNA breaks. Nature, 432(7014), 187–193. [PubMed: 15538360]

SINHA KM, UNCIULEAC MC, GLICKMAN MS & SHUMAN S (2009). AdnAB: a new DSB-resecting motor-nuclease from mycobacteria. Genes Dev, 23(12), 1423–1437. [PubMed: 19470566]

SOKOLOWSKA M, CZAPINSKA H & BOCHTLER M (2009). Crystal structure of the beta beta alpha-Me type II restriction endonuclease Hpy99I with target DNA. Nucleic Acids Res, 37(11), 3799–3810. [PubMed: 19380375]

SOKOLOWSKA M, KAUS-DROBEK M, CZAPINSKA H, TAMULAITIS G, SZCZEPANOWSKI RH, URBANKE C, SIKSNYS V & BOCHTLER M (2007). Monomeric restriction endonuclease BcnI in the apo form and in an asymmetric complex with target DNA. J Mol Biol, 369(3), 722–734. [PubMed: 17445830]

SOLARO PC, BIRKENKAMP K, PFEIFFER P & KEMPER B (1993). Endonuclease VII of phage T4 triggers mismatch correction in vitro. J Mol Biol, 230(3), 868–877. [PubMed: 8478939]

SOREK R, KUNIN V & HUGENHOLTZ P (2008). CRISPR--a widespread system that provides acquired resistance against phages in bacteria and archaea. Nat Rev Microbiol, 6(3), 181–186. [PubMed: 18157154]

SPIEGEL PC, CHEVALIER B, SUSSMAN D, TURMEL M, LEMIEUX C & STODDARD BL (2006). The structure of I-CeuI homing endonuclease: Evolving asymmetric DNA recognition from a symmetric protein scaffold. Structure, 14(5), 869–880. [PubMed: 16698548]

STAHL MM, THOMASON L, POTEETE AR, TARKOWSKI T, KUZMINOV A & STAHL FW (1997). Annealing vs. invasion in phage lambda recombination. Genetics, 147(3), 961–977. [PubMed: 9383045]

STAHLEY MR & STROBEL SA (2005). Structural evidence for a two-metal-ion mechanism of group I intron splicing. Science, 309(5740), 1587–1590. [PubMed: 16141079]

STAHLEY MR & STROBEL SA (2006). RNA splicing: group I intron crystal structures reveal the basis of splice site selection and metal ion catalysis. Curr Opin Struct Biol, 16(3), 319–326. [PubMed: 16697179]

STEC B, HOLTZ KM & KANTROWITZ ER (2000). A revised mechanism for the alkaline phosphatase reaction involving three metal ions. J Mol Biol, 299(5), 1303–1311. [PubMed: 10873454]

STEINIGER-WHITE M, RAYMENT I & REZNIKOFF WS (2004). Structure/function insights into Tn5 transposition. Curr Opin Struct Biol, 14(1), 50–57. [PubMed: 15102449]

STEITZ TA (1998). A mechanism for all polymerases. Nature, 391(6664), 231–232. [PubMed: 9440683]

STEITZ TA & STEITZ JA (1993). A general two-metal-ion mechanism for catalytic RNA. Proc Natl Acad Sci U S A, 90(14), 6498–6502. [PubMed: 8341661]

STEPHENSON JB (2008). Aicardi-Goutieres syndrome (AGS). Eur J Paediatr Neurol, 12(5), 355–358. [PubMed: 18343173]

STETSON DB, KO JS, HEIDMANN T & MEDZHITOV R (2008). Trex1 prevents cell-intrinsic initiation of autoimmunity. Cell, 134(4), 587–598. [PubMed: 18724932]

STODDARD BL (2005). Homing endonuclease structure and function. Q Rev Biophys, 38(1), 49–95. [PubMed: 16336743]

STUCKEY JA & DIXON JE (1999). Crystal structure of a phospholipase D family member. Nat Struct Biol, 6(3), 278–284. [PubMed: 10074947]

SUBRAMANYA HS, ARCISZEWSKA LK, BAKER RA, BIRD LE, SHERRATT DJ & WIGLEY DB (1997). Crystal structure of the site-specific recombinase, XerD. Embo J, 16(17), 5178–5187. [PubMed: 9311978]

SUCK D, OEFNER C & KABSCH W (1984). Three-dimensional structure of bovine pancreatic DNase I at 2.5 A resolution. Embo J, 3(10), 2423–2430. [PubMed: 6499835]

SUN W, PERTZEV A & NICHOLSON AW (2005). Catalytic mechanism of Escherichia coli ribonuclease III: kinetic and inhibitor evidence for the involvement of two magnesium ions in RNA phosphodiester hydrolysis. Nucleic Acids Res, 33(3), 807–815. [PubMed: 15699182]

SYSON K, TOMLINSON C, CHAPADOS BR, SAYERS JR, TAINER JA, WILLIAMS NH & GRASBY JA (2008). Three metal ions participate in the reaction catalyzed by T5 flap endonuclease. J Biol Chem, 283(42), 28741–28746. [PubMed: 18697748]

SZANKASI P & SMITH GR (1995). A role for exonuclease I from S. pombe in mutation avoidance and mismatch correction. Science, 267(5201), 1166–1169. [PubMed: 7855597]

SZANKASI P & SMITH GR (1996). Requirement of S. pombe exonuclease II, a homologue of S. cerevisiae Sep1, for normal mitotic growth and viability. Curr Genet, 30(4), 284–293. [PubMed: 8781170]

TADOKORO T & KANAYA S (2009). Ribonuclease H: molecular diversities, substrate binding domains, and catalytic mechanism of the prokaryotic enzymes. FEBS J, 276(6), 1482–1493. [PubMed: 19228197]

TAKEUCHI M, LILLIS R, DEMPLE B & TAKESHITA M (1994). Interactions of Escherichia coli endonuclease IV and exonuclease III with abasic sites in DNA. J Biol Chem, 269(34), 21907–21914. [PubMed: 7520446]

TANAKA N, ARAI J, INOKUCHI N, KOYAMA T, OHGI K, IRIE M & NAKAMURA KT (2000). Crystal structure of a plant ribonuclease, RNase LE. J Mol Biol, 298(5), 859–873. [PubMed: 10801354]

THORE S, MAUXION F, SERAPHIN B & SUCK D (2003). X-ray structure and activity of the yeast Pop2 protein: a nuclease subunit of the mRNA deadenylase complex. EMBO Rep, 4(12), 1150–1155. [PubMed: 14618157]

TOCK MR & DRYDEN DT (2005). The biology of restriction and anti-restriction. Curr Opin Microbiol, 8(4), 466–472. [PubMed: 15979932]

TOMLINSON CG, ATACK JM, CHAPADOS B, TAINER JA & GRASBY JA (2010). Substrate recognition and catalysis by flap endonucleases and related enzymes. Biochem Soc Trans, 38(2), 433–437. [PubMed: 20298197]

TON-HOANG B, GUYNET C, RONNING DR, COINTIN-MARTY B, DYDA F & CHANDLER M (2005). Transposition of ISHp608, member of an unusual family of bacterial insertion sequences. Embo J, 24(18), 3325–3338. [PubMed: 16163392]

TOOR N, KEATING KS & PYLE AM (2009). Structural insights into RNA splicing. Curr Opin Struct Biol, 19(3), 260–266. [PubMed: 19443210]

TOOR N, RAJASHANKAR K, KEATING KS & PYLE AM (2008). Structural basis for exon recognition by a group II intron. Nat Struct Mol Biol, 15(11), 1221–1222. [PubMed: 18953333]

TORRES-LARIOS A, SWINGER KK, PAN T & MONDRAGON A (2006). Structure of ribonuclease P--a universal ribozyme. Curr Opin Struct Biol, 16(3), 327–335. [PubMed: 16650980]

TRAN PT, ERDENIZ N, DUDLEY S & LISKAY RM (2002). Characterization of nuclease-dependent functions of Exo1p in Saccharomyces cerevisiae. DNA Repair (Amst), 1(11), 895–912. [PubMed: 12531018]

TRUGLIO JJ, RHAU B, CROTEAU DL, WANG L, SKORVAGA M, KARAKAS E, DELLAVECCHIA MJ, WANG H, VAN HOUTEN B & KISKER C (2005). Structural insights into the first incision reaction during nucleotide excision repair. Embo J, 24(5), 885–894. [PubMed: 15692561]

TSUTAKAWA SE, JINGAMI H & MORIKAWA K (1999). Recognition of a TG mismatch: the crystal structure of very short patch repair endonuclease in complex with a DNA duplex. Cell, 99(6), 615–623. [PubMed: 10612397]

TUCKER PW, HAZEN EE, JR. & COTTON FA (1978). Staphylococcal nuclease reviewed: a prototypic study in contemporary enzymology. I. Isolation; physical and enzymatic properties. Mol Cell Biochem, 22(2–3), 67–77. [PubMed: 370553]

UESUGI Y & HATANAKA T (2009). Phospholipase D mechanism using Streptomyces PLD. Biochim Biophys Acta, 1791(9), 962–969. [PubMed: 19416643]

UNCIULEAC MC & SHUMAN S (2009). Characterization of the mycobacterial AdnAB DNA motor provides insights into the evolution of bacterial motor-nuclease machines. J Biol Chem, 285(4), 2632–2641. [PubMed: 19920138]

URAKUBO Y, IKURA T & ITO N (2008). Crystal structural analysis of protein-protein interactions drastically destabilized by a single mutation. Protein Sci, 17(6), 1055–1065. [PubMed: 18441234]

USUI T, OHTA T, OSHIUMI H, TOMIZAWA J, OGAWA H & OGAWA T (1998). Complex formation and functional versatility of Mre11 of budding yeast in recombination. Cell, 95(5), 705–716. [PubMed: 9845372]

VAN GENT DC, MIZUUCHI K & GELLERT M (1996). Similarities between initiation of V(D)J recombination and retroviral integration. Science, 271(5255), 1592–1594. [PubMed: 8599117]

VAN ROEY P, MEEHAN L, KOWALSKI JC, BELFORT M & DERBYSHIRE V (2002). Catalytic domain structure and hypothesis for function of GIY-YIG intron endonuclease I-TevI. Nat Struct Biol, 9(11), 806–811. [PubMed: 12379841]

VASU K, SARAVANAN M, BUJNICKI JM & NAGARAJA V (2008). Structural integrity of the beta beta alpha-Metal finger motif is required for DNA binding and stable protein-DNA complex formation in R.KpnI. Biochim Biophys Acta, 1784(2), 269–275. [PubMed: 18329982]

VERHOEVEN EE, VAN KESTEREN M, MOOLENAAR GF, VISSE R & GOOSEN N (2000). Catalytic sites for 3' and 5' incision of Escherichia coli nucleotide excision repair are both located in UvrC. J Biol Chem, 275(7), 5120–5123. [PubMed: 10671556]

VIADIU H & AGGARWAL AK (1998). The role of metals in catalysis by the restriction endonuclease BamHI. Nat Struct Biol, 5(10), 910–916. [PubMed: 9783752]

VIADIU H & AGGARWAL AK (2000). Structure of BamHI bound to nonspecific DNA: a model for DNA sliding. Mol Cell, 5(5), 889–895. [PubMed: 10882125]

VICENS Q & CECH TR (2006). Atomic level architecture of group I introns revealed. Trends Biochem Sci, 31(1), 41–51. [PubMed: 16356725]

VISWANATHAN M & LOVETT ST (1999). Exonuclease X of Escherichia coli. A novel 3'−5' DNase and Dnaq superfamily member involved in DNA repair. J Biol Chem, 274(42), 30094–30100. [PubMed: 10514496]

VITKUTE J, MANELIENE Z, PETRUSYTE M & JANULAITIS A (1998). BfiI, a restriction endonuclease from Bacillus firmus S8120, which recognizes the novel non-palindromic sequence 5'-ACTGGG(N)5/4–3'. Nucleic Acids Res, 26(14), 3348–3349. [PubMed: 9649617]

VOEGTLI WC, WHITE DJ, REITER NJ, RUSNAK F & ROSENZWEIG AC (2000). Structure of the bacteriophage lambda Ser/Thr protein phosphatase with sulfate ion bound in two coordination modes. Biochemistry, 39(50), 15365–15374. [PubMed: 11112522]

VOET D & VOET JG (2004). Biochemistry. Hoboken, NJ: Wiley.

VOZIYANOV Y, PATHANIA S & JAYARAM M (1999). A general model for site-specific recombination by the integrase family recombinases. Nucleic Acids Res, 27(4), 930–941. [PubMed: 9927723]

WALKER D, LANCASTER L, JAMES R & KLEANTHOUS C (2004). Identification of the catalytic motif of the microbial ribosome inactivating cytotoxin colicin E3. Protein Sci, 13(6), 1603–1611. [PubMed: 15133158]

WANG JC (2002). Cellular roles of DNA topoisomerases: a molecular perspective. Nat Rev Mol Cell Biol, 3(6), 430–440. [PubMed: 12042765]

WANG LK & SHUMAN S (2005). Structure-function analysis of yeast tRNA ligase. RNA, 11(6), 966–975. [PubMed: 15923379]

WANG Y, JURANEK S, LI H, SHENG G, TUSCHL T & PATEL DJ (2008). Structure of an argonaute silencing complex with a seed-containing guide DNA and target RNA duplex. Nature, 456(7224), 921–926. [PubMed: 19092929]

WANG Y, JURANEK S, LI H, SHENG G, WARDLE GS, TUSCHL T & PATEL DJ (2009). Nucleation, propagation and cleavage of target RNAs in Ago silencing complexes. Nature, 461(7265), 754–761. [PubMed: 19812667]

WANG YT, YANG WJ, LI CL, DOUDEVA LG & YUAN HS (2007). Structural basis for sequence-dependent DNA cleavage by nonspecific endonucleases. Nucleic Acids Res, 35(2), 584–594. [PubMed: 17175542]

WANG Z, FAST W, VALENTINE AM & BENKOVIC SJ (1999). Metallo-beta-lactamase: structure and mechanism. Curr Opin Chem Biol, 3(5), 614–622. [PubMed: 10508665]

WEST SC & CONNOLLY B (1992). Biological roles of the Escherichia coli RuvA, RuvB and RuvC proteins revealed. Mol Microbiol, 6(19), 2755–2759. [PubMed: 1435254]

WESTON SA, LAHM A & SUCK D (1992). X-ray structure of the DNase I-d(GGTATACC)2 complex at 2.3 A resolution. J Mol Biol, 226(4), 1237–1256. [PubMed: 1518054]

WHITE MF & LILLEY DM (1997). Characterization of a Holliday junction-resolving enzyme from Schizosaccharomyces pombe. Mol Cell Biol, 17(11), 6465–6471. [PubMed: 9343409]

WIDLAK P (2000). The DFF40/CAD endonuclease and its role in apoptosis. Acta Biochim Pol, 47(4), 1037–1044. [PubMed: 11996094]

WIDLAK P & GARRARD WT (2005). Discovery, regulation, and action of the major apoptotic nucleases DFF40/CAD and endonuclease G. J Cell Biochem, 94(6), 1078–1087. [PubMed: 15723341]

WIEDENHEFT B, ZHOU K, JINEK M, COYLE SM, MA W & DOUDNA JA (2009). Structural basis for DNase activity of a conserved protein implicated in CRISPR-mediated genome defense. Structure, 17(6), 904–912. [PubMed: 19523907]

WILLIAMS RS, MONCALIAN G, WILLIAMS JS, YAMADA Y, LIMBO O, SHIN DS, GROOCOCK LM, CAHILL D, HITOMI C, GUENTHER G, MOIANI D, CARNEY JP, RUSSELL P & TAINER JA (2008). Mre11 dimers coordinate DNA end bridging and nuclease processing in double-strand-break repair. Cell, 135(1), 97–109. [PubMed: 18854158]

WINKLER FK, BANNER DW, OEFNER C, TSERNOGLOU D, BROWN RS, HEATHMAN SP, BRYAN RK, MARTIN PD, PETRATOS K & WILSON KS (1993). The crystal structure of EcoRV endonuclease and of its complexes with cognate and non-cognate DNA fragments. Embo J, 12(5), 1781–1795. [PubMed: 8491171]

WOO EJ, KIM YG, KIM MS, HAN WD, SHIN S, ROBINSON H, PARK SY & OH BH (2004). Structural mechanism for inactivation and activation of CAD/DFF40 in the apoptotic pathway. Mol Cell, 14(4), 531–539. [PubMed: 15149602]

WORRALL JA & LUISI BF (2007). Information available at cut rates: structure and mechanism of ribonucleases. Curr Opin Struct Biol, 17(1), 128–137. [PubMed: 17189683]

WU M, REUTER M, LILIE H, LIU Y, WAHLE E & SONG H (2005). Structural insight into poly(A) binding and catalytic mechanism of human PARN. Embo J, 24(23), 4082–4093. [PubMed: 16281054]

WU SI, LO SK, SHAO CP, TSAI HW & HOR LI (2001). Cloning and characterization of a periplasmic nuclease of Vibrio vulnificus and its role in preventing uptake of foreign DNA. Appl Environ Microbiol, 67(1), 82–88. [PubMed: 11133431]

WYCKOFF HW, HARDMAN KD, ALLEWELL NM, INAGAMI T, JOHNSON LN & RICHARDS FM (1967). The structure of ribonuclease-S at 3.5 A resolution. J Biol Chem, 242(17), 3984–3988. [PubMed: 6037556]

WYCKOFF HW, TSERNOGLOU D, HANSON AW, KNOX JR, LEE B & RICHARDS FM (1970). The three-dimensional structure of ribonuclease-S. Interpretation of an electron density map at a nominal resolution of 2 A. J Biol Chem, 245(2), 305–328. [PubMed: 5460889]

XIANG S, COOPER-MORGAN A, JIAO X, KILEDJIAN M, MANLEY JL & TONG L (2009). Structure and function of the 5'-->3' exoribonuclease Rat1 and its activating partner Rai1. Nature, 458(7239), 784–788. [PubMed: 19194460]

XU QS, ROBERTS RJ & GUO HC (2005). Two crystal forms of the restriction enzyme MspI-DNA complex show the same novel structure. Protein Sci, 14(10), 2590–2600. [PubMed: 16195548]

XUE S, CALVIN K & LI H (2006). RNA recognition and cleavage by a splicing endonuclease. Science, 312(5775), 906–910. [PubMed: 16690865]

XUE Y, BAI X, LEE I, KALLSTROM G, HO J, BROWN J, STEVENS A & JOHNSON AW (2000). Saccharomyces cerevisiae RAI1 (YGL246c) is homologous to human DOM3Z and encodes a protein that binds the nuclear exoribonuclease Rat1p. Mol Cell Biol, 20(11), 4006–4015. [PubMed: 10805743]

YAJIMA S, INOUE S, OGAWA T, NONAKA T, OHSAWA K & MASAKI H (2006). Structural basis for sequence-dependent recognition of colicin E5 tRNase by mimicking the mRNA-tRNA interaction. Nucleic Acids Res, 34(21), 6074–6082. [PubMed: 17099236]

YAKOVLEVA L, CHEN S, HECHT SM & SHUMAN S (2008). Chemical and traditional mutagenesis of vaccinia DNA topoisomerase provides insights to cleavage site recognition and transesterification chemistry. J Biol Chem, 283(23), 16093–16103. [PubMed: 18367446]

YAMAGATA A, KAKUTA Y, MASUI R & FUKUYAMA K (2002). The crystal structure of exonuclease RecJ bound to Mn2+ ion suggests how its characteristic motifs are involved in exonuclease activity. Proc Natl Acad Sci U S A, 99(9), 5908–5912. [PubMed: 11972066]

YANG K, ZHANG L, XU T, HEROUX A & ZHAO R (2008). Crystal structure of the beta-finger domain of Prp8 reveals analogy to ribosomal proteins. Proc Natl Acad Sci U S A, 105(37), 13817–13822. [PubMed: 18779563]

YANG W (2008). An equivalent metal ion in one- and two-metal-ion catalysis. Nat Struct Mol Biol, 15(11), 1228–1231. [PubMed: 18953336]

YANG W, LEE JY & NOWOTNY M (2006). Making and breaking nucleic acids: two-Mg2+-ion catalysis and substrate specificity. Mol Cell, 22(1), 5–13. [PubMed: 16600865]

YANG W & MIZUUCHI K (1997). Site-specific recombination in plane view. Structure, 5(11), 1401–1406. [PubMed: 9384556]

YANG W & STEITZ TA (1995a). Crystal structure of the site-specific recombinase gamma delta resolvase complexed with a 34 bp cleavage site. Cell, 82(2), 193–207. [PubMed: 7628011]

YANG W & STEITZ TA (1995b). Recombining the structures of HIV integrase, RuvC and RNase H. Structure, 3(2), 131–134. [PubMed: 7735828]

YANG X, GERCZEI T, GLOVER LT & CORRELL CC (2001). Crystal structures of restrictocin-inhibitor complexes with implications for RNA recognition and base flipping. Nat Struct Biol, 8(11), 968–973. [PubMed: 11685244]

YANG XC, SULLIVAN KD, MARZLUFF WF & DOMINSKI Z (2009). Studies of the 5’ exonuclease and endonuclease activities of CPSF-73 in histone pre-mRNA processing. Mol Cell Biol, 29(1), 31–42. [PubMed: 18955505]

YARUS M (2002). Primordial genetics: phenotype of the ribocyte. Annu Rev Genet, 36, 125–151. [PubMed: 12429689]

YOSHIDA H (2001). The ribonuclease T1 family. Methods Enzymol, 341, 28–41. [PubMed: 11582784]

YOSHIKAWA M, IWASAKI H & SHINAGAWA H (2001). Evidence that phenylalanine 69 in Escherichia coli RuvC resolvase forms a stacking interaction during binding and destabilization of a Holliday junction DNA substrate. J Biol Chem, 276(13), 10432–10436. [PubMed: 11152689]

YU M, SOUAYA J & JULIN DA (1998). The 30-kDa C-terminal domain of the RecB protein is critical for the nuclease activity, but not the helicase activity, of the RecBCD enzyme from Escherichia coli. Proc Natl Acad Sci U S A, 95(3), 981–986. [PubMed: 9448271]

ZALATAN JG, FENN TD & HERSCHLAG D (2008). Comparative enzymology in the alkaline phosphatase superfamily to determine the catalytic role of an active-site metal ion. J Mol Biol, 384(5), 1174–1189. [PubMed: 18851975]

ZAMEL R, POON A, JAIKARAN D, ANDERSEN A, OLIVE J, DE ABREU D & COLLINS RA (2004). Exceptionally fast self-cleavage by a Neurospora Varkud satellite ribozyme. Proc Natl Acad Sci U S A, 101(6), 1467–1472. [PubMed: 14755053]

ZEGERS I, LORIS R, DEHOLLANDER G, FATTAH HAIKAL A, POORTMANS F, STEYAERT J & WYNS L (1998). Hydrolysis of a slow cyclic thiophosphate substrate of RNase T1 analyzed by time-resolved crystallography. Nat Struct Biol, 5(4), 280–283. [PubMed: 9546218]

ZHANG J, XING X, HERR AB & BELL CE (2009). Crystal structure of E. coli RecE protein reveals a toroidal tetramer for processing double-stranded DNA breaks. Structure, 17(5), 690–702. [PubMed: 19446525]

ZHANG Y, BUCHHOLZ F, MUYRERS JP & STEWART AF (1998). A new logic for DNA engineering using recombination in Escherichia coli. Nat Genet, 20(2), 123–128. [PubMed: 9771703]

ZHU CX & TSE-DINH YC (2000). The acidic triad conserved in type IA DNA topoisomerases is required for binding of Mg(II) and subsequent conformational change. J Biol Chem, 275(8), 5318–5322. [PubMed: 10681504]

ZUO Y, VINCENT HA, ZHANG J, WANG Y, DEUTSCHER MP & MALHOTRA A (2006). Structural basis for processivity and single-strand specificity of RNase II. Mol Cell, 24(1), 149–156. [PubMed: 16996291]

ZUO Y, WANG Y & MALHOTRA A (2005). Crystal structure of Escherichia coli RNase D, an exoribonuclease involved in structured RNA processing. Structure, 13(7), 973–984. [PubMed: 16004870]

ZUO Y, ZHENG H, WANG Y, CHRUSZCZ M, CYMBOROWSKI M, SKARINA T, SAVCHENKO A, MALHOTRA A & MINOR W (2007). Crystal structure of RNase T, an exoribonuclease involved in tRNA maturation and end turnover. Structure, 15(4), 417–428. [PubMed: 17437714]

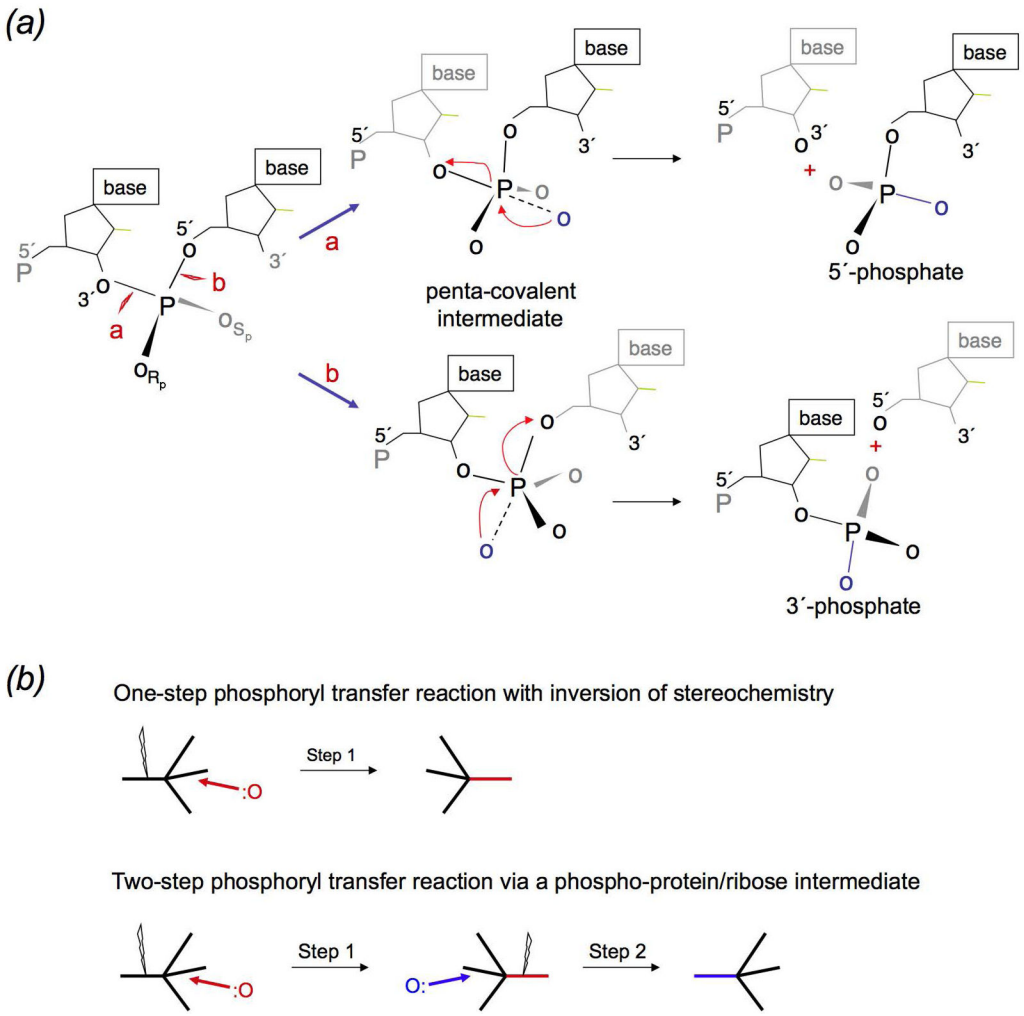

Fig. 1.

Adjacent nucleotides in RNA and DNA are linked by 3′ and 5′ O-P phosphodiester bonds. **a.** Nucleases degrade nucleic acid by breaking either one of these two bonds labeled as a and b. A nucleophile attacking in-line from the 5′ side breaks the 3′ O-P bond and produces 5′-phosphate and 3′-OH. Alternatively, a nucleophile attacking the scissile phosphate from the 3′ side breaks the 5′ O-P bond and produces 3′-phosphate and 5′ -OH. **b.** The S_N2 type associative reaction inverts the stereo configuration of phosphate. A two-step trans-esterification reaction can set the stereochemistry back to the original.

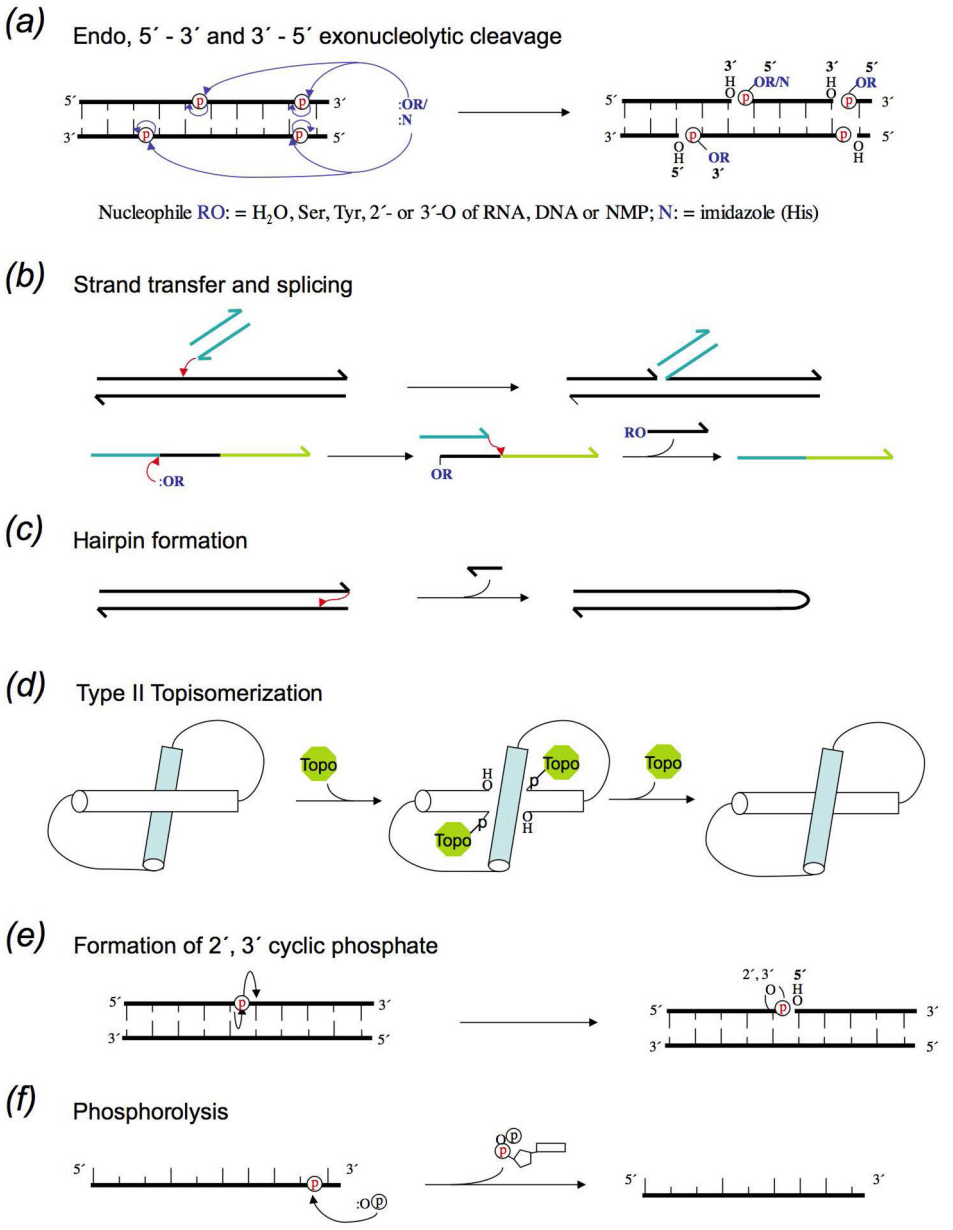

Fig. 2.

Phosphodiester bond cleavage. **a.** Nucleases can attack a scissile phosphate in the middle of nucleic acids (endo) or at the 5′ or 3′ ends (exo). The nucleophiles can be the hydroxyl groups of water molecules, Ser or Tyr sidechains, hydroxyls of ribose (2′ or 3’) or deoxyribose (3′) in RNA and DNA, or free nucleophiles. PLD- family (phospholipase D) nucleases use the imidazole of His as the nucleophile. When a protein sidechain serves as a nucleophile, the phosphodiester bond to be cleaved is transferred to the protein. Similarly, when the hydroxyl of a nucleotide or nucleic acid serves as the nucleophile, it is transferred to the nucleic acid. Both are indicated as R. **b.** DNA transposition by cut-and-paste mechanism. The donor DNA uses its cleaved 3′-OH to attack a phosphate in a target DNA. Thus the donor DNA is inserted into the target in this strand transfer reaction. RNA splicing

is similar. The cleavage of the 5′ exon-intron junction frees the 3′-OH of the first exon. This 3′-OH than attacks the 3′ exon-intron junction and results in a linked two exons and free intron. **c.** DNA Hairpin formation. When a 3′ -OH of a duplex DNA attacks a phosphate of its complementary strand, the two strands of that duplex are linked and become one. **d.** Type II topoisomerization. Both strands of one DNA segment are cleaved and form covalent bonds with a dimeric (or tetrameric) topoisomerase. The second DNA segment shown in light blue passes through the cleaved segment thus changing the linking number and topology. The cleaved DNA is then religated and the topoisomerase regenerated. **e.** The 2′ -OH immediate adjacent to a scissile phosphate can serve as a nucleophile and hydrolysis of 5′ O-P bond leads to 2′,3′ cyclic phosphate and 5′-OH. **f.** RNase PH and PNPase are 3′ exonucleases. They use inorganic phosphate as nucleophiles and degrade RNA to nucleotide diphosphates.

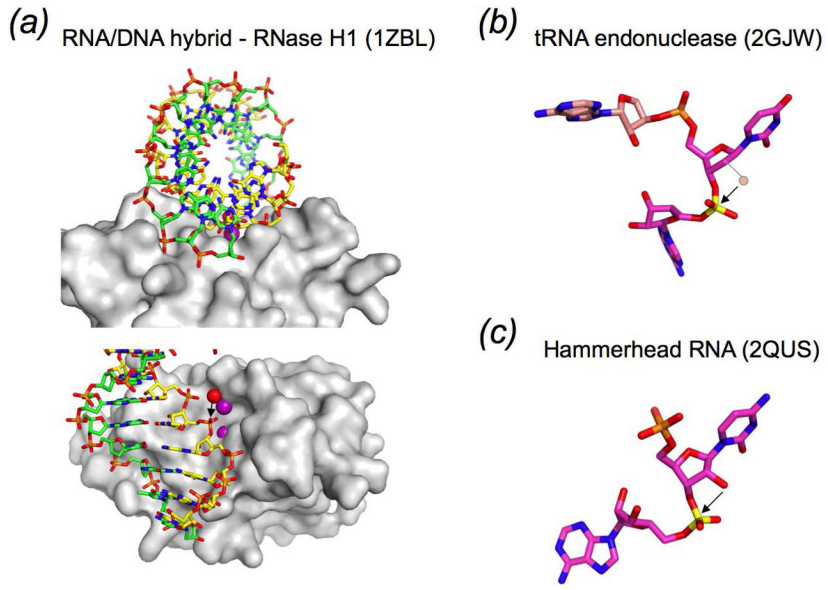

Fig. 3.

Double versus single stranded nucleic acid substrate. **a.** To cleave a double helix the nucleophile can attack from outside of the duplex only. Show here is an RNA/DNA hybrid in a mixed A and B form, which is approached by RNase H1 from the minor groove side. A water molecule is coordinated by the Mg^{2+} ion in the active site to attack the phosphate from the 5′ side and produce a 5′ phosphate and 3′ -OH. **b.** A scissile phosphate in pre-tRNA to be cleaved by tRNA endonuclease using the 2′-OH as the nucleophile. The nucleotides surrounding the scissile phosphate are not base paired and splayed. The phosphate itself is distorted. **c.** Self-cleaving hammerhead ribozyme distorts the scissile phosphate in a similar way because the double helix conformation is incompatible with the reaction coordinates of using a 2′-OH to attack the adjacent phosphate.

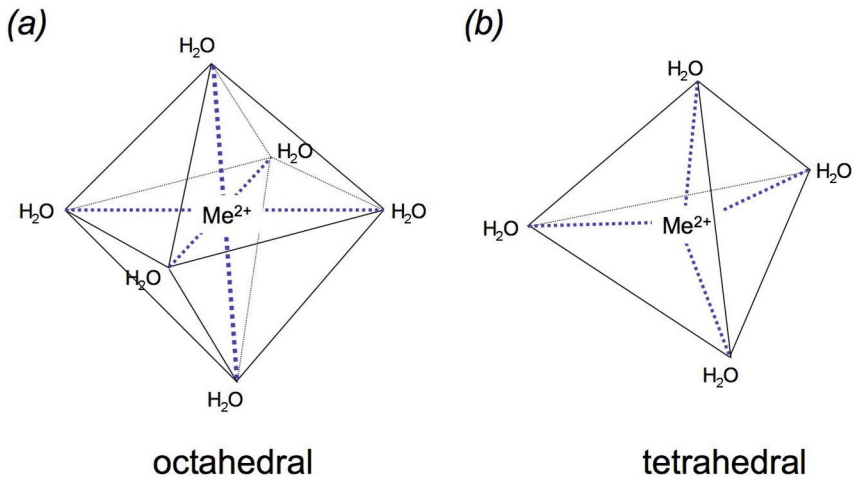

Fig. 4.

Metal-dependent nucleases most often use Mg^{2+} and Zn^{2+} to facilitate phosphodiester bond breakage. **a.** Diagram of octahedral coordination preferred by Mg^{2+} and can also be adopted by Zn^{2+}. **b.** Tetrahedral coordination favored by Zn^{2+}.

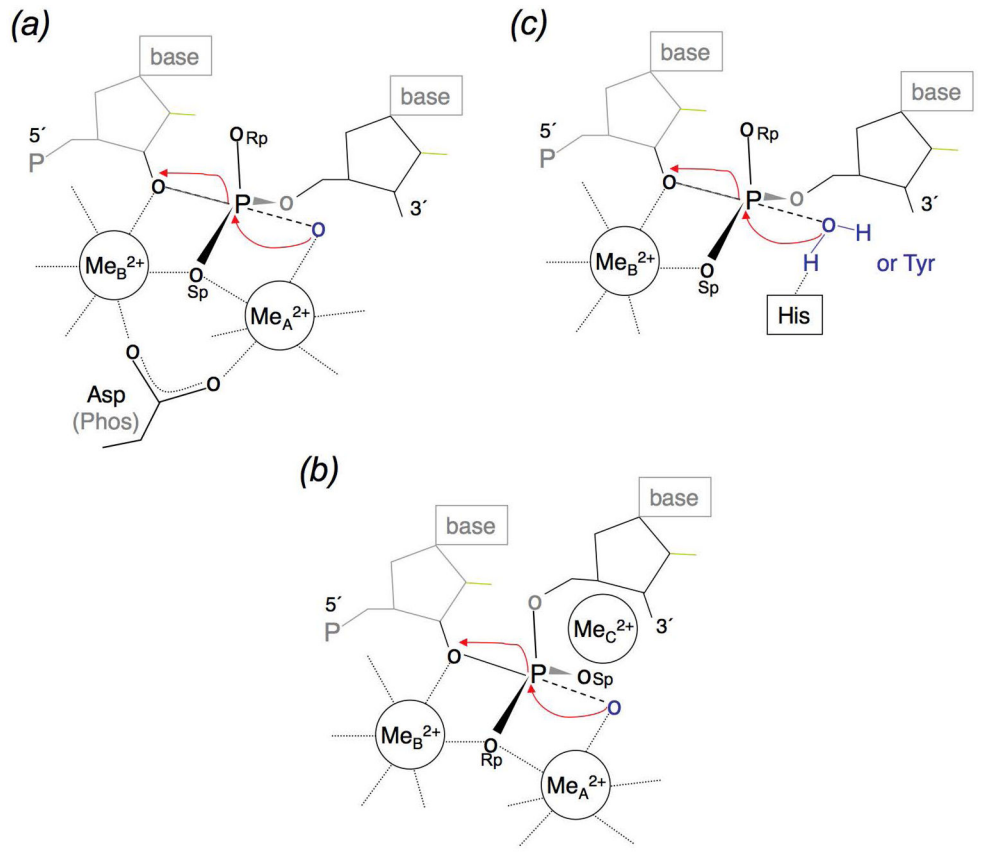

Fig. 5.

Metal-ion dependent catalysis. **a**. Two-metal-ion mechanism. The pro-Sp oxygen of a scissile phosphate coordinates both metal ions, one on the 5′ side and the other on the 3′ side. The pro-Rp oxygen is exposed to solvent. When labeling, pro-Sp is abbreviated as Sp and pro-Rp as Rp. **b.** The three-metal-ion mechanism is a variation of the two-metal-ion mechanism. The scissile phosphate is turned and the pro-Rp oxygen coordinates the two catalytic metal ions and, the pro-Sp oxygen is stabilized by the third divalent cation. **c**. The one-metal-ion mechanism is an alternative to the two-metal-ion mechanism. One metal ion (A) is eliminated and may be replaced by a positively charged protein sidechain. In the cases where water is the nucleophile, a conserved His often acts as the general base to deprotonate it for nucleophilic attack. Alternatively, Tyr is the nucleophile as in topoisomerases, relaxases and RCR-related recombinases. In all three metal-ion-dependent mechanisms, the nucleophile is always on the 5′ side, and cleavage results in 5′-phosphate and 3′-OH.

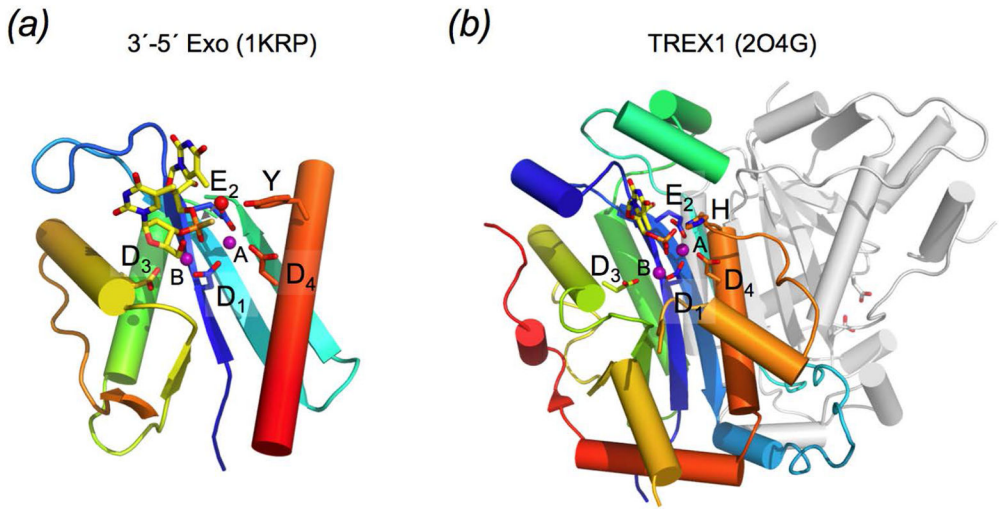

Fig. 6.

The DEDD superfamily consists of DnaQ-like exonucleases. **a.** The core of the 3′ - 5′ exonuclease domain of *E. coli* DNA polymerase I (PDB code is shown in parenthesis) represents the DEDDy nucleases. **b.** Dimeric TREX1 (2O4G) represents the DEDDh exonucleases. Proteins are shown in ribbon diagrams. One subunit of each enzyme is shown in rainbow colors from the blue N- to red C-terminus. Divalent cations are shown as purple spheres, and the nucleophile water as a red sphere. The sidechains of the conserved DEDDy/h motifs and nucleic acid/nucleotide are shown in sticks with oxygen in red and nitrogen in blue. All DEDD-family members use the two-metal-ion mechanism as represented in the enzyme-nucleic acid or nucleotide complex structures.

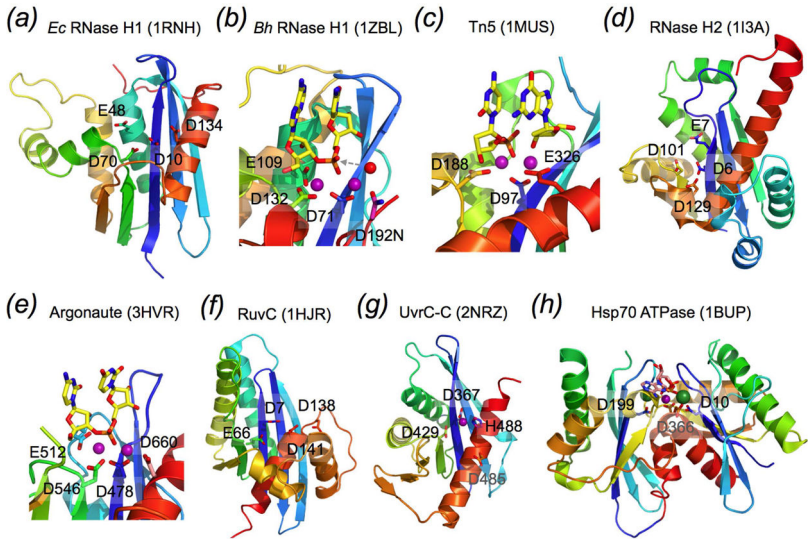

Fig. 7.

The RNase H superfamily consists of various endonucleases. **a.** *E. coli* RNase H1 is the prototype of this superfamily. **b.** The active site of *B. halodurans* RNase H complexed with an RNA/DNA hybrid substrate. **c.** Tn5 transposase (complexed with a cleaved DNA product) represents the HIV integrase-like recombinases with the DDE motif. **d.** RNase H2 has the same topology as RNase H1 but the second and fourth conserved carboxylates are located differently. **e.** The active site of *Tth* Argonaute, essential for RNAi pathways is similar to that of RNase H1. **f.** RuvC is a Holliday-junction resolvase. **g.** The C-terminal nuclease domain of UvrC may use two conserved carboxylates and a His for metal ion coordination and catalysis. **h.** Monomeric Hsp70 ATPases contain two RNase H-like domains. The duplicated domains are both shown in blue to red color gradients. The Asp residues in the first β strand (D10 and D199) are conserved throughout the Hsp70 family and essential for the ATPase activity. Proteins, nucleic acids and divalent cations are shown in the same scheme as in Fig. 6. The green spheres represent the K^+ ions.

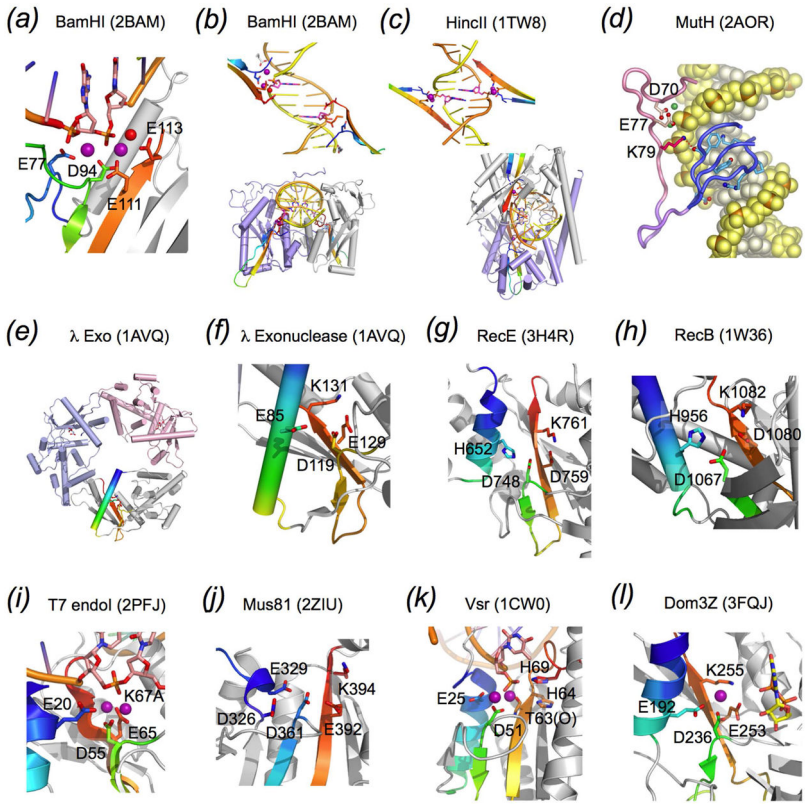

Fig. 8.

The DEK superfamily consists of sequence- or structure-specific endonucleases and processive 3′ - 5′ exonucleases. **a.** The active site of BamHI contains (E)DEE, a variation of DEK. Except for panel b, the region containing the catalytic residues is shown in rainbow colored ribbon diagrams. The rest of the protein is colored grey. Divalent cations and the nucleophilic water are shown in purple and red spheres, respectively. **b.** Orthogonal views of BamHI-DNA interactions. The two BamHI subunits are shown in grey and light purple. The uneven β hairpins containing the DEK motif are highlighted in the rainbow colors. Only the β hairpins are shown when looking into the DNA major groove. BamHI cleaves DNA to form 4nt 5′ overhangs. The nucleotides containing the scissile phosphate are highlighted in pink sticks. **c.** Orthogonal views of HincII-DNA interactions. HincII cleaves DNA to blunt ends. The dimerization interface of HincII is nearly perpendicular to that of BamHI when looking down the DNA helical axis. **d.** *E. coli* MutH is a sequence- and methyl-specific endonucleaese with the DEK motif. The conserved Lys (K79) bridges the DNA sequence-specific binding in the major groove (shown in blue) and catalytic center approaching the minor groove (shown in pink). The divalent cations (Ca^{2+}) are shown as green spheres. **e.** The trimeric phage λ exonuclease has a toroidal shape and degrades ssDNA processively. The three subunits are shown in grey, pink and blue ribbon diagrams. The active site region of the grey subunit is highlighted in rainbow colors. **f.** A zoom-in view of the active site with the eDEK motif. **g.** RecE, which is a processive exonuclease and promotes DNA recombination, is shown in the same color scheme as BamHI. **h.** The active site of RecB has the DEK motif with a His at its N-terminus like RecE. **i.** The Holliday-junction resolvase T7 endonuclease I has the (E)DEK motif like MutH and binds two metal ions. **j.** The structure

specific endonuclease Mus81 and XPF also contain the DEK motif with two conserved carboxylates N-terminal to it. **k.** Vsr is a sequence-specific endonuclease. The DEK motif may be replaced by DHH, and the two metal ions in the active site are coordinated by a carbonyl oxygen (of T63) in addition to the conserved Asp and scissile phosphate. **l.** Dom3Z and Rai1 have the conserved DEK motif and can hydrolyze GTP.

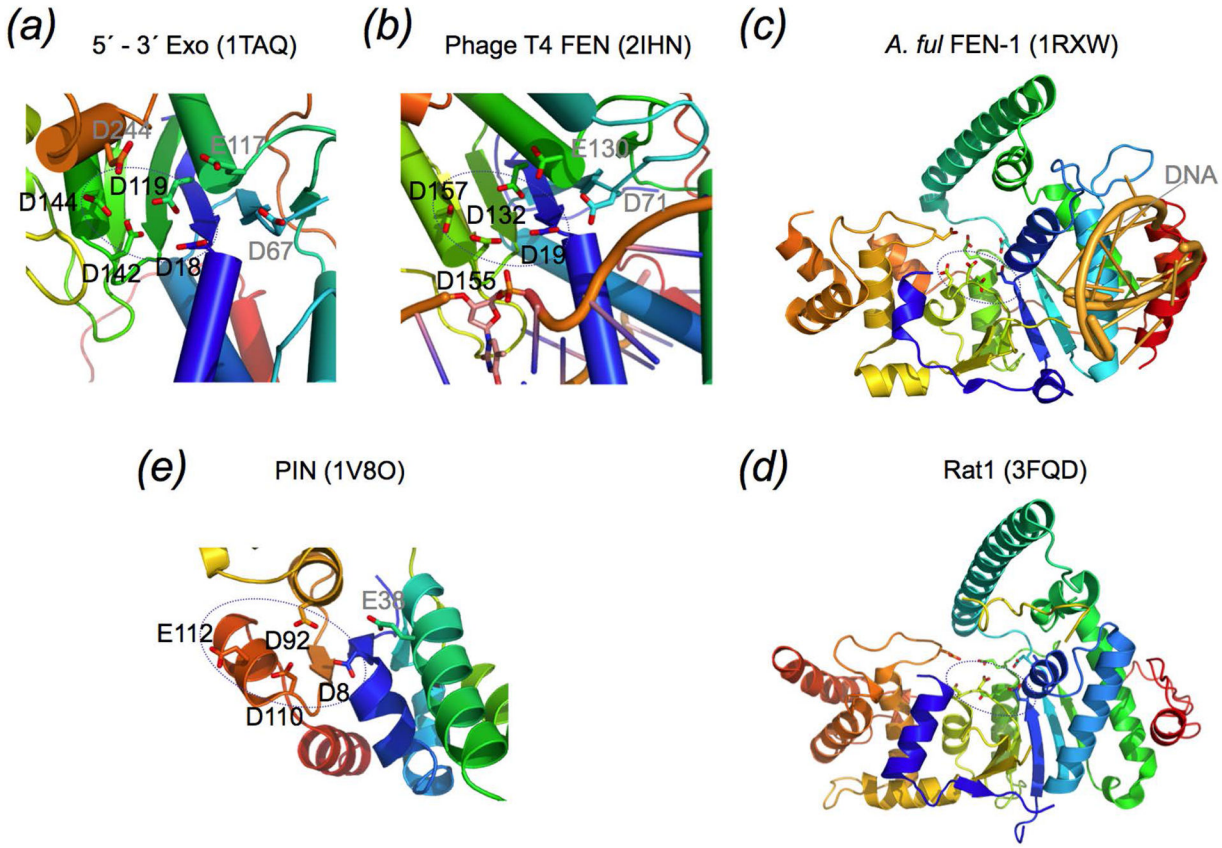

Fig. 9.

The FEN1 and 5′ - 3′ exonuclease superfamily. **a.** The active site of the 5′ - 3′ exonuclease domain of Taq DNA polymerase. Four of seven conserved carboxylates (encircled) likely participate in metal-ion binding and catalysis. **b.** Phage T4 FEN1, previously known as T4 RNase H. The structure was determined in the complex with DNA substrate, but the scissile phosphate is too far away from the catalytic residues in the absence of divalent cations. **c.** The archaeal FEN1 has the same active site composition as the bacterial and phage orthologues. The bound DNA is far away from the nuclease active site. **d.** Rat1, which is an RNase, has the same overall structure and conserved active site as archaeal FEN1. **e.** The PIN domain represents the minimal catalytic core of the nucleases in this superfamily. In all panels, the protein topology is shown in the color gradient from the blue N- to red C-terminus.

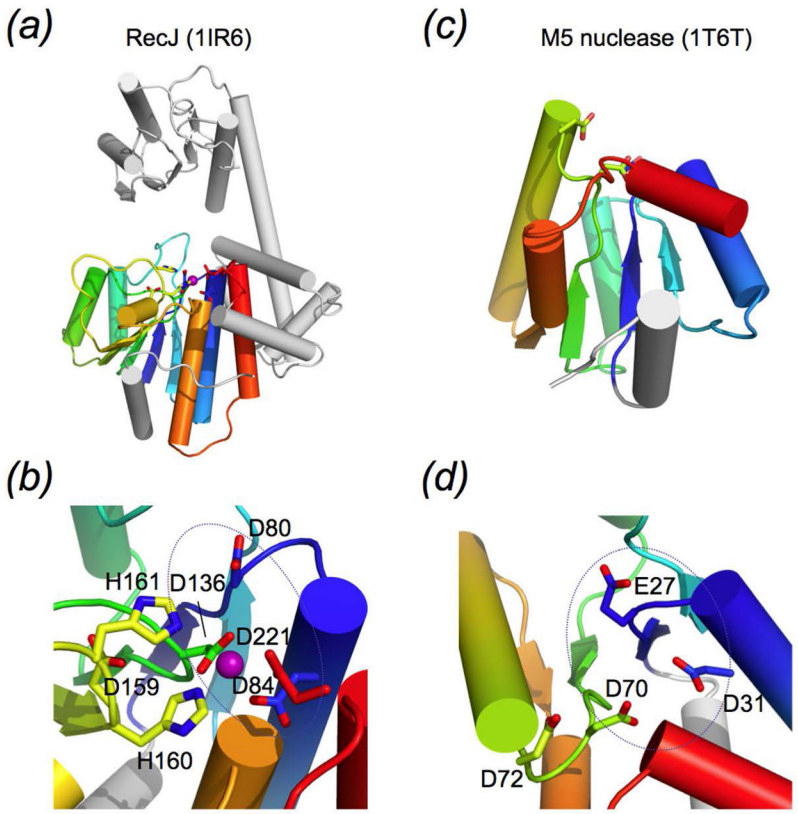

Fig. 10.

Two nuclease families related to FEN1. **a.** RecJ is a representative member of the DHH family. The catalytic and DNA binding domain of RecJ are shown in ribbon diagrams. The catalytic domain containing the DHH motif is shown in rainbow colors with the gradient of blue N- to red C-terminus. The rest of RecJ is shown in grey. **b.** A divalent cation is found in the carboxylate-rich active site in the absence of substrate. **c.** TOPRIM M5 nuclease family has a βα fold of a central parallel 4-stranded β sheet surrounded by α helices. The catalytic carboxylates are located on the loops linking secondary structures. **d.** The active site of M5 nuclease. The four carboxylates are shown as sticks.

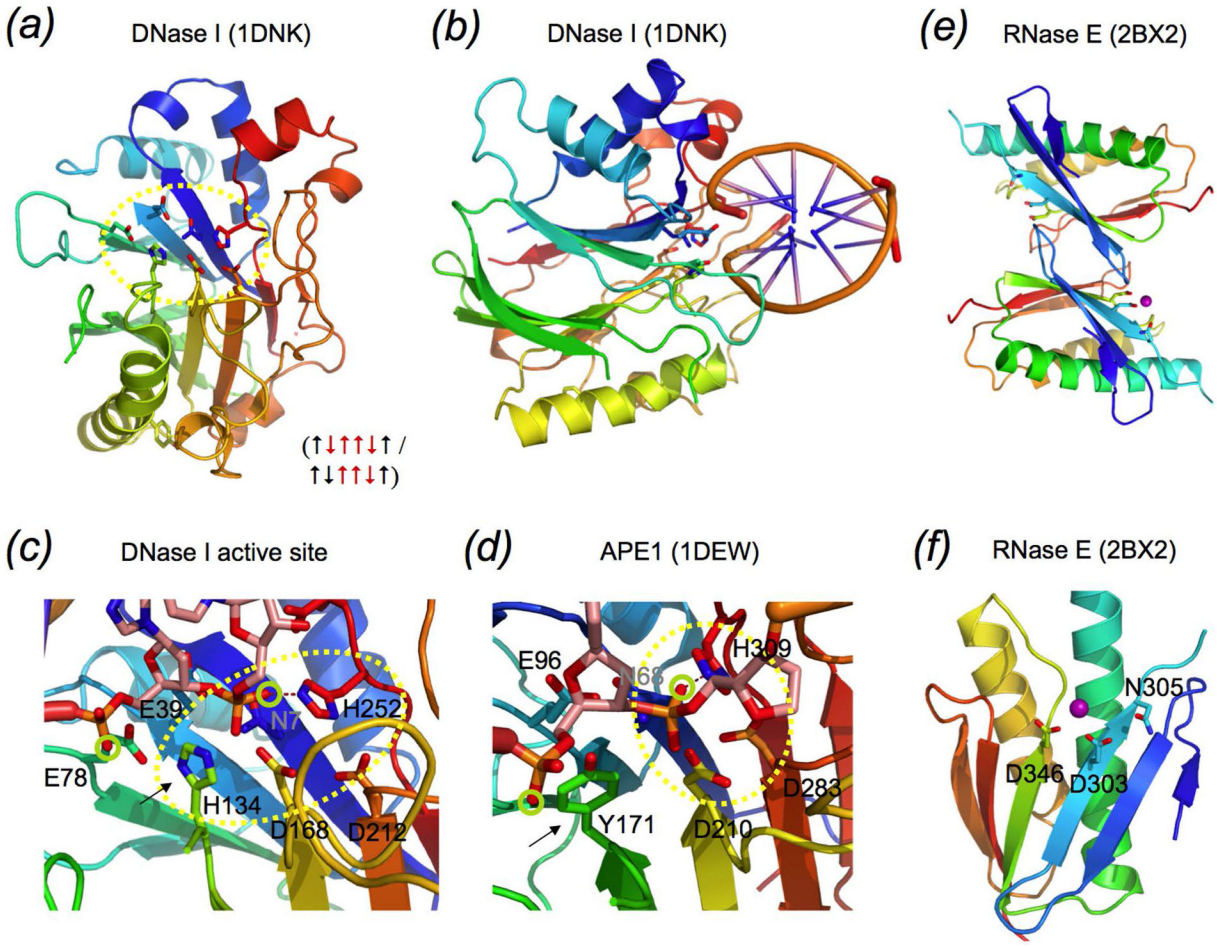

Fig. 11.

DNase I family. **a.** The overall structure of DNase I. Directions of strands are indicated in the parenthesis at the foot of the panel and, the strands contributing catalytic residues are highlighted in red. The active site is encircled. **b**. DNase I with bound substrate. The view is roughly orthogonal to panel a. The two β sheets are related by a pseudo dyad axis lying in the plane of the page and roughly parallel to the strands. **c.** The active site of DNase I. The pro-Sp oxygens of the scissile phosphate and the neighboring phosphate are encircled in green. Note the distortion of the scissile phosphate. **d.** Similar distortion of the scissile phosphate is also observed in the APE1-substrate complex. Most of catalytic residues are conserved between DNase I and APE1 except for the alternative His and Tyr as indicated by the black arrowheads. **e.** The catalytic domain of RNase E upon dimerization is proposed to be similar to DNase I. Both subunits are shown as rainbow-colored ribbon diagrams from blue N- to red C-terminus. The dyad axis between the two subunits is perpendicular to the plane of the page. **f.** The catalytic domain of a single RNase E subunit. The divalent cation is shown as a purple sphere.

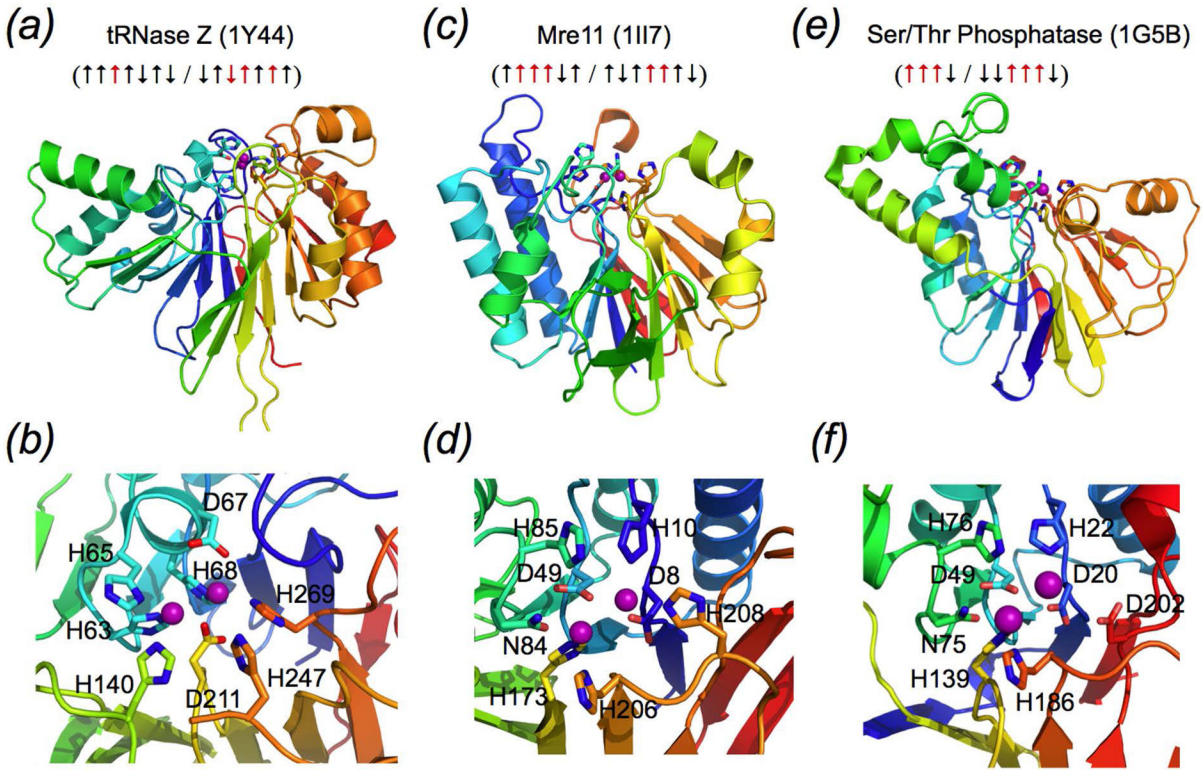

Fig. 12.

Nucleases of the metallo-β−lactamase and protein phosphatase (PP2A) families. **a.** The overall structure of tRNase Z of the metallo-β−lactamase family. Directions of strands in the two β sheets are indicated by the array of arrows. Strands contributing the catalytic residues are highlighted in red. **b.** The active site of tRNase Z consists of six His and two Asp residues. Two metal ions are bound independent of substrate **c.** The overall structure of Mre11. It bears significant similarity to tRNase Z in the topology, tertiary structure, active site composition and metal-ion binding. However, the composition and locations of the catalytic residues are different. **d.** The active site of Mre11 consists of five His, one Asn and two Asp. **e.** A Ser/Thr phosphatase structure is shown for comparison. Its topology has some differences from tRNase Z and Mre11. **f.** The active site of the protein phosphatase is nearly superimposable with that of Mre11.

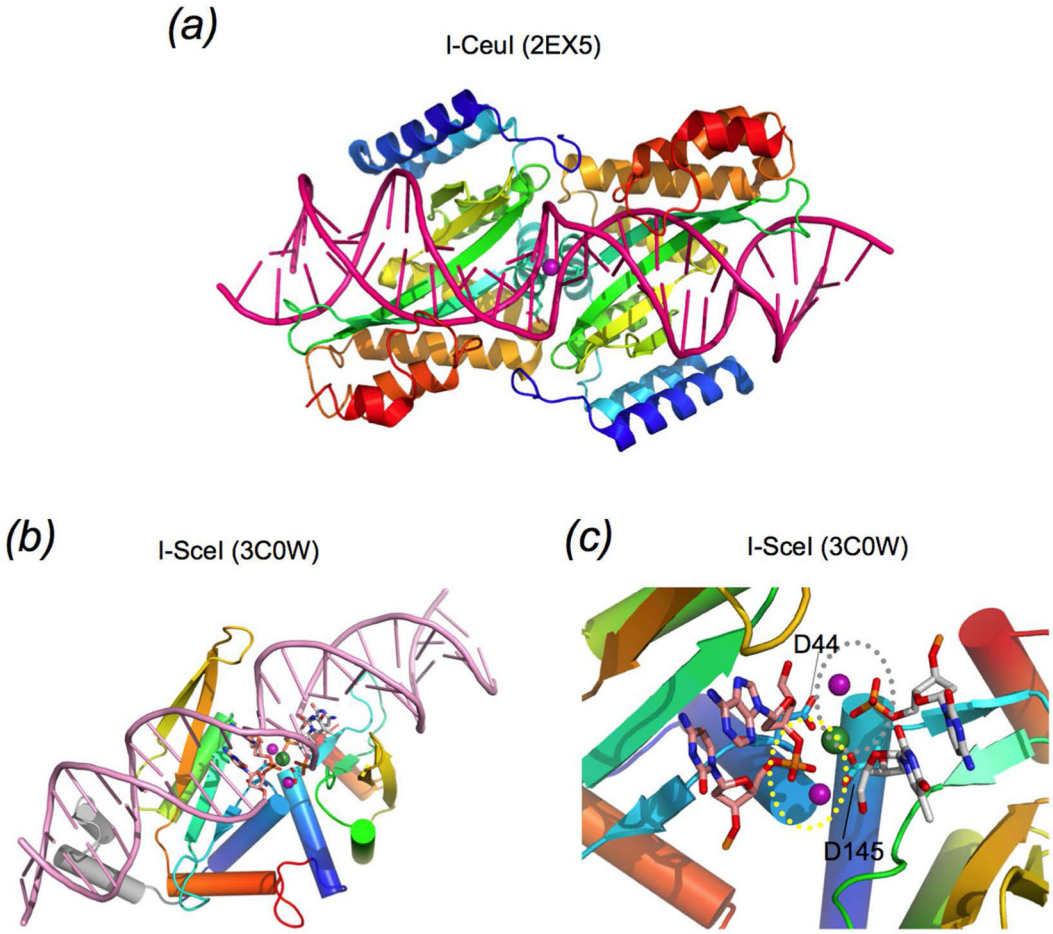

Fig. 13.

The LAGLIDADG homing endonucleases. **a.** The structure of homodimeric I-CeuI in complex with DNA substrate. Each subunit is shown in a rainbow color gradient from blue N- to red C-terminus. The DNA is shown in hot pink ribbon diagrams. The divalent cation bound in the active site is shown as a purple sphere. **b.** Structure of the monomeric I-SceI with two homologous domains in one polypeptide chain. Each domain is colored in blue to red gradient from N- to C-terminus. The green and purple spheres represent the divalent and monovalent cations, respectively. **c.** The active site of I-SceI consists of three cations and two overlapping catalytic centers, which are encircled in grey and yellow. The two scissile phosphates and surrounding nucleotides are colored pink (not cleaved) and white (cleaved). The most conserved Asp residues of the LAGLIDA**D**G motif are shown in sticks.

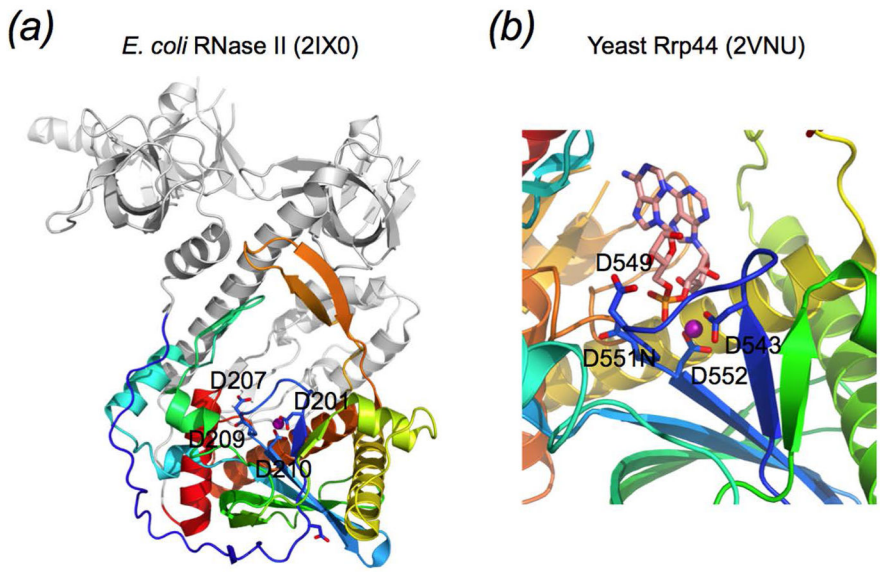

Fig. 14.

Bacterial and eukaryotic RNases II. **a.** *E. coli* RNase II. The catalytic domain is highlighted in rainbow colors, and the remaining domains are shown in grey. The active site is marked by four conserved Asp residues and a bound metal ion (purple sphere). **b.** The active site of Rrp44 in complex with ssRNA. Rrp44 is the yeast homolog of RNase II and is a part of exosome. The four Asp residues are all located on the loop of a β hairpin.

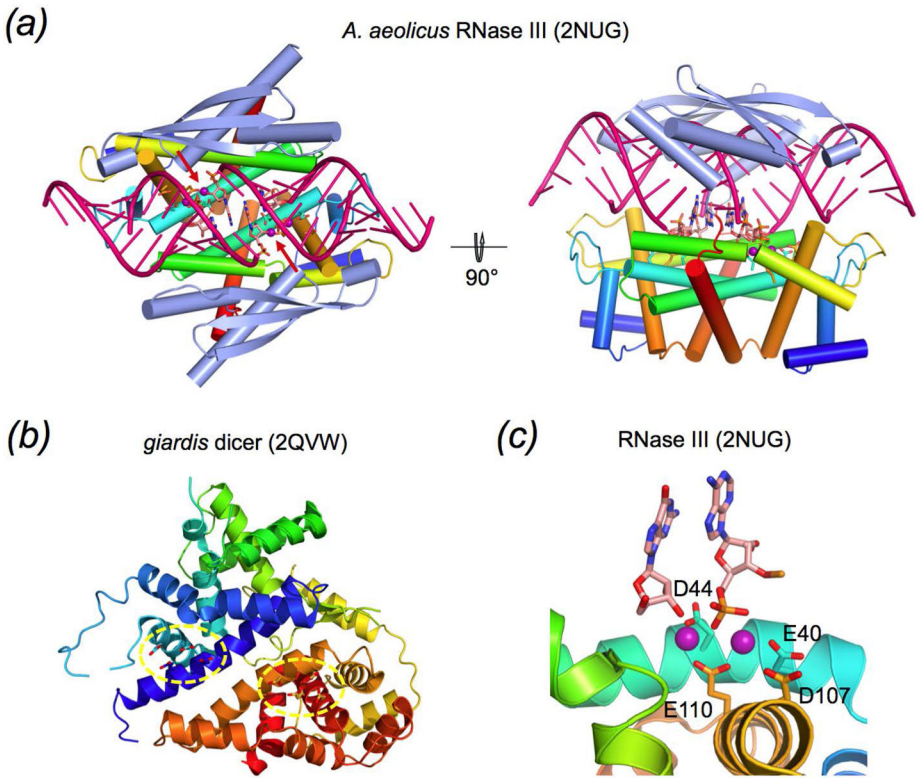

Fig. 15.

RNase III and dicers. **a.** The orthogonal views of a homodimeric RNase III. Each subunit consists of a catalytic domain (rainbow color) and the RNA-binding domain (light blue). The two active sites are marked by the bound divalent cations (purple spheres). The red arrowheads point at the scissile bonds. The catalytic residues and nucleotides flanking the scissile phosphates are shown in sticks. **b.** A eukaryotic dicer is shown in a similar orientation as in panel a. It contains two RNase III-like domains. The region of the duplicated catalytic domain is shown in rainbow color from the blue N to red C terminus, and the two active sites are encircled in yellow. **c.** The active site of the bacterial RNase III and the cleaved RNA.

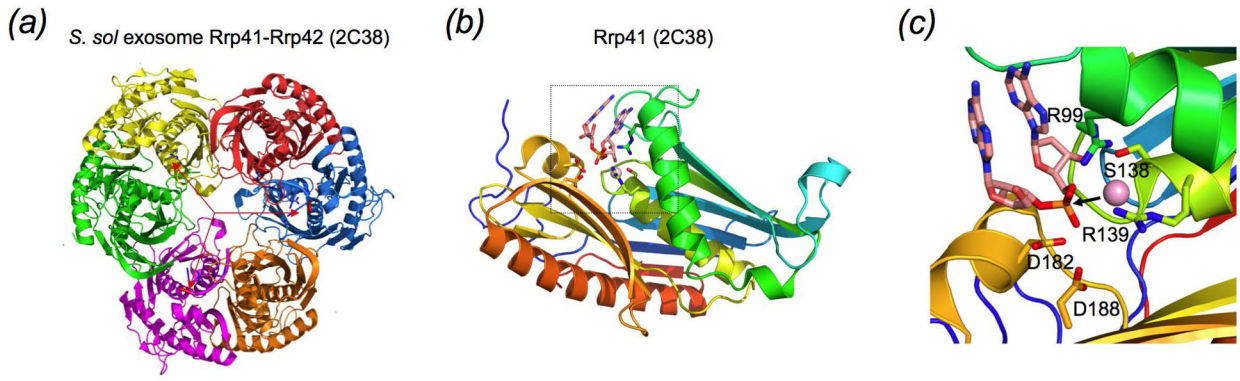

Fig. 16.

Archaeal and eukaryotic RNase PH (PNPase). **a.** The RNase PH core of an archaeal exosome consists of a trimer of Rrp41-Rrp42 heterodimer. The red arrowheads indicate the active sites. **b.** The catalytically active Rrp41 is shown as rainbow colored ribbon diagrams. The pink sphere represents the Cl^- observed in the crystal structure. The two 3′ nucleotides of ssRNA and the residues in the active site are shown as sticks. **c.** A zoom-in view of the catalytic center as boxed in b. The Cl^- mimicking the nucleophile Pi is poised for nucleophilic attack to produce a fresh 3′-OH and NDP.

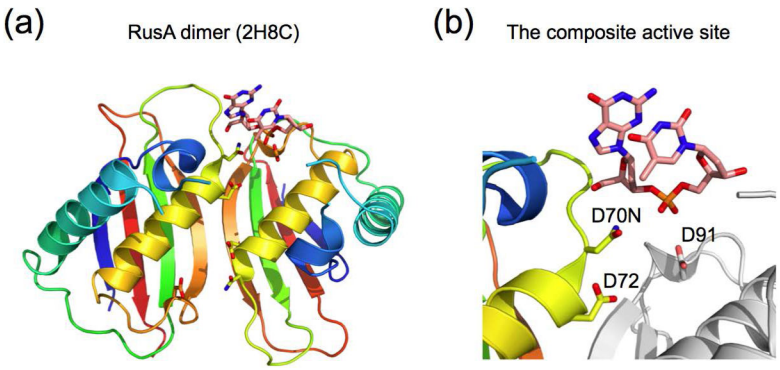

Fig. 17.

Holliday junction resolvase RusA. **a.** An overall view of RusA homodimer. Each subunit is shown in rainbow colors. The active site residues and bound DNA near one active site are depicted in sticks. **b.** A close-up view of the active site. Each active site consists of residues from both subunits (one in rainbow color and the other in silver). Hence it is composite. The catalytic sidechains and two nucleotides surrounding the scissile phosphate are shown as sticks.

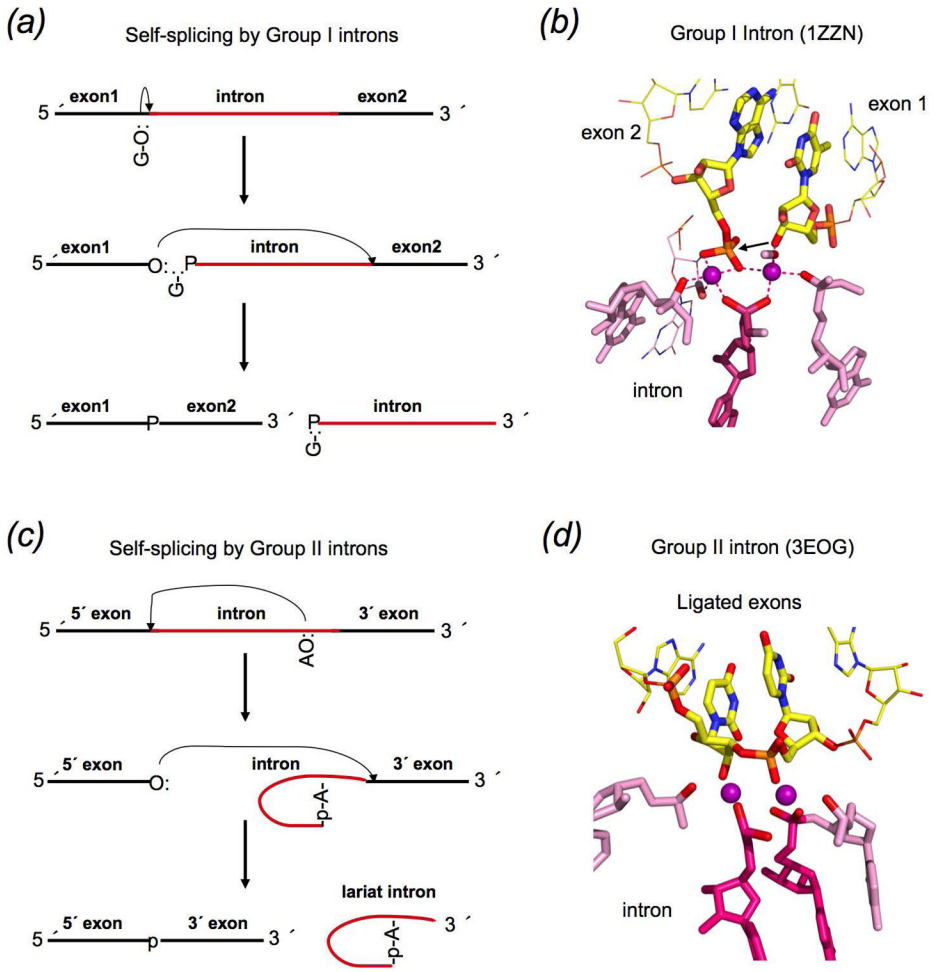

Fig. 18.

Self-splicing introns. **a.** A schematic drawing of phosphoryl transfer reactions catalyzed by group I introns. G-O: represents a free guanosine with its 2′-O serving as the nucleophile. **b.** Structure of the catalytic center of Group I introns. The exons to be ligated are shown in yellow and the nucleotides of the intron involved in catalyses are highlighted in pink and hot pink. Two Mg^{2+} (purple spheres) are jointly coordinated by the scissile phosphate and a backbone phosphate that mimics the sidechain of Asp in protein enzymes. **c.** A schematic drawing of phosphoryl transfer reactions catalyzed by Group II introns. A-O: represents an internal adenosine with its 2′-O serving as the nucleophile. **d.** Structure of the catalytic center of a group II intron in complex with ligated exons as the product of splicing. Two metal ions (purple spheres) again are found in the active site.

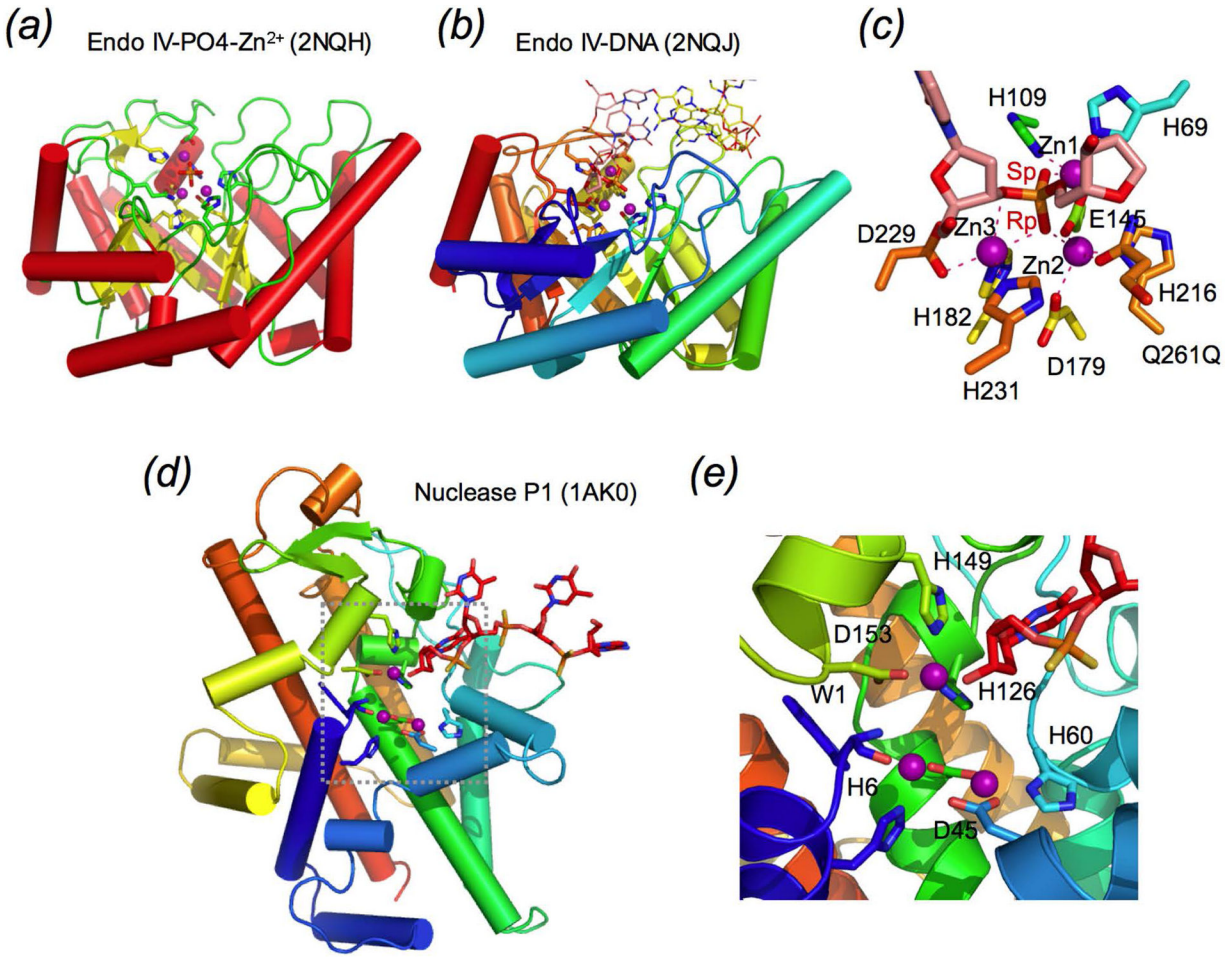

Fig. 19.

Nucleases using the three-metal-ion mechanism. **a.** The structure of AP endonuclease IV (Endo IV) has a TIM barrel fold. The ribbon diagram of Endo IV is colored according to the secondary structures: red α helices, yellow β strands and green loops. A bound phosphate ion is shown as sticks and three Zn^{2+} ions are shown as purple spheres. **b.** The structure of the Endo IV-DNA complex. The protein is shown in rainbow colors from blue N- to red C-terminus. DNA substrate is shown as sticks. The cleavage strand is shown in pink and the other strand in yellow. **c.** A close-up view of the active site. The scissile phosphate is turned so that both pro-Rp and pro-Sp oxygen atoms are coordinated by metal ions. **d.** Nuclease P1 consists of mostly α helices and a β hairpin. The structure represents an enzyme-ssDNA product complex. **e.** A close-up view of the Nuclease P1 active site as boxed in d. In spite of the unrelated structures, the three Zn^{2+} ions and the coordination ligands are reminiscent of Endo IV.

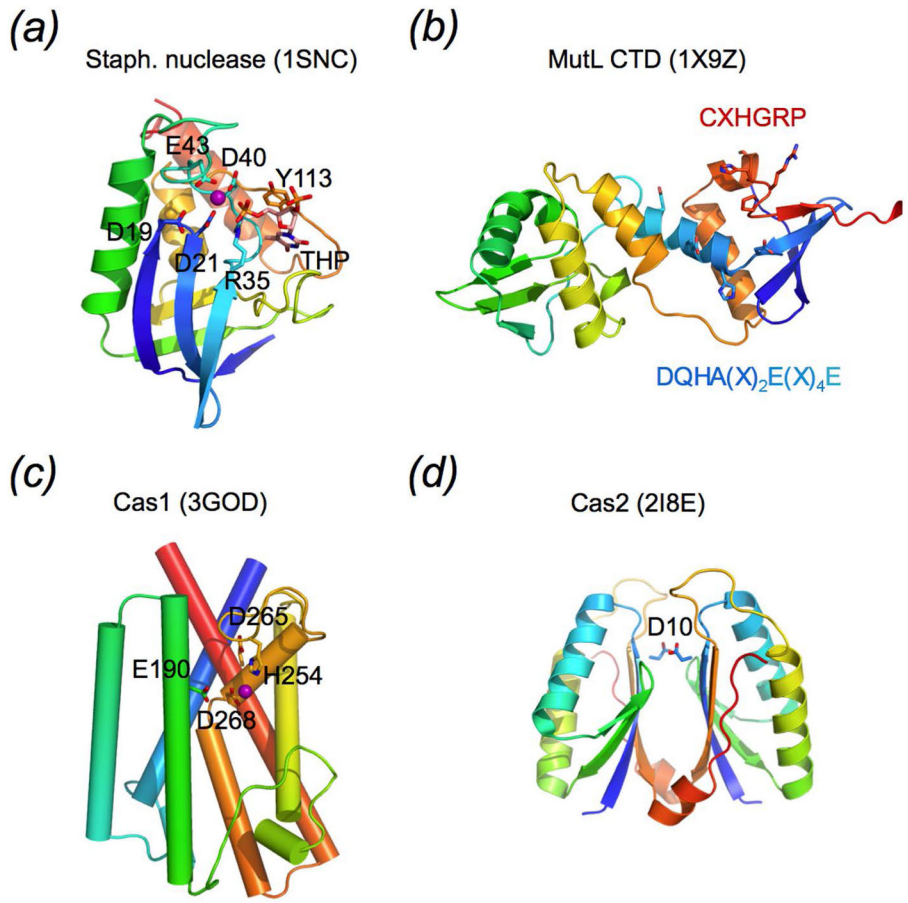

Fig. 20.

Nucleases that may use the two-metal-ion mechanism. **a.** Staphylococcal nuclease (SNase). Thymidine diphosphate (pdTp, THP) co-crystallized and the catalytic residues are shown in sticks. A Ca^{2+} ion captured in the structure is shown as a purple sphere. **b**. The MutL endonuclease activity resides in its C-terminal domain (CTD), The crystal structure of *E. coli* MutL CTD (known as LC20) is shown in a rainbow-colored ribbon diagram. Conserved sequence motifs surrounding the metal-ion-binding site are shown in matching colors of the ribbon diagram and modeled onto the structure with sidechains shown as sticks. **c.** Cas1 is a CRISPR nuclease. The dimerization domain is not shown here. One catalytic domain is shown in rainbow colored ribbon diagrams with helices shown as rods. The active site is composed of three carboxylates and one His. A bound Mn^{2+} is shown as a purple sphere. **d.** The structure of Cas2. Cas2 is a CRISPR RNase with the ferredoxin fold. Both subunits of the homodimer Cas2 are shown in rainbow color from blue N- to red C-terminus. The active site is located at the dimer interface with the conserved and catalytically essential Asp shown in sticks and labeled.

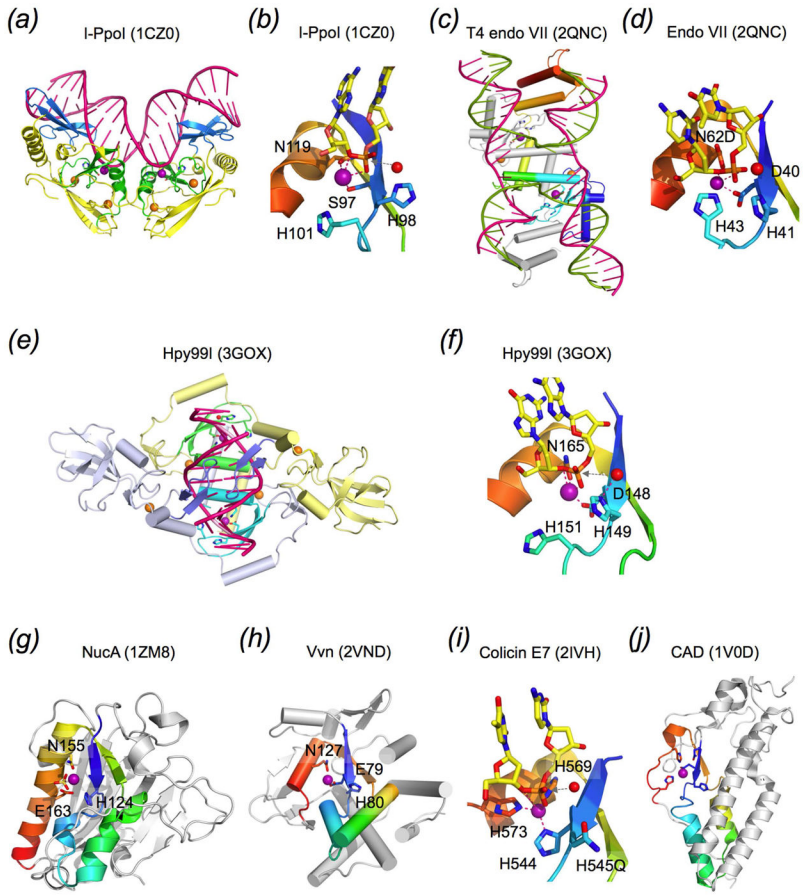

Fig. 21.

The ββα-Me nucleases. **a.** The overall structure of homing endonuclease I-PpoI. It is homodimeric, and the identical protein subunits are shown in the same color schemes. The catalytic domain is shown in green, DNA recognition domain in blue and the connection region in yellow. The cations in the active sites are shown as purple spheres, and structurally important Zn^{2+} ions are shown as orange spheres. DNA is shown in hot pink. **b.** A close-up of the active site. The ββα structural motif is shown in rainbow colors. The scissile phosphate and surrounding nucleotides are shown as yellow sticks. A Na^{+} mimicking the catalytic divalent cation in this structure is shown in purple. The catalytic residues are shown in sticks and labeled. The potential nucleophilic water is shown as a red sphere. **c.** T4 endonuclease VII (Endo VII) resolves Holliday junctions. One of the two subunits is shown in rainbow color (from blue N- to red C-terminus) and the other in silver. The lime-green DNA strands are to be cleaved. The Mg^{2+} ions in the active site are shown as purple spheres, and structural Zn^{2+} ions as orange spheres. One ββα motif in this panel is colored cyan. **d.** A close-up view of the active site of Endo VII. The presentaion scheme is same as in panel b. **e.** The structure of restriction endonuclease Hpy99I in complex with DNA substrate. The two subunits of Hpy99I are shown as pale blue and yellow ribbon diagrams. The DNA-binding modules of both subunits are highlighted in blue, and the twp ββα-Me motifs in green and cyan. The catalytically essential Mg^{2+} ions are substituted by Na^{+} ions and shown as purple spheres. Zn^{2+} ions (orange spheres) play a structural role. DNA is colored pink and

the scissile phosphates are indicated in light pink. **f.** The active site of Hpy99I. **g** and **h.** The overall structures of NucA/EndoG and Vvn. The ββα-Me motif in each structure is highlighted in rainbow colors and the metal ion shown as a purple sphere. The remaining protein structures are shown in silver grey. **i**. The active site (ββα-Me motif) of colicin E7 in complex with DNA substrate. The catalytic Zn^{2+} is coordinated by three His sidechains and two oxygens of the scissile phosphate. The general base H545 is mutated to Q to stop the cleavage reaction. **j.** The catalytic domain of CAD. The ββα-Me motif is highlighted as in panels f and g.

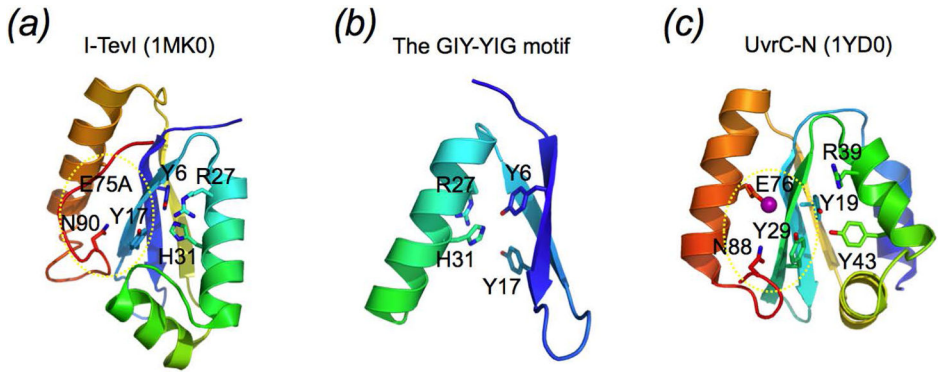

Fig. 22.

GIY-YIG nucleases. **a.** I-TevI homing endonuclease. The catalytic domain is shown in rainbow-colored ribbon diagram. **b.** A close-up view of the GIY-YIG motif, which forms a β hairpin. The conserved Tyr are labeled. With the following α helix, the structure resembles the ββα-Me motif, but the GIY-YIG motif doesn't bind metal ion. **c.** The N-terminal domain of UvrC has the GIY-YIG motif. A divalent cation is coordinated by E76 and probably marks the active site. The catalytic residues Y (of YIG), E and N near the C-terminus are conserved in both and are encircled in yellow.

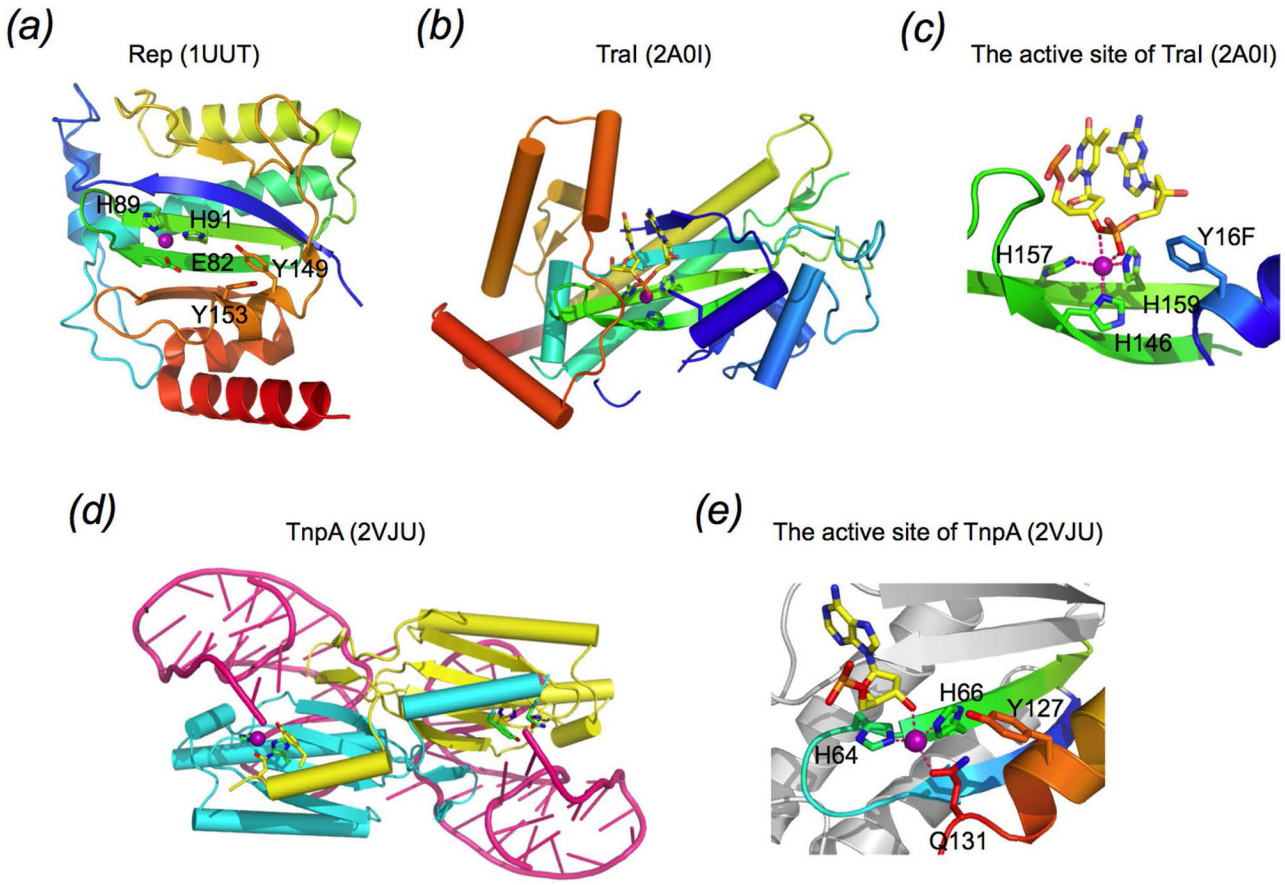

Fig. 23.

The HuH nucleases. **a.** The nuclease domain of Adeno-associated virus (Aav5) Rep shown in rainbow colored ribbon diagrams. The associated metal ion is shown in purple. **b.** The structure of TraI relaxase (Y16F mutant) representing the mob family. Only two nucleotides surrounding the scissile phosphate of the ssDNA substrate are shown as sticks. **c.** A close-up view of the TraI active site. Three His sidechains coordinate the Mg^{2+}, which in turn aligns the scissile phosphate for nucleophilic attach by Y16. **d.** Ribbon diagrams of the DNA transposase (TnpA) of IS608 complexed with a 3′-end cleavage product. TnpA is homodimeric. The two domain-swapped protein subunits are shown in yellow and cyan, and the two DNAs in hot pink. **e.** A close-up view of the composite TnpA active site. The last nucleotide at the 3′ end is also shown. The metal-chelating His residues (of the HUH motif) are from one subunit. The third metal ligand (Q131) and the nucleophile Y127 are from the other subunit.

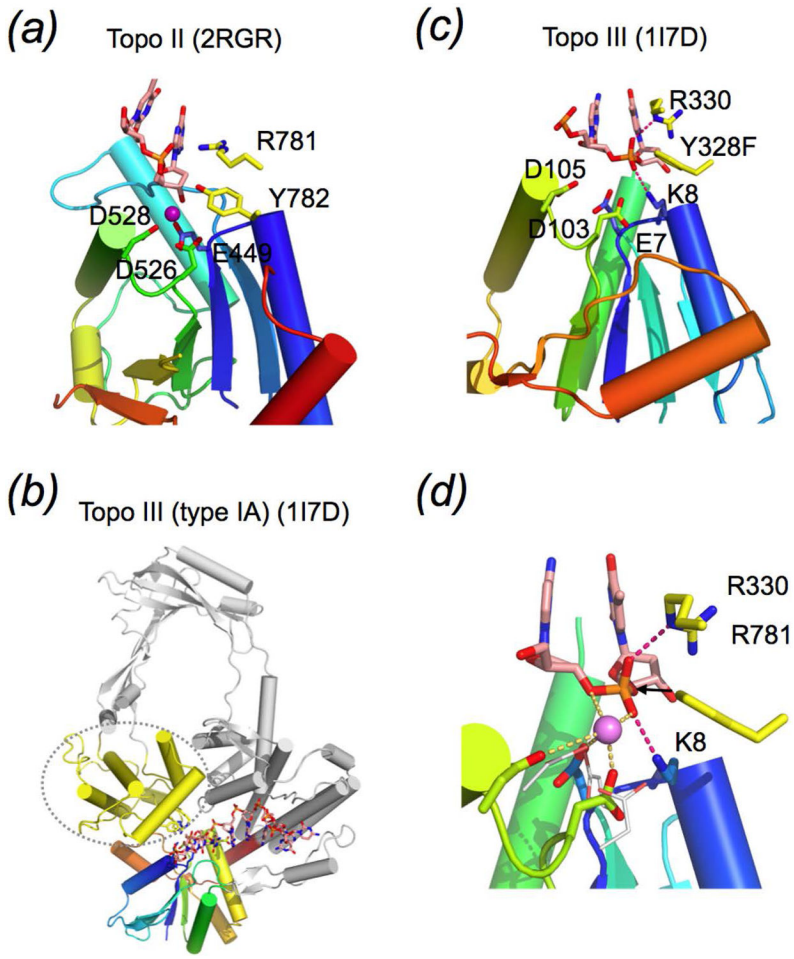

Fig. 24.

Topoisomerases containing the TOPRIM motif. **a.** The active site of *S. cerevisiae* Topo II in complex with dsDNA substrate. The TOPRIM domain is shown in rainbow-colored ribbon diagram. The nucleophile Y782 and its neighbor R781 are supplied in trans by the other subunit of the dimeric Topo II and shown as yellow sticks. The scissile phosphate and surrounding nucleotides are shown as pink sticks. Nitrogen and oxygen atoms are colored blue and red, respectively. A Mg^{2+} ion (purple sphere) is coordinated by the conserved carboxylates in the TOPRIM domain. **b.** Ribbon diagrams of *E. coli* Topo III (Type IA) in complex with ssDNA substrate. The α-helices are represented by cylinders. The TOPRIM domain (aka domain I) is shown in rainbow colors, and the catalytic domain (domain III) carrying the Tyr nucleophile is shown in yellow. The ssDNA substrate in shown as sticks. **c.** A close-up view of the active site of Topo III. The scissile phosphate, the conserved carboxylates, and the nuclephile Y328 are nearly superimposable with that of Topo II shown in panel a. **d.** A model of the reaction coordinates of DNA cleavage by type IA and type II topoisomerases. The active sites of the two types of TOPRIM topoisomerase are superimposed. The metal ion observed in Topo II is incorporated in the composite active site and shown as a lilac sphere. A Lys (K8) of Topo III approximately occupies the metal ion A position. The Arg next to the nucleophile (R781 of Topo II or R330 of Topo III) in the

catalytic domain further stabilizes the scissile phosphate and neutralizes the developing negative charges.

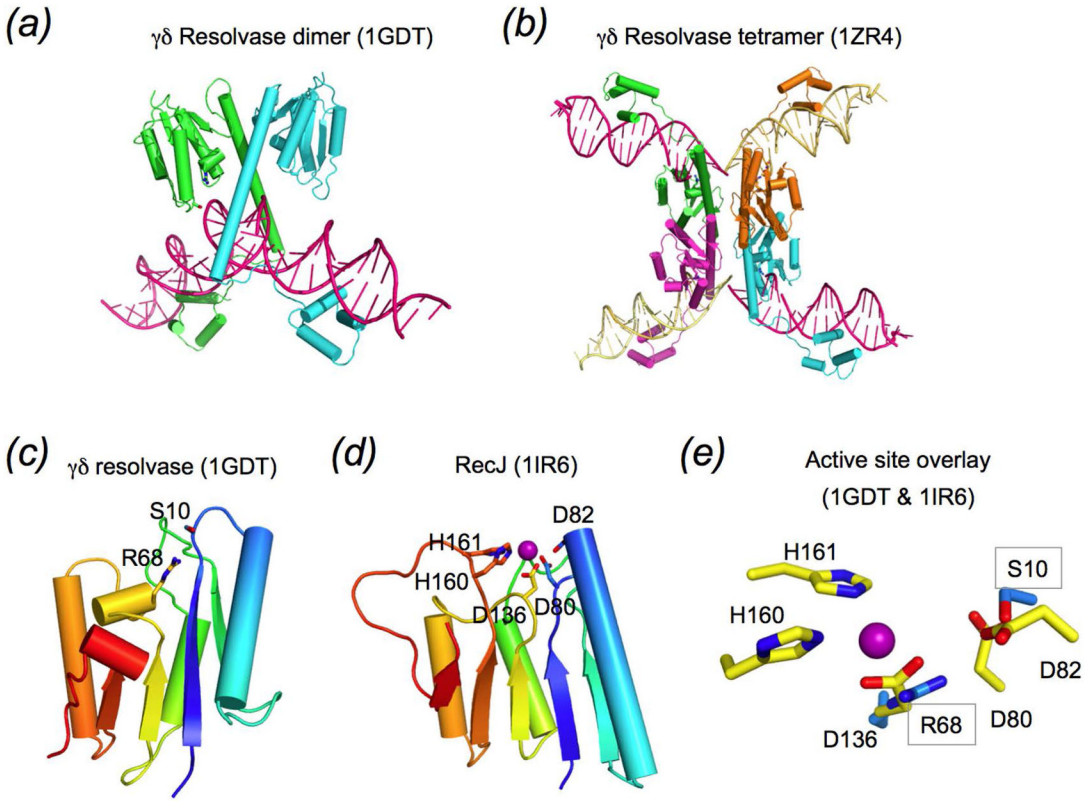

Fig. 25.

Metal-independent Ser recombinases. **a.** The structure of γδ resolvase dimer complexed with a palindromic DNA cleavage site (site I). Each protein subunit and DNA are shown in different colors. The catalytic residues are shown as sticks. **b.** The γδ resolvase tetramer complexed with two cleaved DNA site I. Each protein dimer and DNA site are rearranged extensively. **c.** The catalytic domain of resolvase is shown in rainbow colors from blue N- to red C-terminus. The catalytic residues S10and R68 are shown in sticks. **d.** The catalytic domain of RecJ. The metal coordinating carboxylates and the DHH motif are shown as sticks. **e.** Superposition of the catalytic residues of resolvase (blue) and RecJ (yellow).

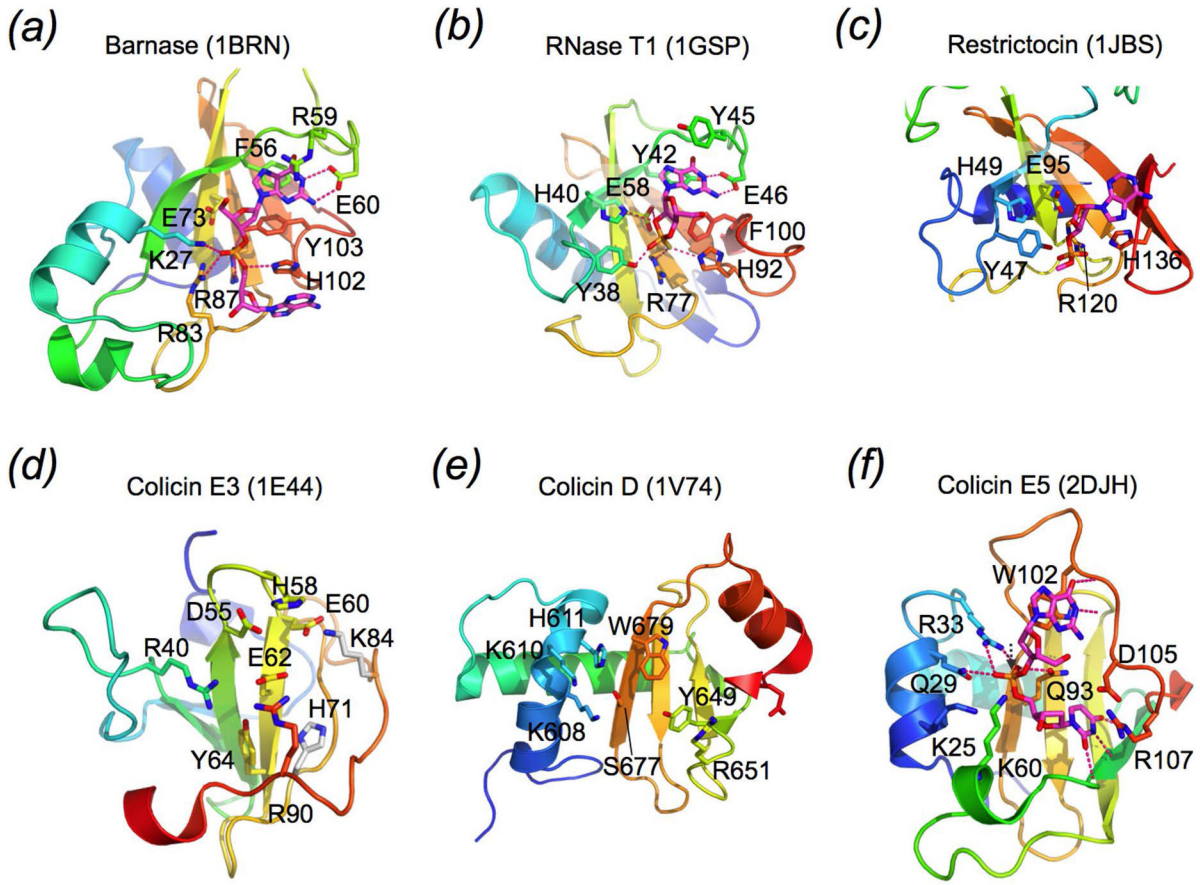

Fig. 26.

Metal-independent RNases of T1 family and colicins. **a.** Barnase in complex with a substrate mimic d(GGAC). The RNase is shown in rainbow-colored ribbon diagrams. The scissile phosphate and surrounding nucleotides are shown as magenta sticks. The active site residues are shown in sticks and labeled. Hydrogen bonds with the scissile phosphate and the surrounding bases are shown as dashed lines. **b.** RNase T1 complexed with a phosphorothioate cleavage product. The sulfur atom in the 2′, 3′ cyclophosphrothioate is shown in light yellow. **c.** Sarcin homolog restrictocin in complex with the mimic of sarcin/ricin loop. Only the active site is shown. The RNA is not positioned for cleavage. **d.** The ribonuclease domain of colicin E3. The potential active site residues are shown as sticks in the same colors as their Cα atoms. Those, whose mutations don't decrease the nuclease activity, are shown in silver. **e.** The nuclease domain of colicin D with the active site residues shown in sticks. **f.** Colicin E5 complexed with d(GU). Sequence specificity is determined by the numerous hydrogen bonds between the RNase and the bases surrounding the scissile phosphate. The nucleophilic attack would take place as indicated by the black dashed arrowhead if 2′ -OH is present.

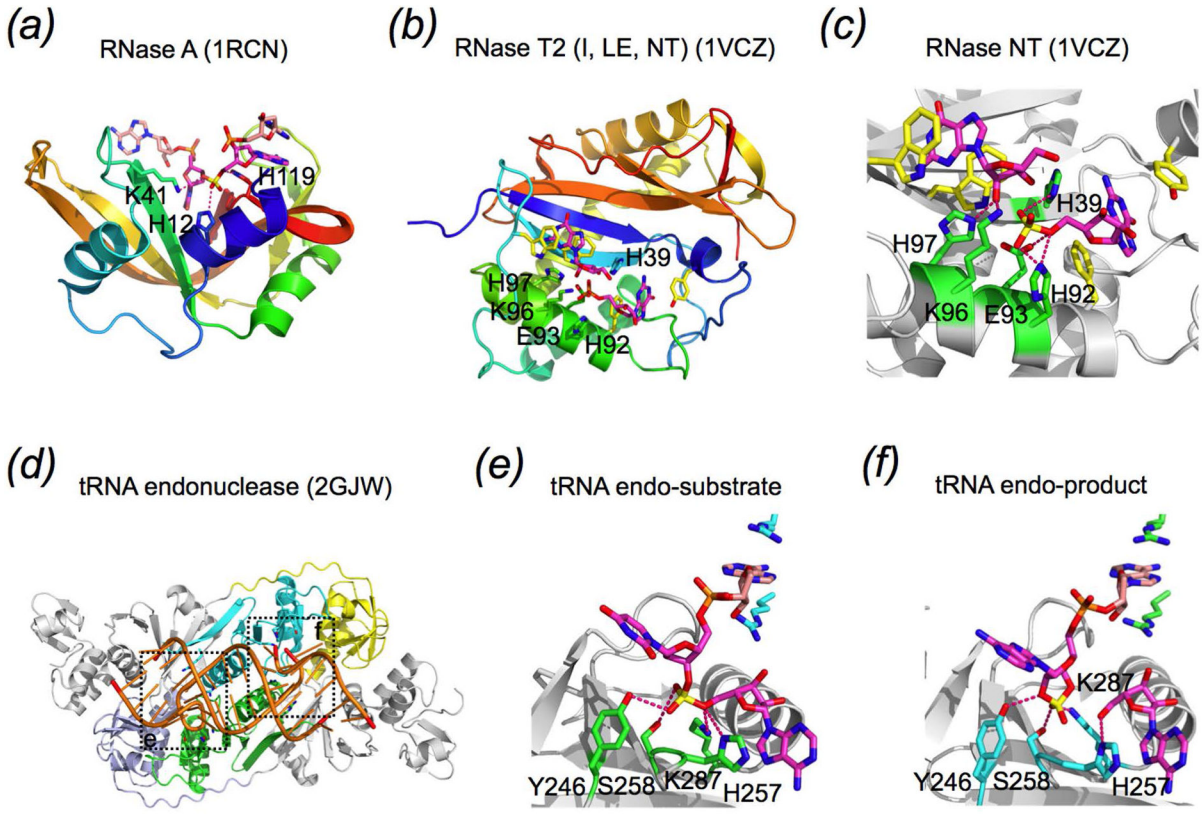

Fig. 27.

RNase A and related RNases. **a.** RNase A in complex with d(ATAAG) substrate mimic. RNase A is shown in rainbow-colored ribbon diagrams with the catalytic triad (HKH) shown as sticks. The scissile phosphate is shown in yellow, the surrounding nucleotides in magenta and other nucleotides in pink sticks. **b.** An example of RNase T2 family, RNase NT, complexed with two GMP. The structure is shown in the same scheme as in panel a. **c.** A close-up view of the substrate recognition by RNase NT. The two bases surrounding the putative scissile phosphate are sandwiched by aromatic sidechains (shown in yellow). The HKH catalytic triad (shown in green sticks) appears to be conserved, and the two His sidechains serve as general acid and base. **d.** The overall structure of a homodimeric tRNA splicing endonuclease. Each catalytic unit consists of a catalytic domain (shown in blue and cyan) and an associated unique domain (shown in yellow and steel blue). Two structural units are shown in silver grey and are homologous to the catalytic units (green+yellow or cyan+light) by gene duplication. The four units can be independent polypeptide chains in other orthologs. The pre-tRNA mimic is shown in orange ribbon diagrams. The uncleaved and cleaved scissile phosphates are boxed and labeled as e and f, respectively. **e.** A close-up view of the active site (green subunit) with uncleaved RNA (substrate). Hydrogen bonds with the scissile phosphate are shown as hot pink dashed lines. RNA substrate is stabilized by cation-**π**-cation stacking with a neighboring subunit (cyan). **f.** The active site (cyan subunit) with the cleavage product, 2′,3′-cyclic phosphate.

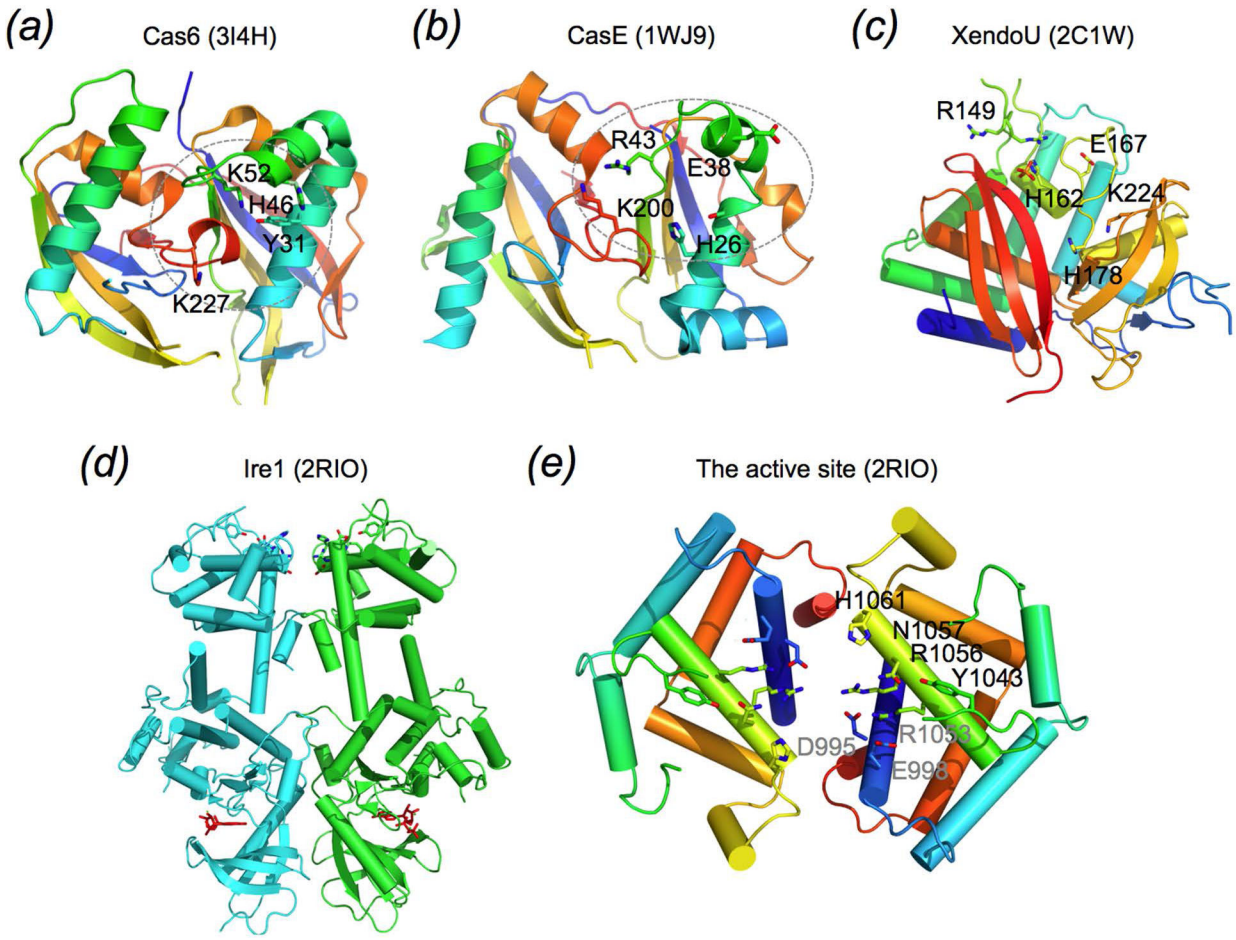

Fig. 28.

Other metal-independent RNases. **a.** *Pyrococcus furiosus* Cas6. The two ferredoxin-like domains arranged in a direct repeat are both shown in rainbow-colored ribbon diagrams, from blue N- to red C-terminus. Putative catalytic residues are shown as sticks. **b.** *Thermus thermophilus* CasE is related to Cas6 and shown in the same color scheme. Only the Lys near the C-terminal is conserved between Cas6 and CasE. **c.** Ribbon diagram of XendoU. The protein is in rainbow color from blue N- to red C-terminus. A pseudodyad symmetry relates the two 3-stranded β sheets. A bound phosphate is shown as orange and red sticks. The conserved and catalytic essential residues are also shown and labeled. **d.** The overall structure of IreI homodimer. The two subunits are shown in green and cyan, and the bound ADPs in the kinase domains are shown in red sticks. The nuclease domains (top) are highlighted with the catalytic residues shown in sticks. **e.** A close-up view of the putative active site of IreI. Each nuclease domain is shown in rainbow colors. The residues (in one subunit) with strong effects on catalysis are labeled in black, and those of with medium effects in grey.

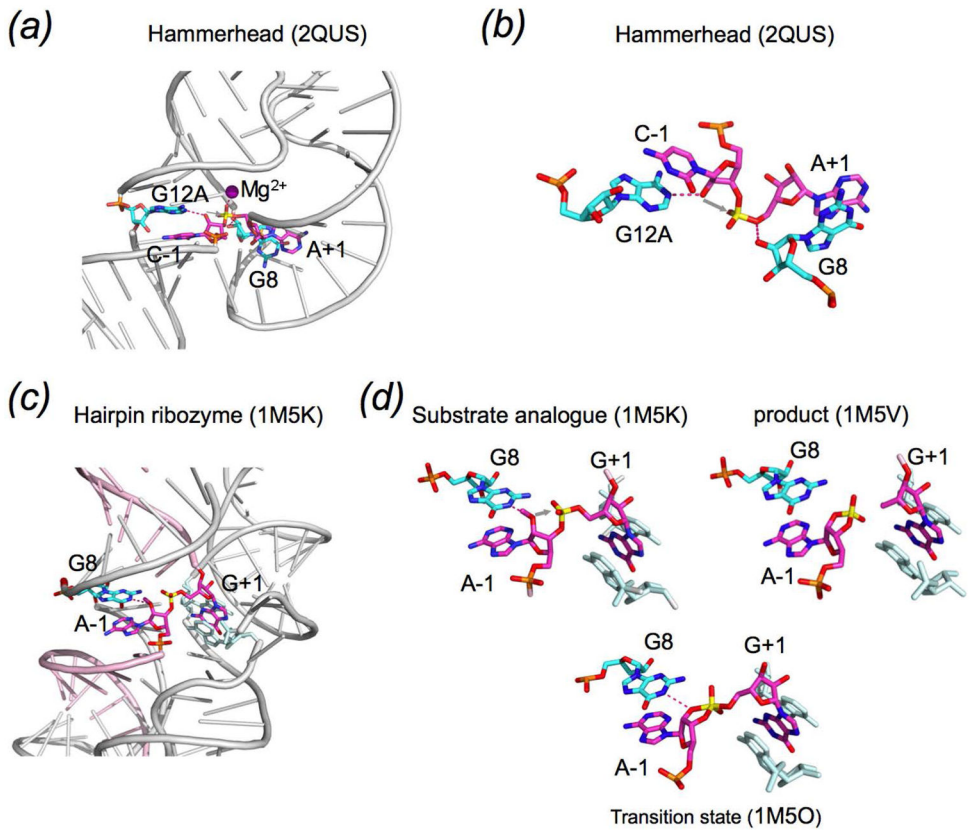

Fig. 29.

Metal-independent ribozymes. **a.** Hammerhead ribozyme. The RNA is shown in silver ribbon diagrams. The scissile phosphate is shown in yellow, the surrounding nucleotides (C-1 and A+1) in magenta, and the catalytic nucleotides in cyan. A Mg^{2+} (purple sphere) happens to be coordinated by the scissile phosphate. **b.** A close-up view of the catalytic center in the hammerhead. The Mg^{2+} is omitted for clarity. The reaction is stopped because of the G12A mutation, which reduces the effectiveness of the general base. The 2′-OH of G8 is proposed to be the general acid. **c.** The overall structure of a catalytically active Hairpin ribozyme. The RNA substrate is shown in pink ribbon diagrams, and the others are shown in the same scheme as in panel a. **d.** Close-up views of the active site of the hairpin ribozyme complexed with a substrate analog (A-1 is 2′-O-methylated), transition state analog (vanadate) and product (2′, 3′ cyclic phosphate).

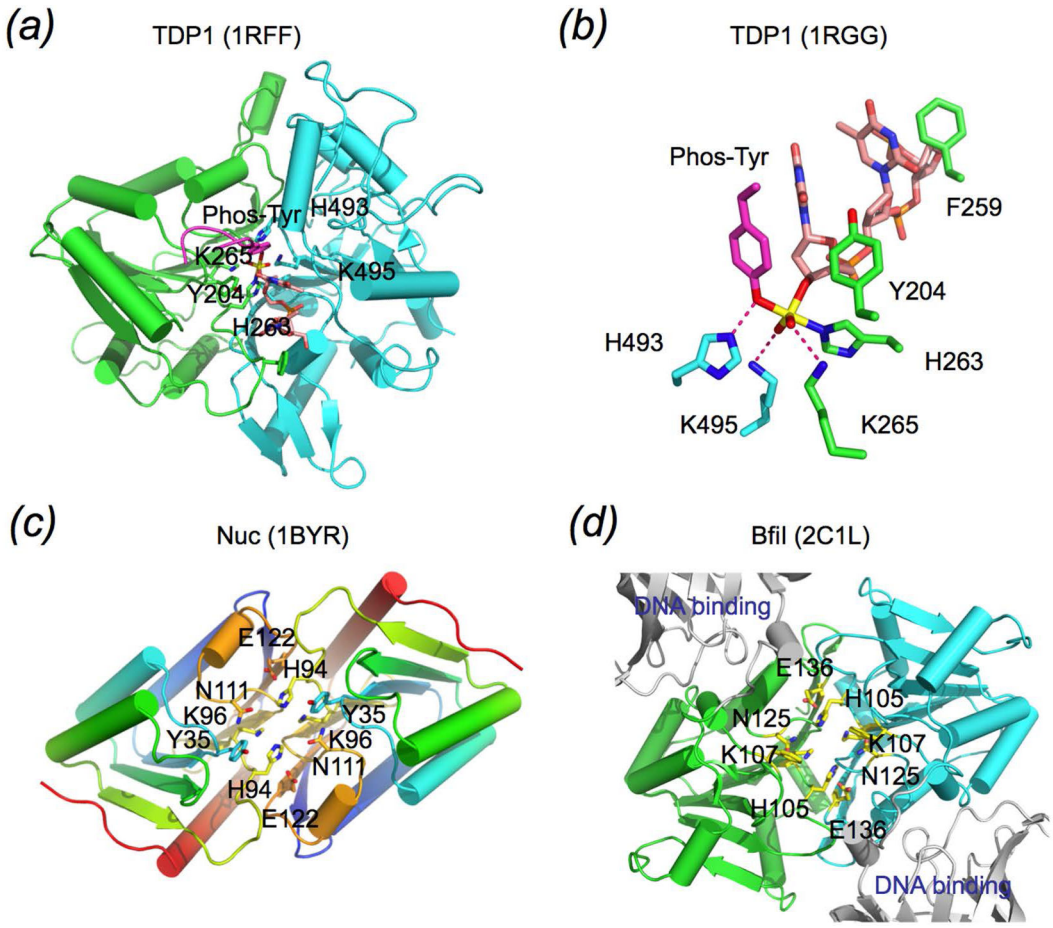

Fig. 30.

Metal-independent DNases of the PLD family. **a.** The overall structure of Tyrosine dephosphatase (TDP1). TDP1 serves as a paradigm of phosphoryl transferases using His as the nucleophile. Two gene-duplicated domains are shown in green and cyan. The phosphorylated Tyr is shown in magenta, the scissile phosphate in yellow sticks, and remaining oligonucleotides in pink. The catalytic residues are shown in sticks and colored in green and cyan as the Cα atoms. **b.** A close-up view of the catalytic center. A mimic of the covalent intermediate (vanadate) is shown in yellow. The duplicated His and Lys are directly involved in catalysis. **c.** The overall structure of *S. typ* Nuc shown in the orientation similar to TDP1 in panel a. The two identical subunits are both shown in rainbow colors. **d.** The catalytic domains of dimeric restriction endonuclease BfiI. The catalytic domains of two subunits are shown in green and cyan and oriented similarly as TDP1 and Nuc. Sequence-specific DNA-binding domains are shown in silver grey.

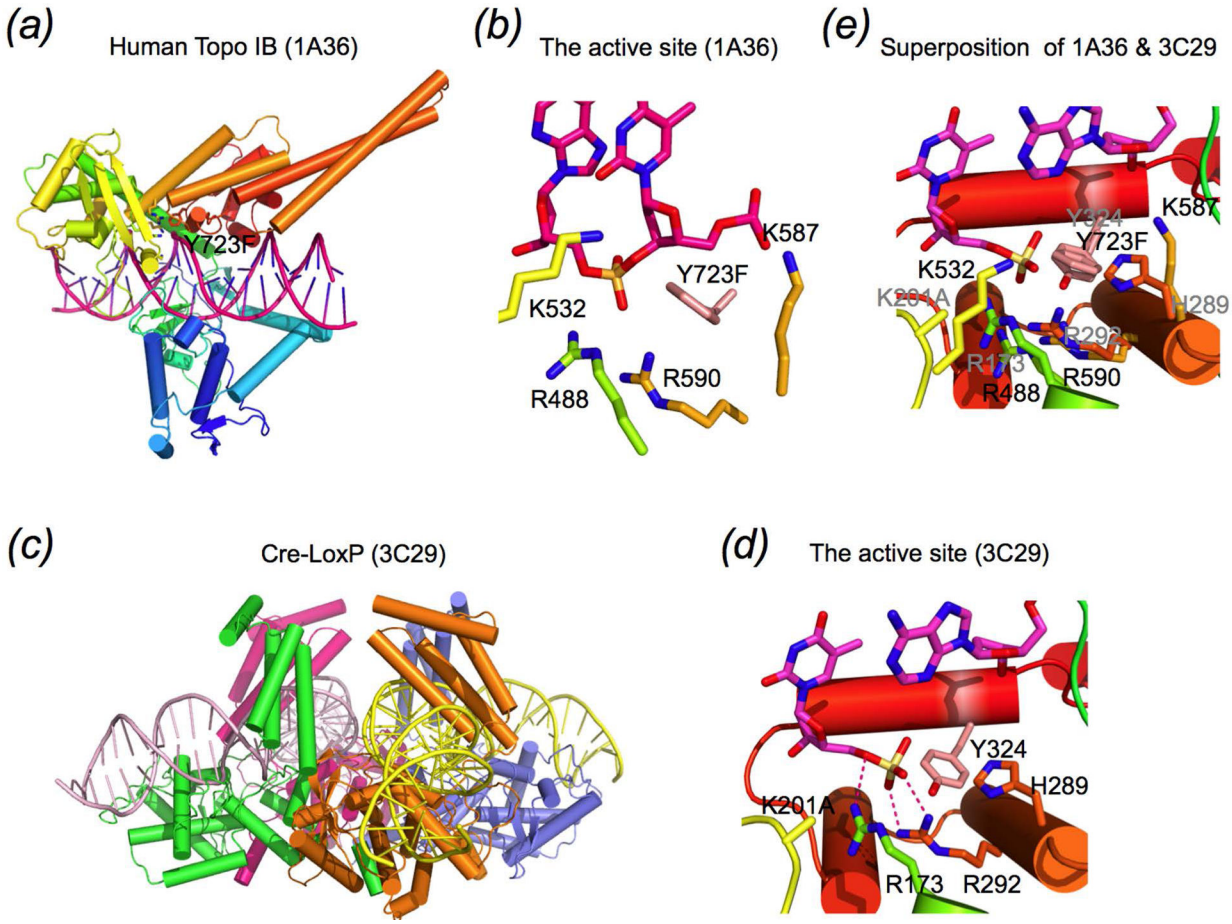

Fig. 31.

Metal-independent topoisomerases and Tyr recombinases. **a.** The overall structure of Human Topo IB. The protein is shown in rainbow-colored ribbon diagrams. The DNA duplex is shown in pink/blue ribbons. The active site is highlighted with the catalytic residues shown in sticks. The nucleophile Y723 (mutated to Phe) is labeled. **b.** A close-up view of the active site of Topo IB. The reaction is stopped because of the Y723F (shown in pink) mutation. The scissile phosphate is neutralized by Arg and Lys sidechains. **c.** The overall structure of the Cre recombinase complexed with substrate LoxP site. The tetrameric Cre is shown in four colors and the two LoxP in pink and yellow. The DNA binding domains are above the DNA and the catalytic domains are below. **d.** A close-up view of the active site of Cre-LoxP. The scissile phosphate is already pre-nicked. **e.** Superposition of the catalytic residues of Topo IB and Cre.

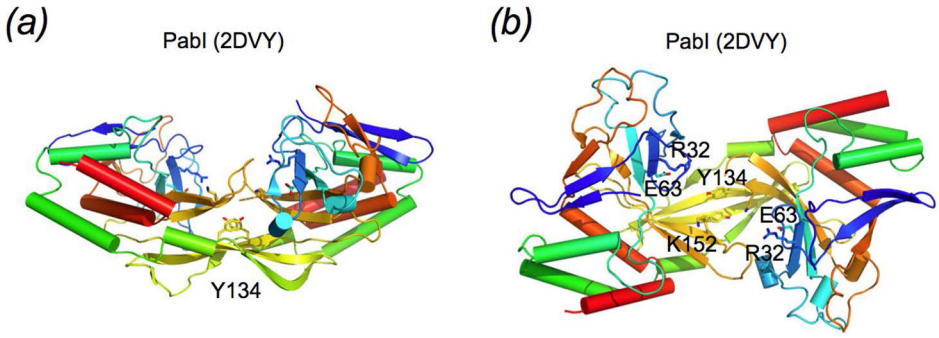

Fig. 32.

PabI family of restriction endonuclease. **a.** The overall structure of homodimeric PabI. Two subunits are both shown in rainbow colors. The shape is likened to a halfpipe. The catalytically essential Y134 from both subunits are close together at the bottom of the central groove. **b.** An orthogonal view of PabI. The catalytically essential residues are shown in sticks and labeled.